Cylopalladated Complexes with Some Acid and Thioacid Hydrazide Based Ligands and Their Catalytic Applications

A Thesis
Submitted for the Degree of
Doctor of Philosophy

By

GORINTLA NARENDRA BABU

School of Chemistry
University of Hyderabad
Hyderabad 500 046
India

June 2017

Dedicated to

My Parents and Family members

CONTENTS

STATEMENT

I hereby declare that the matter embodied in this thesis entitled "**Cyclopalladated Complexes with Some Acid and Thioacid Hydrazide Based Ligands and Their Catalytic Applications"** is the result of the investigation carried out by me in the School of Chemistry, University of Hyderabad, under the supervision of **Prof. Samudranil Pal**.

In keeping the general practice of reporting scientific observations, due acknowledgement has been made wherever the work described is based on findings of other investigations. Any omission which might have occurred by oversight or error is regretted.

30th June, 2017 **Gorintla Narendra Babu**

DECLARATION

I **Gorintla Narendra Babu** hereby declare that this thesis entitled "***Cyclopalladated Complexes with Some Acid and Thioacid Hydrazide Based Ligands and Their Catalytic Applications***" submitted by me under the supervision and guidance **Prof. Samudranil Pal**, School of Chemistry, University of Hyderabad is a bonafide research work which is also free from plagiarism. I also declare that it has not been submitted previously in part or full to this University or any other University or Institution for the award of any degree or diploma. I hereby agree that my thesis can be deposited in shodhganga/INFLIBNET.

Date: 30th June 2017

Gorintla Narendra Babu

Reg.No:12CHPH03

Signature of the supervisor:

Prof. Samudranil Pal

CERTIFICATE

This is to certify that the thesis entitled "**Cyclopalladated Complexes with Some Acid and Thioacid Hydrazide Based Ligands and Their Catalytic Applications"** submitted by **Gorintla Narendra Babu** bearing registration number **12CHPH03** in partial fulfillment of the requirements for award of Doctor of Philosophy in the School of Chemistry is a bonafide work carried out by him under my supervision and guidance. This thesis is free from plagiarism and has not been submitted previously in part or in full to this or any other University or Institution for award of any degree or diploma. Further the student has seven publications before submission of the thesis for adjudication and has produced evidences for the same in the form of reprints.

Parts of this thesis have been published in the following three publications:

1. G. N. Babu, S. Pal, *J. Organomet. Chem*. 805 (2016) 19–26. (Chapter 2)
2. G. N. Babu, S. Pal, *Tetrahedron Lett*. 58 (2017) 1000–1005. (Chapter 3)
3. G. N. Babu, S. Pal, *J. Organomet. Chem.* 824 (2016) 42–47. (Chapter 4)

He has also made presentations in the following conferences:

1. Poster presentation in the 17th CRSI National Symposium in Chemistry, National Chemical Laboratories, Pune, India (6–8 February, 2015).
2. Poster presentation in the Symposium on Modern Trends in Inorganic Chemistry (MTIC-XVI), Jadavpur University, Kolkata (3–5 Dec., 2015).
3. Oral and Poster presentation at CHEMFEST-2016, 13th Annual In-house Symposium, University of Hyderabad (18–19 March, 2016).

Further the student has passed the following courses towards fulfillment of coursework requirement for Ph. D.:

Course	Title	Credits	Pass/Fail
1. CY-801	Research Proposal	3	Pass
2. CY-805	Instrumental Methods A	3	Pass
3. CY-806	Instrumental Methods B	3	Pass
4. CY-810	Basic Concepts and Coordination Chemistry	3	Pass

Prof. Samudranil Pal
(Thesis Supervisor)

Dean
School of Chemistry

ACKNOWLEDGEMENTS

First and foremost, I would like to express deepest gratitude and great respect to my research supervisor ***Prof. Samudranil Pal*** *for his constant guidance, fruitful suggestions, encouragement and support throughout my research work that helped me to grow as a successful research scholar and person. It has been great privilege for me to work with him.*

I would like to thank the former and present Deans, School of Chemistry for providing all essential facilities to carry out my research work without any interruption. I am extremely thankful individually to all the faculty members of the school particularly my doctoral committee members Prof. Samar Kumar Das and Prof. K. Muralidharan for their, cooperation and encouragement at various stages of my stay in the school.

I thank all non-teaching staff of the School of Chemistry for their help and cooperation to execute my research work. I am thankful to IGM library for providing an excellent collection of books and journals.

I sincerely thank Council of Scientific and Industrial Research (CSIR), New Delhi for a research fellowship (No. 09/414(1025)/2012-EMR-I). Financial support and instrumental facilities provided by the Department of Science and Technology, New Delhi through the FIST and the PURSE programs and by the University Grants Commission, New Delhi through the CAS and the UPE programs are gratefully acknowledged.

I am extremely thankful to my seniors in the lab: Dr. Tulika, Dr. Nagaraju, Dr. swamy, Dr. Balavardhana Rao, Dr. Sathish Kumar and post-doctoral fellows Dr. Rupesh Narayana Prabhu and Dr. Srinivas for their help and cooperation. I thank my present labmates: Sabari Ghosh, Ankit Kumar Srivastava and Mohammed Ishtiyak for their help and creating a cheerful atmosphere in the lab.

I know that I do not speak to all my friends every day but I have lots of great friends and it is difficult to mention to all of them here. I would like to thank my B.Sc. friends Ramesh and Sadhana, Mahesh, Y.V.K. Prasad, srekhar, Ravibabu, Koti, pasha, Krishna, Rajender, Mohan, Sandeep, Harilal, Vijayalaxmi, Anusha, my entire school friends Medhara, Suresh, Adapa, Narapongu, Enupanuri, Guru, Thati, Neelam brothers, Laxman, Narasimharao, Guruswamy, Dasari, Bandela, Yadagiri, Bharath, Kranthi, Rambabu, Veeru, Sanjay, saidulu, Jerripotula, Porella Krishna, Prabhakar,

Ramachandra, Rayala, Adham, Hanumathu, Apparao, Gopalakrishna, Thatha, Sridhar, Kiran, Anandh, Inter friends Ashok, Gopinath, Amarlapudi, Sheshu, Suresh, Arun, Pullarao, Anji, Mekala, Raghu, Johny, Ravi. My M.Sc. friends Laxman, Praveen, Sridhar, Sampath, Srinu, Srujan, Chaithanya, Gopal, Khadahr, Mahender, Srinivas, Gupta, Curd Mamatha, Jyothi, Sushma, Tejaswi, Rani, Rupa and Mamatha, I extend my heart thanks to my friends in School of Chemistry, Uday, Harish, Srinu, Ramakrishna, Tulasi, Dr. Nayudu, Dr. shivaramakrishna, Dr. Chandu, Dr. Sudheer, Anandh, Mohan, satyanarayana, Ramesh, Sagar, shivareddy, Shankar, Shashi, Keshav, Mittapalli, Anil, Allu, Dr. Kiran, Prabhakarreddy, Surender, Dr. Madhavachary, Dr. Murali, Dr. Bharani, Dr. Shiva, Dr. Naveen, Chandrahas, Basha, Tamilarasan, Shaktivelu, Nagamaiah, Obaiah, Vikranth, Shuvankar, Satheesh, Dr. Babu, Dr. Bhargavi, Dr. Krishnachary, Kondareddy, Dr. Kondareddy, Billa, Rambabu, Dr. Raju, Velpuri, Dr. Hanees, Dr. Vignesh, Dr. Ganesh, Dr. Dharavath, Dr. Ashok, Ugander, Naveen, Ranjani, Indravath, Suresh, satheesh, Dr. Kishore, Dr. Paulami, Krishna, Venkata Ramudu, Dr. Venu, Rangu, Majji, Koushik…are few to mention.

My special thanks to my beloved cousins Ashwini, Ashok, Anil, Murali, Venkat, Hanumanthu, Kiran, Rakesh, Rajesh, Mahesh, Babu, Naresh, Lazar, Reddy, Srinu, Mamatha, Aneepa, Abhinay and all my relatives.

I owe everything to god and my parents Nageswara Rao and Jayamma for their love, support and care. They have offered me the highest degree of freedom in life. No words, only gratitude to them. My special thanks to my beloved Annaiah-Vadina Suresh Kumar-Mithili and Suman Babu-Srilatha for their lots of love, values and care from them. I would like to thank my uncut diamonds son and daughter Surya Teja and Sahasya for their precious smile. Thank you

G. Narendra Babu

SYNOPSIS

This thesis entitled **"Cyclopalladated Complexes with Some Acid and Thioacid Hydrazide Based Ligands and Their Catalytic Applications"** consists of five chapters. These are: (**1**) Introduction, (**2**) Mono- and dinuclear cyclopalladated complexes with 4-R-*N'*-(mesitylidene)benzohydrazides and mono- and diphosphines, (**3**) Mono- and dinuclear cyclopalladated complexes as catalysts for Suzuki–Miyaura cross-coupling reactions in predominantly aqueous media, (**4**) Syntheses, structures and catalytic applications of mono- and tetranuclear cyclopalladated complexes with *N'*-(9-anthracenylidene)benzothiohydrazide and (**5**) Syntheses, characterization and catalytic properties of two cyclopalladated complexes with *N'*-(2-naphthaldimine)benzohydrazide. Except for the first chapter (Introduction), each of the remaining chapters is divided into following sections: Introduction, Experimental Section, Results and Discussion, Conclusions and References.

Chapter 1

Introduction

In this chapter, cyclopalladated complexes and their applications in biology, materials science and catalysis have been briefly described.

Chapter 2

Mono- and dinuclear cyclopalladated complexes with 4-R-*N'* (mesitylidene)benzohydrazides and mono- and diphosphines

Reactions of $PdCl_2$, LiCl, 4-R-*N'*-(mesitylidene)benzohydrazides (H_2L^n; n = 1 and 2 for R = H and OMe, respectively) and $NaO_2CH \cdot 3H_2O$ in 1:2:1:1 mole ratio in methanol produce $[Pd(HL^n)Cl]$ (**1** (n = 1) and **2** (n = 2)) in ~77% yields.

Scheme 1. (i) $PdCl_2$, LiCl and $NaOAc{\cdot}3H_2O$ (1:2:1 mole ratio) in methanol at room temperature. (ii) PPh_3 (2 mole equivalents) in acetone at room temperature. (iii) $Ph_2P(CH_2)_4PPh_2$ (0.5 mole equivalent) in acetone at room temperature. (iv) $[Fe(C_5H_4PPh_2)_2]$ (0.5 mole equivalent) in acetone at room temperature.

Reactions of [Pd(HL^n)Cl] (**1** and **2**) with PPh_3 in 1:2 mole ratio in acetone provide [Pd(L^n)(PPh_3)] (**3** (n = 1) and **4** (n = 2)) in ~76% yields. Whereas, treatment of two mole equivalents of [Pd(HL^n)Cl] (**1** and **2**) with one mole equivalent of 1,4-bis(diphenylphosphino)butane (dppb) in acetone affords the dinuclear [Pd_2(μ-dppb)(L^n)$_2$] (**5** (n = 1) and **6** (n = 2)) in ~74% yields. Analogous reaction between [Pd(HL^2)Cl] (**2**) and 1,1'-bis(diphenylphosphino)ferrocene (dppf) provides [Pd_2(μ-dppf)(L^2)$_2$] (**7**) in 67% yield (Scheme 1). Elemental (CHN) analysis, X-ray crystallographic and spectroscopic (IR, UV-Vis and NMR) measurements have been used to characterize all the complexes. In these complexes, the metal centers are in square-planar CNOCl or CNOP coordination geometry formed by the 6,5-membered fused chelate rings forming methylene-C, azomethine-N and amide- or amidate-O donor $(HL^n)^-$ or $(L^n)^{2-}$ and the ancillary ligand chloride or phosphine. The spectroscopic properties of the complexes are consistent with the corresponding molecular structures established by X-ray crystallography.

Chapter 3

Mono- and dinuclear cyclopalladated complexes as catalysts for Suzuki–Miyaura cross-coupling reactions in predominantly aqueous media

Suzuki–Miyaura cross-coupling reactions of aryl halides with arylboronic acids were performed in predominantly aqueous media employing two mono- and two dinuclear cyclopalladated complexes as catalysts. These complexes are [Pd(HL)Cl] (**I**), [Pd(L)(PPh_3)] (**II**), [Pd_2(μ-dppb)(L)$_2$] (**III**) and [Pd_2(μ-dppf)(L)$_2$] (**IV**); where H_2L, dppb and dppf represent 4-methoxy-*N*′-(mesitylidene)benzohydrazide, 1,4-bis(diphenylphosphino)butane and 1,1′-bis(diphenylphosphino)ferrocene, respectively. The reactions were conducted

using potassium carbonate as base in presence of tetrabutylammonium bromide (TBAB) at 70/90 °C in dimethylformamide–water (1:20) mixture (Scheme 2). Among the four catalysts used, the dinuclear complex **IV** turned out to be the most effective and afforded moderate to excellent yields with broad substrate scope.

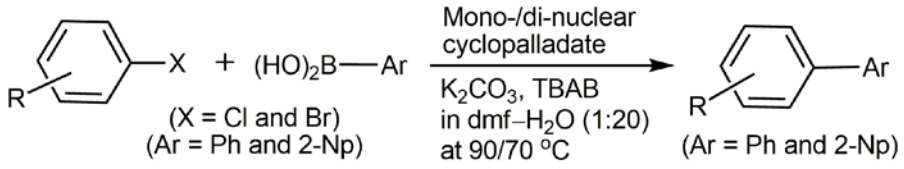

Scheme 2. Conditions for the Suzuki–Miyaura reactions.

Chapter 4

Syntheses, structures and catalytic applications of mono- and tetranuclear cyclopalladated complexes with *N′*-(9-anthracenylidene)benzothio-hydrazide

Reaction of $PdCl_2$, LiCl, N′-(9-anthracenylidene)benzothiohydrazide (H_2L, 2 Hs represent the thioamide NH proton and the 9-anthracenyl *peri* proton) and $NaOAc{\cdot}3H_2O$ in 1:2:1:1 mole ratio in methanol produced $[Pd_4(L)_4]$ (**1**) in 75 % yield. Treatment of **1** with PPh_3 (1:4.5 mole ratio) in acetone provided $[Pd(L)(PPh_3)]$ (**2**) in 72% yield (Scheme 3). The molecular formulas of the diamagnetic and non-electrolytic **1** and **2** were established by elemental analyses. Molecular structures of **1** and **2** were determined by single crystal X-ray diffraction studies. In the tetranuclear **1**, the palladium(II) centers are in distorted square-planar CNS_2 coordination environments created by four $(L)^{2-}$, each of which acts as 5,6-membered fused chelate rings forming thioamidate-S, azomethine-N and 9-anthracenyl *peri*-C donor to one metal center and uses the thioamidate-S atom to bridge a second metal center. In the mononuclear **2**,

$(L)^{2-}$ and PPh_3 assemble a distorted square-planar CNSP coordination environment around the palladium(II) center. Spectroscopic (IR, NMR and UV-Vis) measurements were also used to characterize **1** and **2**. The catalytic properties of both complexes in the oxidative phenylacetylene homocoupling reaction were examined.

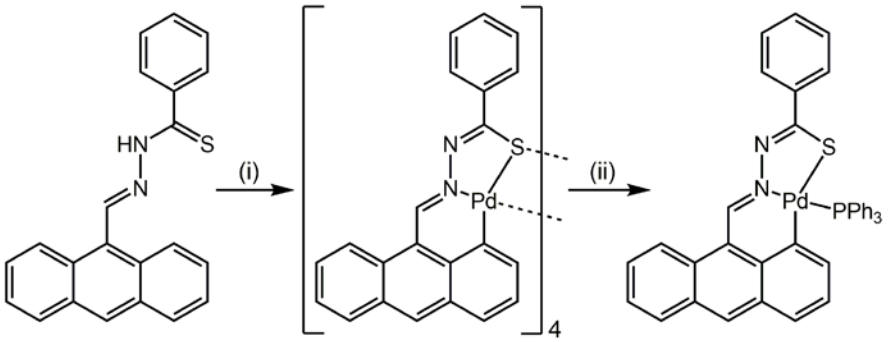

Scheme 3. (i) $PdCl_2$, LiCl and $NaOAc{\cdot}3H_2O$ (1:2:1 mole ratio) in methanol at 298 K. (ii) PPh_3 (4.5 mole equivalents) in acetone at 298 K.

Chapter 5

Syntheses, characterization and catalytic properties of two cyclopalladated complexes with *N'*-(2-naphthaldimine)benzohydrazide

Condensation reaction of 2-naphthaldehyde with one equivalent of benzohydrazide in presence of acetic acid in refluxing methanol yielded the Schiff base *N'*-(2-naphthaldimine)benzohydrazide (H_2L) in 86% yield. Reaction of equimolar amounts of Li_2PdCl_4 (generated in situ from $PdCl_2$ and LiCl taken in 1:2 mole ratio), H_2L and $NaOAc{\cdot}3H_2O$ in methanol at room temperature provided the complex [Pd(HL)Cl] (**1**) in 82% yield. Treatment of one mole equivalent of **1** with two mole equivalents of PPh_3 in acetone at room temperature produced the complex [Pd(L)(PPh_3)] (**2**) in 72% yield. The Schiff base and the two complexes were characterized by elemental analysis,

mass spectrometric and various spectroscopic (IR, UV-Vis and ^{1}H-NMR) measurements. The molecular structures of both complexes (**1** and **2**) were determined by single crystal X-ray crystallography. In each square-planar complex, the tridentate ligand (HL^{-} in **1** and L^{2-} in **2**) acts as pincer-like CNO-donor. The fourth coordination site is occupied by chloride in **1**, while that in **2** is satisfied by the P-atom of PPh_3. The 2-naphthyl fragment of both $(HL)^{-}$ and $(L)^{2-}$ is palladated at the 3-position. Complex **2** was found to be an effective catalyst for one-pot Suzuki-Miyaura double cross-coupling reactions of 3,5-dihalosalicylaldehydes with a variety of arylboronic acids to provide the corresponding triaryl products in moderate to excellent yields (Scheme 4).

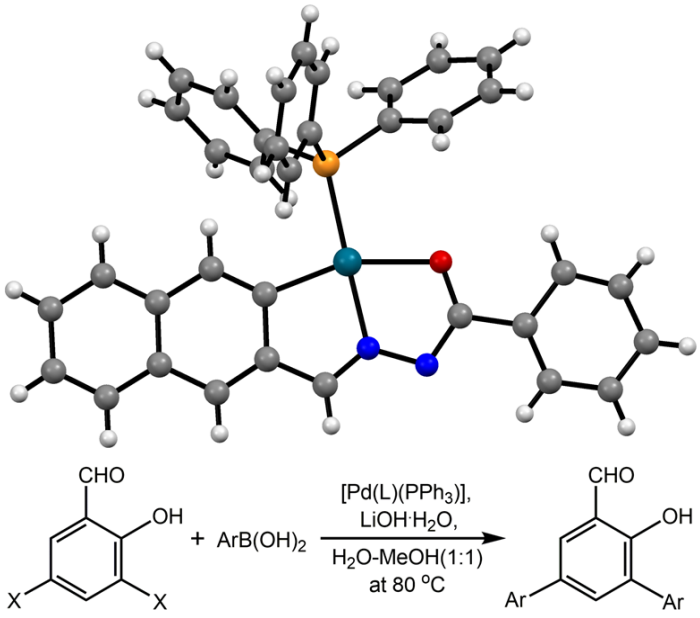

Scheme 4. Structure of [Pd(L)(PPh_3)] (top) and conditions for Suzuki–Miyaura double cross–coupling reactions (bottom).

Chapter 1

Introduction

In this chapter, cyclopalladated complexes and their applications in biology, materials science and catalysis have been briefly described.

1.1. Cyclopalladated complexes

Since the discovery of first cyclometallated nickel(II) complex (Scheme 1.1) in 1963 by Klienman and Dubeck [1], this chemistry was quickly extended to other transition metals, particularily the platinum group metals (Os, Ru, Rh, Ir, Pt and Pd) [2−8]. Among the platinum group metals cyclopalladation chemistry has received the maximum attention [6−8].

Scheme 1.1. The first cyclometallated complex

In 1965, Cope and Siekmen [9] carried out the reactions of azobenzene and its derivatives with $PdCl_2$ to synthesize the first examples of cycopalladated complexes (Scheme 1.2). Since then a vast number of cyclopalladated complexes have been synthesized using a variety of ligands such as azoaryls, aryl-heteroaryls, aryl phosphines and Schiff bases [10−23].

Scheme 1.2. One of the first examples of cyclopalladated species

Cyclopalladallation reactions and cyclopalladated complexes continue to be of immense interest due to their uses and applications in design and synthesis of complex and intricate organic molecules, biological studies, medicinal chemistry, materials science and catalysis [24−30].

1.2. Some applications

1.2.1. Biological and medicinal chemistry

Cyclopalladated complexes have been found to exhibit a wide range of biological activities such as antibacterial, antifungal, antimycobacterial and antiprotozoal [31−36]. Over the past few decades, cisplatin and their analogues (carboplatin and oxaliplatin) [37,38] have been extensively used as anticancer agents. However these cisplatin derivatives are known to have several limitations which restrict their utility to a great extent. Thus many other transition metals instead of platinum are in focus to reduce side effects and to improve effectiveness of the anticancer activities. Palladium has structural preferences similar to those of platinum and can exhibit significant cytotoxic effect on cancer cells. Thus palladium compounds can be an alternative to platinum based anticancer agents. Cyclopalladated complexes have the ability to bind a wide variety of ancillary monodentate ligands (e.g. halides, O-, S-, N-and P-donor). Such complexes are described as promising antitumor agents [39−44]. Some of the biologically and pharmaceutically important cyclopalladated complexes are shown in Figure 1.1.

Figure 1.1. Examples of some biologically active cyclopalladates

1.2.2. Materials science

Cyclopalladated complexes have found applications in photonic, photocatalytic, polymer and liquid crystalline materials research [45−52]. Liquid crystalline cyclopalladated complexes have received much attention over the last few years due to their promising properties and potential use in photoresponsive devices for optical data storage, photomechanics, and nonlinear optics. The cyclopalladated complexes with aliphatic chain bearing Schiff base ligands are most common liquid crystalline compounds. In recent times, considerable efforts have been devoted on developing new cyclometallated complexes for use as emissive materials in light emitting device (LED) based display and lighting applications. Heavy metal cyclometallated complexes particularly those containing platinum and iridium are known to be very effective for LEDs. Besides Pt and Ir, cyclopalladated complexes have also shown promising results for use in LEDs [53−60].

1.2.3. Catalysis

Cyclopalladated complexes have received considerable attention because the cyclopalladation reaction represents probably the mildest route for activating strong carbon–hydrogen and carbon–heteroatom bonds. Indeed these complexes are intermediates for various organic transformation reactions. Apart from this, due to their stability, easy handling, air and moisture insensitivity, these complexes have found many successful applications in catalysis. In 1986, Lewis [61] first used cyclopalladated complexes as catalysts for the hydrogenation of alkenes and alkynes. Palladacycles have been efficiently used as catalysts in selective reduction of nitro-aromatic compounds, nitro-alkenes, nitriles and aromatic carbonyl compounds [62−65]. Palladacycle catalysts have been used quite extensively in C–C and C–heteroatom bond cross coupling reactions [66−77] as compared to hydrogenation reactions.

Figure 1.2. Some examples of cyclopalladated catalysts

Cross coupling reactions catalyzed by cyclopalladated complexes have several advantages such as air and moisture tolerance, mild conditions and enhanced catalytic activities compared to simple palladium salts/complexes, e.g., $Pd(OAc)_2$, $PdCl_2$, $[PdCl_2(CH_3CN)_2]$, $[Pd(PPh_3)_4]$, $[PdCl_2(PPh_3)_2]$ etc. Cyclopalladates were first successfully introduced by Hermann and co-workers [66] as catalysts for C–C cross–coupling reactions, which demonstrate broad substrate scope. Since then various types of cyclopalladated complexes have been synthesized for use as catalysts (Figure 1.2). In addition to the complexes bearing bidentate C,P-; C,S- and C,N-donor ligands and pincer and pincer type ligands, complexes with Schiff base ligands have also been successfully employed in common carbon–carbon and carbon–hetero atom cross coupling reactions such as Suzuki, Heck, Sonogashira, Stille, Buchwald and Negishi reactions and in number of other organic transformation reactions [67−79].

Suzuki–Miyaura cross-coupling reactions

The most convenient and useful method for the single step synthesis of a biaryl or biheteroaryl is the Csp^2–Csp^2 Suzuki–Miyaura cross–coupling reaction (Equation 1.1). Biaryls and biheteroaryls are an important class of compounds as they are significant building blocks for a variety of natural products, pharmaceuticals, agrochemicals and functional materials such as sensors and liquid crystals [80−85]. Suzuki–Miyaura cross-coupling reactions have several advantages. These are as follows: commercial availability of the reagents, mild reaction conditions, broad range of products, unaffected by the presence of water and biproducts of the reaction are nontoxic and easily removable.

Equation 1.1

R^1 = aryl, allyl and alkenyl.

X = Cl, Br, I and OTf.

R^2 = aryl and alkenyl.

Since the discovery of this catalytic coupling reaction, there is a continuous effort to develop new catalyst systems which will be effective for a wide range of products. Among the catalytic systems developed for Suzuki–Miyaura coupling reactions till date, not many are cyclopalladate based systems [86−89]. The cycloapalladate catalyzed coupling reactions can proceed in organic media as well as in aqueous media. Besides this, cyclopalladated species are also effective catalysts for not only aryl/heteroaryl iodides and bromides but also for various functionalized aryl/heteroaryl chlorides as cross coupling partners [90−93]. Generally cyclopalladates bearing electron rich phosphines and bidentate phosphines as ancillary ligands promote the oxidative addition step and hence are very effective towards cross coupling reactions [94−98].

1.3. Cyclopalladated complexes with Schiff bases

Schiff bases were first discovered by Hugo Schiff [99]. Schiff base ligands are considered privileged ligands because they have shown excellent selectivity, stability and are easily prepared by simple condensation of aldehydes/ketones and primary amines. The chemistry of Schiff bases are well known with first row transition metals [100−105], whereas their cyclopalladation chemistry is relatively less explored. In 1969 Molnar and Orchin [106] reported the first cyclopalladated species with Schiff base ligands. Generally bi- and tridentate Schiff base ligands form stable cyclopalladated complexes. Most of the cyclopalladates are with bidentate CN-donor Schiff base ligands and exist as

acetate or halogen bridged dimers. The halide/acetate bridges could be easily cleaved by mono-/bidentate neutral or anionic ligands [107−110]. A few representative examples of such complexes are shown in Figure 1.3.

Figure 1.3. A few examples of palladacycles with bidentate Schiff bases

In addition to cyclopalladated complexes with bidentate Schiff base ligands, interest is growing to prepare such complexes with terdentate ligands. The process of bidentate chelation followed by cyclometallation of a pendant aryl group is the most effective and commonly used strategy for the synthesis of cyclometallated complexes with tridentate ligands. Majority of these cyclopalladated complexes have been derived from imine based ligands, e.g., hydrazone, semicarbazone and thiosemicarbazone derivatives [111−118]. In these complexes, the ligands act as either 5,5- or 5,6-membered fused chelate rings forming pincer like CNO-, CNN-, CNS- and CNP-donors (Figure 1.4).

Figure. 1.4. Examples of cyclopalladates with pincer-like Schiff bases

1.4. About the present work

In the present study, the cyclopalladation chemistry of the following three aroyl-and thioaroylhydrazones (Figure 1.5) has been explored. In this effort, several new cyclopalladated complexes have been isolated. Besides, syntheses, and characterization of these cyclopalladated complexes, their catalytic properties in Suzuki-Miyaura cross-coupling and alkyne homocoupling reactions have been also investigated.

Figure 1.5. 4-R-*N*′-(mesitylidene)benzohydrazides (left), N′-(9-anthracenylidene)benzothiohydrazide (middle), *N*′-(2-naphthaldimine)-benzohydrazide (right).

1.5. References

[1] J.P. Klienman, M. Dubeck, *J. Am. Chem. Soc*. 85 (1963) 1544−1545.

[2] M.E. van der Boom and D. Milstein, *Chem. Rev*. 103 (2003) 1759−1792.

[3] J. Dehand and M. Pfeffer, *Coord. Chem. Rev*. 18 (1976) 327−352.

[4] G.R. Newkome, W.E. Puckett, V.K. Gupta and G.E. Kiefer, *Chem. Rev*. 86 (1988) 451−489.

[5] M.I. Bruce, Angew. *Chem. Int. Ed*. 16 (1977) 73−86.

[6] W.A. Herrmann, K. Ofele, D.V. Preysing, S. K. Schneider, *J. Organomet. Chem*. 687 (2003) 229−248.

[7] M. Albrecht, *Chem. Rev*. 110 (2010) 576−623.

[8] V.V. Dunina, O.A. Zalevskaya and V.M. Potapov, *Russian Chem. Rev*. 57 (1988) 434−473.

[9] A.C. Cope, R.W. Siekman, *J. Am. Chem. Soc*. 87 (1965) 3272−3273.

[10] J. Albert, A. González, J. Granell, R. Moragas, X. Solans and M.F-Bardía, *J. Chem. Soc. Dalton Trans*. (1998) 1781−1785.

[11] A. Fernandez, M.L. -Torres, S.C. -Juiz, M. Merino, D.V. -Garcıa, J.M. Vila and J.J. Fernandez, *Organometallics* 30 (2011) 386−395.

[12] I. B1aszczyk, A. Gniewek, A.M. Trzeciak, *J. Organomet. Chem*. 696 (2011) 3601−3607.

[13] K. Karami, M.H. -Kharat, Z.S. -Sarmazeh, R.Z. -Nasab, C. Rizzoli and J. Lipkowski, *J. Coord. Chem*. 69 (2016) 763−778.

[14] S.A. Kurzeev, G.M. Kazankov, A.D. Ryabov, *Inorg. Chim. Acta*. 305 (2000) 1−6.

[15] J.L. Serrano, J. Pérez, L. García, G. Sánchez, J. García, P. Lozano, V. Zende and A. Kapdi, *Organometallics* 34 (2015) 522−533.

[16] C. Xu, Z. Wang, X. Yuan, X. Han, Z. Xiao, W. Fu, B. Ji, X. Hao, M. Song, *J. Organomet. Chem*. 777 (2015) 1−5.

[17] G.–R. Peh, E.A. B. Kantchev, J.–C. Er and J.Y. Ying, *Chem. Eur. J*. 16 (2010) 4010−4017.

[18] M.S. Viciu, R.A. Kelly, E.D. Stevens, F. Naud, M. Studer and S.P. Nolan, *Org. Lett*. 5 (2003) 1479−1482.

[19] K. Karami, S. Abedanzadeh, F. Yadollahi, O. Büyükgüngor, H. Farrokhpour, C. Rizzoli, J. Lipkowski, *J. Organomet. Chem*. 781 (2015) 35−46.

[20] A. Amoedo, L.A. Adrio, J.M. Antelo, J. Martínez, M.T. Pereira, A. Fernández and J.M. Vila, *Eur. J. Inorg. Chem*. (2006) 3016−3021.

[21] M. Juribasic, M. Curic, K. Molcanov, D. Matkovicalogovic and D. Babic, *Dalton Trans*. 39 (2010) 8769−8778.

[22] Md. A. Hossain, S. Lucarini, D. Powell and K.B. -James, *Inorg. Chem*. 43 (2004) 7275−7277.

[23] C. López, M. Salmi, A. Mas, P. Piotrowski, M.F. Bardía and T. Calvet, *Eur. J. Inorg. Chem*. (2012) 1702−1709.

[24] J. Dupont, M. Pfeffer (Eds.), Palladacycles: Synthesis, Characterization and Applications, Wiley-VCH, Weinheim, 2008.

[25] I.P. Beletskaya, A.V. Cheprakov, *J. Organomet. Chem*. 689 (2004) 4055−4082.

[26] I. Omae, Cyclometalation Reactions, Sprindger, Tokyo, 2014.

[27] K. Godula, D. Sames, *Science* 312 (2006) 67−72.

[28] Y. You, W. Nam, *Chem. Soc. Rev*. 41 (2012) 7061−7084.

[29] N. Cutillas, G.S. Yellol, C. de Haro, C. Vicente, V. Rodríguez, J. Ruiz, *Coord. Chem. Rev*. 257 (2013) 2784−2797.

[30] X. Jiang, N. Zhu, D. Zhao, Y. Ma, *Sci. China Chem*. 59 (2016) 40−52.

[31] A.-S.S.H. Elgazwy, N.S.M. Ismail, S.R. Atta-Allah, M.T. Sarg, D.H.S. Soliman, M.Y. Zaki and M.A. Elgamas, *Current Medicinal Chem.* 19 (2012) 3967−3981.

[32] S. Ray, R. Mohan, J.K. Singh, M.K. Samantaray, M.M. Shaikh, D. Panda and P. Ghosh, *J. Am. Chem. Soc*. 129 (2007) 15042−15053.

[33] A.M.A. Velásquez, R.A. de Souza, T.G. Passalacqua, A.R. Ribeiro, M. Scontri, C.M. Chin, L. de Almeida, M.L. Del Cistia, J.A. da Rosa, A.E. Mauro and M.A.S. Graminha, *J. Braz. Chem. Soc*. 27 (2016) 1032−1039.

[34] A. Tahghighi, *J. Organomet. Chem*. 770 (2014) 51−60.

[35] F. Zamora, V.M. Gonzalez, J.M. Pérez, J.R. Masaguer, C. Alonso and C.N. -Ranninger, *appl. Organomet. Chem*. 11 (1997) 659−666.

[36] J. Albert, J. Granell, J.A. Duran, A. Lozano, A. Luque, A. Mate, J. Quirante, M.K. Khosa, C. Calvis, R. Messeguer, L. Baldoma, J. Badia, *J. Organomet. Chem*. 839 (2017) 116−125.

[37] B. Rosenberg, L. Vancamp, J.E. Trosko and V.H. Mansour, *Nature* 222 (1969) 385−386.

[38] L. Kelland, *Nat. Rev. Cancer* 7 (2007) 573−584.

[39] A. Bechara, C.M.V. Barbosa, E.J.P. -Gamero, D.M. Garcia, L.S. Silva, A.L. Matsuo, F.D. Nascimento, E.G. Rodrigues, A.C.F. Caires, S.S. Smaili, C. Bincoletto, *Eur. J. Med. Chem*. 79 (2014) 24−33.

[40] A.–S. H. Elgazwy, M.R. Shehata, M.Y. Zaki, D.H.S. Solima and M.M. Elbakkry, *Med. Chem*. 3 (2013) 254−261.

[41] E.G. Rodrigues, L.S. Silva, D.M. Fausto, M.S. Hayashi, S. Drehrr, E.L. Santos, J.B. Pesquero, L.R. Travassos and A.C.F. Caires, *Int. J. Cancer*: 107 (2003) 498−504.

[42] A.R. Kapdi and I.J.S. Fairlamb, *Chem. Soc. Rev*. 43 (2014) 4751−4777.

[43] S. Aliwaini, J. Peres, W.L. Kröger, A. Blanckenberg, J. Mare, A.L. Edkins, S. Mapolie, S. Prince, *Cancer Lett*. 357 (2015) 206−218.

[44] J. Spencer, R.P. Rathnam, M. Motukuri, A.K. Kotha, S.C.W. Richardson, A. Hazrati, J.A. Hartley, L. Male and M.B. Hursthouse, *Dalton Trans*. (2009) 4299−4303.

[45] D. Kalyani, K.B. McMurtrey, S.R. Neufeldt, and M.S. Sanford, *J. Am. Chem. Soc*. 133 (2011) 18566−18569.

[46] P.–K. Chow, W.–P. To, K. Low and C.M. Che, *Chem. Asian J*. 9 (2014) 534−545.

[47] C. Bronner, S.A. Baudron, M.W. Hosseini, C.A. Strassert, A. Guenet and L.D. Cola, *Dalton Trans*. 39 (2010) 180−184.

[48] M. Ghedini, S. Armentano, R. Bartolino, F. Rustichelli, G. Torquati, N. Kirov and M. Petrov, *Mol. Cryst. Liq. Cryst*. 151 (1987) 75−91.

[49] B. Neumann, T. Hegmann, R. Wolf and C. Tschierske, *Chem. Commun*. (1998) 105−106.

[50] M. Lehmann, T. Sierra, J. Barbera, J.L. Serrano and R. Parker, *J. Mater. Chem*. 12 (2002) 1342−1350.

[51] J.C. Hershberger, L. Zhang, G. Lu and H.C. Malinakova, *J. Org. Chem*. 71 (2006) 231−235.

[52] Y. Kong, L. Wen, H. Song, S. Xu, M. Yang, B. Liu and B. Wang, *Organometallics* 30 (2011) 153−159.

[53] D. Pucci, G. Barberio, A. Bellusci, A. Crispini, M. Ghedini, *J. Organomet. Chem*. 691 (2006) 1138−1142.

[54] M. Ilis¸ M. Micutz, V. Cîrcu, *J. Organomet. Chem*. 836−837 (2017) 81−89.

[55] G. Zhang, H.–H. Chou, X. Jiang, P. Sun, C. –H. Cheng, Y. Ooyama, Y. Harima, *Organic Electronics* 11 (2010) 632−640.

[56] L. Murphy, P. Brulatti, V. Fattori, M. Cocchi and J. A. G. Williams, *Chem. Commun*. 48 (2012) 5817−5819.

[57] E. Baranoff, B.F.E. Curchod, J. Frey, R. Scopelliti, F. Kessler, I. Tavernelli, U. Rothlisberger, M. Gratzel and Md. K. Nazeeruddin, *Inorg. Chem*. 51 (2012) 215−224.

[58] S.M. Borisov, A.S. Vasylevska, C. Krause and O.S. Wolfbies, *Adv. Funct. Mater*. 16 (2006) 1536−1542.

[59] I. Aiello, D. Dattilo, M. Ghedini, A. Bruno, R. Termine and A. Golemme, *Adv. Mater*. 14 (2002) 1233−1236.

[60] M. Ghedini, I. Aiello, A. Crispini, A. Golemme, M. La Deda and D. Pucci, Coord. *Chem. Rev*. 250 (2006) 1373−1390.

[61] L.N. Lewis, *J. Am. Chem. Soc*. 108 (1986) 743−749.

[62] P.K. Santra, C.R. Saha, *J. Mol. Catal*. 39 (1987) 279−292.

[63] S.M. Islam, B.K. Palit, D.K. Mukherjee and C.R. Saha, *J. Mol. Catal A: Chemical* 124 (1997) 5−20.

[64] A.M. Kluwer, T.S. Koblenz, T. Jonischkeit, K. Woelk and C.J. Elsevier, *J. Am. Chem. Soc*. 127 (2005) 15470−15480.

[65] S. Sabater, J.A. Mata and E. Peris, *ACS Catal*. 4 (2014) 2038−2047.

[66] W.A. Herrmann, C. Brossmer, K. Öfele, C. -P. Reisinger, T. Priermeier, M. Beller, H. Fischer, *Angew. Chem. Int. Ed*. 34 (1995) 1844−1848.

[67] D. Zim, A.S. Gruber, G. Ebeling, J. Dupont and A.L. Monteiro, *Org. Lett*. 2 (2000) 2881−2884.

[68] J. Dupont, C.S. Consorti and J. Spencer, *Chem. Rev*. 105 (2005) 2527−2572.

[69] E.A.B. Kantchev, C.J. OBrien and M.G. Organ, *Angew. Chem. Int. Ed*. 46 (2007) 2768−2813.

[70] G.C. Fortman and S.P. Nolan, *Chem. Soc. Rev*. 40 (2011) 5151−5169.

[71] B. Ines, R. SanMartin, F. Churruca, E. Domınguez, M.K. Urtiaga and M.I. Arriortua, *Organometallics* 27 (2008) 2833−2839.

[72] A. Suzuki, *Angew. Chem. Int. Ed*. 50 (2011) 6722−6737.

[73] N.J. Whitecombe, K.K. Hii and S.E. Gibson, *Tetrahedron* 57 (2001) 7449−7476.

[74] P.G. Gildner and T.J. Colacot, *Organometallics* 34 (2015) 5497−5508.

[75] S.D. Friis, T. Skrydstrup and S.L. Buchwald, *Org. Lett*. 16 (2014) 4296−4299.

[76] C.W. Cheung, D.S. Surry and S.L. Buchwald, *Org. Lett*. 15 (2013) 3734−3737.

[77] D. Haas, J.M. Hammann, R. Greiner and P. Knochel, *ACS Catal*. 6 (2016) 1540−1552.

[78] C. Mateo, D.J. Cardenas, C.F. -Rivas and A.M. Echavarren, *Chem. Eur. J*. (1996) 1596−1606.

[79] W. Susanto, C.-Y. Chu, W.J. Ang, T.-C. Chou, L.-C Lo and Y. Lam, *J. Org. Chem*. 77 (2012) 2729−2742.

[80] H. Aldemir, R. Richarz and T.A.M. Gulder, *Angew. Chem. Int. Ed*. 53 (2014) 8286−8293.

[81] G.-X. Zhong, L.-L. Chen, H.-B. Li, F.-J. Liu, J.-Q. Hu and W.-X. Hu, *Biorg. Med. Chem. Lett*. 19 (2009) 4399−4402.

[82] S. Dadiboyena, *Eur. J. Med. Chem*. 51 (2012) 17−34.

[83] T. Chai, W. Yang, J. Qiu and S. Hou, *Chirality* 27 (2015) 32−38.

[84] L. Pu, *Acc. Chem. Res*. 45 (2012) 150−163.

[85] G. Solladie and G. Gottarelli, *Tetrahedron* 43 (1987) 1425−1437.

[86] R.B. Bedford, *Chem. Commun*. (2003) 1787−1796.

[87] A. Suzuki, *J. Organomet. Chem*. 576 (1999) 147−168.

[88] L. Yin and J. Liebscher, *Chem. Rev*. 107 (2007) 133−173.

[89] D.A. Alonso, C. Najera and M. Pacheco, *J. Org. Chem*. 67 (2002) 5588−5594.

[90] A. F. Littke and G.C. Fu, *Angew. Chem. Int. Ed*. 41 (2002) 4176−4211.

[91] L. Botella and C. Najera, *Angew. Chem. Int. Ed*. 41 (2002) 179−181.

[92] X. Han, H.-M. Li, C. Xu, Z.-Q Xiao, Z.-Q Wang, W.-J Fu, X.-Q. Hao and M.-P. Song, *Transition Met. Chem*. 41 (2016) 403−411.

[93] R.B. Bedford, C.S.J. Cazin, M.B. Hursthouse, M.E. Light and V.J.M. Scordia, *Dalton Trans*. (2004) 3864−3868.

[94] M. Beller, H. Fischer, W.A. Herrmann, K. Ofele and C. Brossmer, *Angew. Chem. Int. Ed*. 34 (1995) 1848−1849.

[95] X. Bei, H.W. Turner, W.H. Weinberg and A.S. Guram, *J. Org. Chem*. 64 (1999) 6797−6803.

[96] H. Yan, P. Chellan, T. Li, J. Mao, K. Chibale and G.S. Smith, *Tetrahedron Letters* 54 (2013) 154−157.

[97] M. Joshaghani, M. Daryanavard, E. Rafiee, S. Nadri, *J. Organomet. Chem*. 693 (2008) 3135−3140.

[98] A.N. Marziale, D. Jantke, S.H. Faul, T. Reiner, E. Herdtweck and J. Eppinger, *Green Chem*. 13 (2011) 169−177.

[99] H. Schiff, *Ann. Chem. Suppl*. 3 (1864) 343.

[100] L.L. Merritt, C. Guare and A.E. Lessor, *Acta Cryst*. 9 (1956) 253−256.

[101] L. Sacconi and U. Campig, *Inorg. Chem*. 5 (1966) 606−611.

[102] A. Chakravorty, J.P. Fennessey and R.H. Helm, *Inorg. Chem*. 4 (1965) 26−33.

[103] B. Dede, I. Ozmen, F. Karipcin, *Polyhedron* 28 (2009) 3967−3974.

[104] B. Dutta, S. Jana, R. Bera, P.K. Saha, S. Koner, *Applied Catalysis A: General*, 318 (2007) 89−94.

[105] U. Basu, I. Pant, A. Hussain, P. Kondaiah and A.R. Chakravarty, *Inorg. Chem*. 54 (2015) 3748−3758.

[106] S.P. Molnar and M. Orchin, *J. Organomet. Chem*. 16 (1969) 196−200.

[107] J.M. Vila , M.T. Pereira , A. Suárez , E. Gayoso , M. Gayoso , J. Selbin & A. Sen, *Synth. React. Inorg. Met.-org. Chem*. 16 (1986) 499−511.

[108] J. Granell, D. Sainz and J. Sales, *J. Chem. Soc. Dalton Trans*. (1986) 1785−1790.

[109] P.S. Pregosin und R. Ruedi, *J. Organomet. Chem*. 273 (1984) 401−413.

[110] J.L. Serrano, L. García, J. Perez, E. Perez, J. García, G. Sanchez, P. Sehnal, S.D. Ornellas, T.J. Williams and I.J.S. Fairlamb, *Organometallics* 30 (2011) 5095−5109.

[111] L. Cuesta, D. Prat, T. Soler, R. Navarro and E.P. Urriolabeitia, *Inorg. Chem*. 50 (2011) 8598−8607.

[112] J. Albert, A. Gonzalez, J. Granell, R. Moragas, C. Puerta and P. Valerga, *Organometallics* 16 (1997) 3775−3778.

[113] G. Zhao, Q.-G. Wang and T.C.W. Mak, *J. Chem. Soc. Dalton Trans*. (1998) 3785−3789.

[114] M. Nonoyama and M. Sugimoto, *Inorg. Chim. Acta*. 35 (1979) 131−134.

[115] S. Tollari, G. Palmisano, F. Demartin, M. Grassi, S. Magnaghi, S. Cenini, *J. Org. met. Chem*. 488 (1995) 79−83.

[116] C. Cativiela, L.R. Falvello, J.C. Gines, R. Navarro and E.P. Urriolabeitia, *New J. Chem*. 25 (2001) 344−352.

[117] A. Fernandez, E. Pereira, J.J. Fernandez, M.L. -Torres, A. Suarez, R. Mosteiro, J.M. Vila, *Polyhedron* 21 (2002) 39−48.

[118] Y.–L. Qiao and G.-X Jin, *Organometallics* 32 (2013) 1932−1937.

Chapter 2

Mono- and dinuclear cyclopalladated complexes with 4-R-*N′*-(mesitylidene)benzohydrazides and mono- and diphosphines[§]

Reactions of $PdCl_2$, LiCl, 4-R-*N′*-(mesitylidene)benzohydrazides (H_2L^n; n = 1 and 2 for R = H and OMe, respectively) and $NaO_2CH \cdot 3H_2O$ in 1:2:1:1 mole ratio in methanol produce $[Pd(HL^n)Cl]$ (**1** (n = 1) and **2** (n = 2)) in ~77% yields. Reactions of $[Pd(HL^n)Cl]$ (**1** and **2**) with PPh_3 in 1:2 mole ratio in acetone provide $[Pd(L^n)(PPh_3)]$ (**3** (n = 1) and **4** (n = 2)) in ~76% yields. Whereas, treatment of two mole equivalents of $[Pd(HL^n)Cl]$ (**1** and **2**) with one mole equivalent of 1,4-bis(diphenylphosphino)butane (dppb) in acetone affords the dinuclear $[Pd_2(\mu\text{-dppb})(L^n)_2]$ (**5** (n = 1) and **6** (n = 2)) in ~74% yields. Analogous reaction between $[Pd(HL^2)Cl]$ (**2**) and 1,1'-bis(diphenylphosphino)ferrocene (dppf) provides $[Pd_2(\mu\text{-dppf})(L^2)_2]$ (**7**) in 67% yield. Elemental (CHN) analysis, X-ray crystallographic and spectroscopic (IR, UV-Vis and NMR) measurements have been used to characterize all the complexes. In these complexes, the metal centers are in square-planar CNOCl or CNOP coordination geometry formed by the 6,5-membered fused chelate rings forming methylene-C, azomethine-N and amide- or amidate-O donor $(HL^n)^-$ or $(L^n)^{2-}$ and the ancillary ligand chloride or phosphine. The spectroscopic properties of the complexes are consistent with the corresponding molecular structures established by X-ray crystallography.

[§] This work has been published in *J. Organomet. Chem*. 805 (2016) 19–26.

2.1. Introduction

The majority of cyclometallated complexes are formed due to activation of a proximal C(sp^2)–H bond of an aryl moiety pendant from a chelated ligand. In comparison, cyclometallated species *via* C(sp^3)–H activation in a similar way are relatively scarce. Generally this scarcity arises due to the chemical inertness and thermodynamic stability of the C(sp^3)–H bond. Our group has been working on cyclometallated complexes of platinum metal ions with aroylhydrazones and thiosemicarbazones of various mono- and polycyclic aromatic aldehydes for the past several years [1–4]. These Schiff bases in presence of base coordinate the metal center *via* the azomethine-N and the amidate-O or the thioamidate-S atoms and form a 5-membered chelate ring [1]. Chelation brings the aromatic ring of the arylidene fragment of the aroylhydrazonate or of the thiosemicarbazonate near to the metal center leading to C(sp^2)–H activation and eventual cyclometallation. In the cyclometallated complexes thus obtained, the ligands act as pincer-like CNO- or CNS-donor and form either 5,5-membered fused chelate rings in the case of *ortho*-metallation or 6,5-membered fused chelate rings in the case of *peri*-metallation. The process of bidentate chelation followed by cyclometallation reaction is the most effective and commonly used strategy for the synthesis of cyclometallated complexes [1,5,6]. In the present chapter, 4-R-*N′*-(mesitylidene)benzohydrazides (H_2L^n; n = 1 and 2 for R = H and OMe, respectively) have been used to examine whether similar NO-chelation followed by activation of the relatively more inert C(sp^3)–H bond in an *ortho*-methyl group of the mesityl fragment is possible or not. We have indeed been able to isolate a new series of cyclometallated palladium(II) complexes of formulas [Pd(HL^n)Cl], [Pd(L^n)(PPh_3)], [Pd_2(μ-dppb)(L^n)$_2$] and [Pd_2(μ-dppf)(L^2)$_2$] where $(HL^n)^-$ and

$(L^n)^{2-}$ behave as 6,5-membered fused chelate rings forming CNO-donor ligands (Scheme 2.1). The syntheses, X-ray structures and spectroscopic properties of these complexes are described in the following sections.

Scheme 2.1. (i) $PdCl_2$, LiCl and $NaOAc{\cdot}3H_2O$ (1:2:1 mole ratio) in methanol at room temperature. (ii) PPh_3 (2 mole equivalents) in acetone at room tem-

perature. (iii) $Ph_2P(CH_2)_4PPh_2$ (0.5 mole equivalent) in acetone at room temperature. (iv) $[Fe(C_5H_4PPh_2)_2]$ (0.5 mole equivalent) in acetone at room temperature.

2.2. Experimental

2.2.1. Materials

All chemicals used in this work were of analytical grade available commercially and were used as received without further purification. The solvents used were purified by standard methods [7].

2.2.2. Physical measurements

A Thermo Finnigan Flash EA-1112 elemental analyzer was used for elemental (CHN) analysis. Purities of H_2L^1 and H_2L^2 were verified with a Shimadzu LCMS 2010 liquid chromatograph mass spectrometer. Room temperature (298 K) magnetic susceptibility measurements were performed with a Sherwood scientific balance. Infrared spectra were recorded on a Thermo Scientific Nicolet 380 FT-IR spectrophotometer. A Digisun DI-909 conductivity meter was used for electrical conductivity measurements in solution. Electronic spectra were recorded with the help of a Shimadzu UV3600 UV-Vis-NIR spectrophotometer. The ^1H (400 MHz) and $^{31}P\{^1H\}$ (160 MHz) NMR spectra were recorded with the help of a Bruker NMR spectrometer.

2.2.3. Synthesis of H_2L^1

Benzohydrazide (1.36 g, 10 mmol) and mesitaldehyde (1.48 g, 10 mmol) were dissolved in methanol (70 ml). To this solution a few drops of acetic acid were added and the mixture was refluxed for 7 h. Upon cooling to room tempera-

ture, the white solid separated was collected by filtration, washed with 20 ml of methanol in three portions and finally dried in air. The compound thus obtained was recrystallized from 30 ml of chloroform. Yield: 2.18 g (81%). Anal. Calcd for $C_{17}H_{18}N_2O$: C, 76.67; H, 6.81; N, 10.52. Found: C, 76.51; H, 6.74; N, 10.38. LCMS in CH_2Cl_2: *m/z* $(M - H)^-$ = 265.2. Selected IR bands: ν (cm^{-1}) = 3199 (N–H), 1657 (C=O), 1606 (C=N). UV-Vis in Me_2NCHO: λ_{max} (nm) (ε (10^3 M^{-1} cm^{-1})) = 300 (12.8). ^{1}H NMR in $(CD_3)_2SO$: δ (ppm) ($J_{H–H}$ (Hz)) = 11.72 (s, 1H, NH), 8.75 (s, 1H, H^{10}), 7.91 (8) (d, 2H, H^{13}, H^{17}), 7.60–7.49 (m, 3H, $H^{14–16}$), 6.90 (s, 2H, H^3, H^5), 2.41 (s, 6H, 2 *o*-Me), 2.23 (s, 3H, *p*-Me).

2.2.4. Synthesis of H_2L^2

H_2L^2 was prepared in methanol medium from equimolar amounts of 4-methoxy benzohydrazide (1.66 g, 10 mmol) and mesitaldehyde (1.48 g, 10 mmol) in presence of 2–3 drops of acetic acid by following the same procedure as described above for H_2L^1. Yield: 2.49 g (84%). Anal. Calcd for $C_{18}H_{20}N_2O_2$: C, 72.95; H, 6.80; N, 9.45. Found: C, 72.85; H, 6.72; N, 9.36. LCMS in CH_2Cl_2: *m/z* $(M - H)^-$ = 295.20. Selected IR bands: ν (cm^{-1}) =: 3224 (N–H), 1650 (C=O), 1603 (C=N). UV-Vis in Me_2NCHO: λ_{max} (nm) (ε (10^3 M^{-1} cm^{-1})) = 300 (16.6). ^{1}H NMR in $(CD_3)_2SO$: δ (ppm) ($J_{H–H}$ (Hz)) = 11.62 (s, 1H, NH), 8.76 (s, 1H, H^{10}), 7.94 (8) (d, 2H, H^{13}, H^{17}), 7.07 (8) (d, 2H, H^{14}, H^{16}), 6.92 (s, 2H, H^3, H^5), 3.84 (s, 3H, OMe), 2.43 (s, 6H, 2 *o*-Me), 2.25 (s, 3H, *p*-Me).

2.2.5. Synthesis of [Pd(HL^1)Cl] (1)

A mixture of $PdCl_2$ (90 mg, 0.5 mmol) and LiCl (43 mg, 1 mmol) was taken in 15 ml of dry methanol and refluxed with stirring for 1 h. The reaction mix-

ture was then cooled to room temperature and filtered. The filtrate containing $Li_2[PdCl_4]$ was added to a methanol (10 ml) solution of H_2L^1 (133 mg, 0.5 mmol) and $NaOAc{\cdot}3H_2O$ (68 mg, 0.5 mmol) and then the mixture was stirred at room temperature for 2 days. The complex **1** separated as a green solid was collected by filtration, washed with methanol and finally dried in air. Yield: 155 mg (76%). Anal. Calcd for $C_{17}H_{17}N_2OClPd$: C, 50.14; H, 4.21; N, 6.88. Found: C, 50.32; H, 4.28; N, 6.71. Selected IR data: ν (cm^{-1}) = 3180 (N–H), 1606 (C=O), 1562 (C=N). UV-Vis in Me_2NCHO: λ_{max} (nm) (ε (10^3 M^{-1} cm^{-1})) = 393^{sh} (2.5), 370 (3.4), 358^{sh} (3.3), 305^{sh} (4.0). ^{1}H NMR in $(CD_3)_2SO$: δ (ppm) ($J_{H–H}$ (Hz)) =11.68 (s, 1H, NH), 8.80 (s, 1H, H^{10}), 7.96 (8) (d, 2H, H^{13}, H^{17}), 7.69 (br, s, 1H, H^{15}), 7.62–7.59 (m, 2H, H^{14}, H^{16}), 7.18 (s, 1H, H^3), 6.99 (s, 1H, H^5), 3.16 (s, 2H, metallated-CH_2), 2.44 (s, 3H, *o*-Me), 2.26 (s, 3H, *p*-Me).

2.2.6. Synthesis of [Pd(HL^2)Cl] (2)

This complex was synthesized in methanol medium by following the same procedure as described above for **1** using $PdCl_2$ (90 mg, 0.5 mmol), LiCl (43 mg, 1mmol), H_2L^2 (148 mg, 0.5 mmol) and $NaOAc{\cdot}3H_2O$ (68 mg, 0.5 mmol). Yield: 170 mg (78%). Anal. Calcd for $C_{18}H_{19}N_2O_2ClPd$: C, 49.45; H, 4.38; N, 6.41. Found: C, 49.58; H, 4.31; N, 6.36. Selected IR data: ν (cm^{-1}) = 3193 (N–H), 1606 (C=O), 1562 (C=N). UV-Vis in Me_2NCHO: λ_{max} (nm) (ε (10^3 M^{-1} cm^{-1})) = 390^{sh} (3.9), 370 (5.0), 355^{sh} (4.9), 328^{sh} (5.8), 290^{sh} (10.9). ^{1}H NMR in $(CD_3)_2SO$: δ (ppm) ($J_{H–H}$ (Hz)) = 11.59 (s, 1H, NH), 8.78 (br, s, 1H, H^{10}), 7.98 (9) (d, 2H, H^{13}, H^{17}), 7.22–6.92 (m, 4H, H^3, H^5, H^{14}, H^{16}), 3.87 (s, 3H, OMe), 3.18 (s, 2H, metallated-CH_2), 2.47 (s, 3H, *o*-Me), 2.29 (s, 3H, *p*-Me).

2.2.7. Synthesis of [Pd(L^1)(PPh$_3$)] (3)

[Pd(HL^1)Cl] (**1**) (122 mg, 0.3 mmol) and PPh_3 (158 mg, 0.6 mmol) were taken in acetone (20 ml) and stirred at room temperature for 24 h. The yellow solid precipitated was collected by filtration, washed with acetone and finally dried in air. Yield: 143 mg (75%). Anal. Calcd for $C_{35}H_{31}N_2OPPd$: C, 66.41; H, 4.94; N, 4.43. Found: C, 66.32; H, 4.85; N, 4.51. Selected IR data: ν (cm^{-1}) = 1599, 1587 (C=N–C=N). UV-Vis in Me_2NCHO: λ_{max} (nm) (ε (10^3 M^{-1} cm^{-1})) = 392^{sh} (2.2), 373 (2.5), 318 (4.9), 290^{sh} (5.7). ^{1}H NMR in $CDCl_3$: δ (ppm) ($J_{H\text{-}H}$ (Hz)) = 8.75 (10) (d, 1H, H^{10}), 8.16 (6) (d, 2H, H^{13}, H^{17}), 7.73–7.68 and 7.52–7.39 (m, m, 7H, 11H, $H^{14–16}$, PPh_3), 6.85 (s, 1H, H^3), 6.65 (s, 1H, H^5), 3.05 (4) (d, 2H, metallated-CH_2), 2.54 (s, 3H, *o*-Me), 2.24 (s, 3H, *p*-Me). ^{31}P NMR in $CDCl_3$: δ (ppm) = 31.67 (s).

2.2.8. Synthesis of [Pd(L^2)(PPh_3)] (4)

This complex was synthesized in acetone medium using one mole equivalent of **2** (132 mg, 0.3 mmol) and two mole equivalents of PPh_3 (158 mg, 0.6 mmol) by following the same procedure as described for **3** in the preceding section. Yield: 155 mg (77%). Anal. Calcd for $C_{36}H_{33}N_2O_2PPd$: C, 65.21; H, 5.02; N, 4.22. Found: C, 65.12; H, 5.08; N, 4.26. Selected IR data: ν (cm^{-1}) = 1597, 1575 (C=N–C=N). UV-Vis in Me_2NCHO: λ_{max} (nm) (ε (10^3 M^{-1} cm^{-1})) = 395^{sh} (1.8), 370 (2.0), 315^{sh} (4.9), 290^{sh} (5.2). ^{1}H NMR in $CDCl_3$: δ (ppm) ($J_{H–H}$ (Hz)) = 8.72 (11) (d, 1H, H^{10}), 8.11 (8) (d, 2H, H^{13}, H^{17}), 7.71–7.66 and 7.57–7.44 (m, m, 9H, 6H, PPh_3), 6.91 (9) (d, 2H, H^{14}, H^{16}), 6.83 (s, 1H, H^3), 6.63 (s, 1H, H^5), 3.86 (s, 3H, OMe), 3.03 (6) (d, 2H, metallated-CH_2), 2.52 (s, 3H, *o*-Me), 2.23 (s, 3H, *p*-Me). ^{31}P NMR in $CDCl_3$: δ (ppm) = 32.69 (s).

2.2.9. Synthesis of [Pd_2(μ-dppb)(L^1)$_2$] (5)

To a suspension of [Pd(HL^1)Cl] (**1**) (122 mg, 0.3 mmol) in 20 ml acetone 1,4-bis(diphenylphosphino)butane (dppb) (66 mg, 0.15 mmol) was added and stirred at room temperature for one day. The yellow solid separated was collected by filtration. It was dissolved in minimum amount of dichloromethane and added to a silica gel column packed with *n*-hexane. The major yellow band eluted with *n*-hexane-ethylacetate (4:1) was evaporated to dryness and the complex thus obtained was collected as a yellow solid. Yield: 128 mg (73%). Anal. Calcd for $C_{62}H_{60}N_4O_2P_2Pd_2$: C, 63.76; H, 5.18; N, 4.80. Found: C, 63.78; H, 5.41; N, 4.65. Selected IR data: ν (cm^{-1}) = 1594 (br) (C=N–C=N). UV-Vis in Me_2NCHO: λ_{max} (nm) (ε (10^3 M^{-1} cm^{-1})) = 400^{sh} (1.4), 370 (1.9), 315 (2.9), 278^{sh} (3.9). ^{1}H NMR in $CDCl_3$: δ(ppm) ($J_{H\text{-}H}$ (Hz)) = 8.71 (11) (d, 1H, H^{10}), 8.13 (7) (d, 2H, H^{13}, H^{17}), 7.73–7.68 (m, 3H, H$^{14–16}$), 7.46–7.28 (m, 10H, PPh_2), 6.81 (s, 1H, H^3), 6.69 (s, 1H, H^5), 2.91 (6) (d, 2H, metallated-CH_2), 2.52 (s, 3H, *o*-Me), 2.45 (br, s, 2H, PCH_2), 2.20 (s, 3H, *p*-Me), 1.91 (br, s, 2H, CCH_2). ^{31}P NMR in $CDCl_3$: δ(ppm) = 24.06 (s).

2.2.10. Synthesis of [Pd$_2$(μ-dppb)(L^2)$_2$] (6)

This complex was synthesized in acetone medium using [Pd(HL^2)Cl] (**2**) (132 mg, 0.3 mmol) and dppb (66 mg, 0.15 mmol) by following the same procedure as described above for **5**. Yield: 138 mg (75%). Anal. Calcd for $C_{64}H_{64}N_4O_4P_2Pd_2$: C, 62.60; H, 5.25; N, 4.56. Found: C, 62.48; H, 5.31; N, 4.46. Selected IR data: ν (cm^{-1}) = 1595, 1574 (C=N–C=N). UV-Vis in Me_2NCHO: λ_{max} (nm) (ε (10^3 M^{-1} cm^{-1})) = 393^{sh} (1.8), 375 (1.9), 356^{sh} (1.8), 314^{sh} (5.1), 298 (5.4). ^{1}HNMR in $CDCl_3$: δ(ppm) ($J_{H\text{-}H}$ (Hz)) = 8.68 (12) (d, 1H, H^{10}), 8.10 (8) (d, 2H, H^{13}, H^{17}), 7.74–7.68 and 7.48–7.39 (m, m, 4H, 6H, PPh_2), 6.90 (s, 1H, H^3), 6.82 (8) (d, 2H, H^{14}, H^{16}), 6.69 (s, 1H, H^5), 3.80 (s, 3H, OMe), 2.91 (6) (d, 2H, metallated-CH_2), 2.51 (s, 3H, *o*-Me), 2.46 (br, s,

2H, PCH_2), 2.19 (s, 3H, *p*-Me), 1.92 (br, s, 2H, CCH_2). ^{31}P NMR in $CDCl_3$: δ (ppm) = 26.92 (s).

2.2.11. Synthesis of [Pd_2(μ-dppf)(L^2)$_2$] (7)

A mixture of [Pd(HL^2)Cl] (**2**) (132 mg, 0.3 mmol) and 1,1'-bis(diphenylphosphino)-ferrocene (dppf) (84 mg, 0.15 mmol) in 20 ml acetone was stirred at room temperature for 1 day. The orange-red solid precipitated was filtered. The solid obtained was dissolved in minimum amount of di-chloromethane and transferred to a silica gel column packed with *n*-hexane. The major orange-red band obtained by elution with *n*-hexane-ethylacetate (7:3) was evaporated to dryness to collect the complex **7**. Yield: 137 mg (67%). Anal. Calcd for $C_{70}H_{64}FeN_4O_4P_2Pd_2$: C, 62.01; H, 4.76; N, 4.13. Found: C, 61.73; H, 5.12; N, 4.23. Selected IR data: ν (cm^{-1}) = 1600, 1581 (C=N–C=N). UV-Vis in Me_2NCHO: λ_{max} (nm) (ε (10^3 M^{-1} cm^{-1})) = 398^{sh} (0.8), 370^{sh} (1.04), 315^{sh} (3.0), 285^{sh} (4.2). ^{1}HNMR in $CDCl_3$: δ (ppm) ($J_{H\text{-}H}$ (Hz)) = 8.74 (11) (s, 1H, H^{10}), 8.27 (10) (d, 2H, H^{13}, H^{17}), 7.63–7.58 and 7.48–7.31 (m, m, 4H, 6H, PPh_2), 6.98 (8) (d, 2H, H^{14}, H^{16}), 6.82 (s, 1H, H^3), 6.44 (s, 1H, H^5), 4.91 (br, s, 2H, ferrocene *o*-protons), 4.20 (br, s, 2H, ferrocene *m*-protons), 3.90 (s, 3H, OMe), 2.84 (6) (d, 2H, metallated-CH_2), 2.52 (s, 3H, *o*-Me), 2.20 (s, 3H, *p*-Me). ^{31}P NMR in $CDCl_3$: δ (ppm) = 23.81 (s).

2.2.12. X-ray crystallography

Diethyl ether vapor diffusion into the dimethylformamide solutions of **1** and **2** provided their single crystals as **1**·Me_2NCHO and **2**·Me_2NCHO, respectively. Single crystals of **3**–**7** were grown as it is without any solvent molecule by slow evaporation of the corresponding acetonitrile or acetonitrile-chloroform

(1:1) or acetonitrile-methanol (1:1) solutions. An Oxford Diffraction Xcalibur Gemini single crystal X-ray diffractometer was used to determine the unit cell parameters and intensity data collection for **1**·Me_2NCHO, **3** and **4** at 298 K. Data collection, reduction and absorption correction were performed using the CrysAlisPro software [8]. Unit cell parameters and intensity data for **2**·Me_2NCHO and **5**–**7** at 298 K were obtained with the help of a Bruker-Nonius SMART APEX CCD single crystal diffractometer. The SMART and the SAINT-Plus packages [9] were used for data acquisition and data extraction, respectively. The absorption corrections were performed with the help of SADABS program [10]. Each structure was solved by direct method and refined on F^2 by full-matrix least-squares procedures. All non-hydrogen atoms were refined anisotropically. The hydrogen atoms were added at geometrically idealized positions and refined using a riding model. Structure solution and refinement were performed using the SHELX-97 programs [11] available in the WinGX suite [12]. The Platon [13] and the Mercury [14] packages were used for graphical representations of thermal ellipsoid plots. Selected crystal data and refinement summary for **1–4** are listed in Table 2.1 and those of **5–7** are listed in Table 2.2. X-ray crystallographic data have been deposited with Cambridge Crystallographic Data Center. Deposition numbers are CCDC 1438903**–**1438909 for **1**·Me_2NCHO, **2**·Me_2NCHO and **3–7** respectively.

2.3. Results and discussion

2.3.1. Synthesis and some properties

4-R-*N′*-(mesitylidene)benzohydrazides (H_2L^1 (R = H) and H_2L^2 (R = OMe) were prepared in ~80% yields by condensation reactions of equimolar amounts mesitaldehyde and the corresponding 4-*R*-benzohydrazides in methanol in presence of a few drops of acetic acid [6–9]. Complexes [Pd(HL^n)Cl] (**1** and **2**) were synthesized in ~77% yields by reacting equimolar amounts of

$Li_2[PdCl_4]$ (prepared in situ), H_2L^n and $NaOAc{\cdot}3H_2O$ in methanol (Scheme 2.1). Treatment of one mole equivalent of $[Pd(HL^n)Cl]$ (**1** and **2**) with two mole equivalents of PPh_3 in acetone leads to the formation of $[Pd(L^n)(PPh_3)]$ (**3** and **4**) in ~76% yields. The dinuclear complexes $[Pd_2(\mu\text{-dppb})(L^n)_2]$ (**5** and **6**) and $[Pd_2(\mu\text{-dppf})(L^2)_2]$ (**7**) have been synthesized in ~76 and 67% yields, respectively by reacting the corresponding chloropalladacycles (**1** and **2**) and the diphosphines in 2:1 mole ratio in acetone. It is very likely that the basic environment created by the phosphine ligands causes the deprotonation of the O-coordinated amide functionality of $(HL^n)^-$ in $[Pd(HL^n)Cl]$. As a result, O-coordinated amide functionality of $(HL^n)^-$ in $[Pd(HL^n)Cl]$. As a result, the Pd-O bond becomes

Table 2.1. Selected crystallographic data for **1**·Me_2NCHO, **2**·Me_2NCHO, **3** and **4**

Complex	**1**·Me_2NCHO	**2**·Me_2NCHO	**3**	**4**
Chemicalformula	$C_{20}H_{24}ClN_3O_2Pd$	$C_{21}H_{26}ClN_3O_3Pd$	$C_{35}H_{31}N_2OPPd$	$C_{36}H_{33}N_2O_2P$
Formula weight	480.27	510.30	632.99	663.01
Crystal system	Tetragonal	Triclinic	Triclinic	Triclinic
λ (Å)	0.71073	0.71073	0.71073	1.54184
Space group	$P4_2/n$	$P\bar{1}$	$P\bar{1}$	$P\bar{1}$
a (Å)	21.2416(12)	8.8606(15)	10.1810(10)	11.2743(5)
b (Å)	21.2416(12)	10.4866(18)	10.6238(11)	11.6592(4)
c (Å)	8.9657(8)	12.161(2)	15.0361(16)	12.1481(6)
α (°)	90	97.028(2)	77.012(9)	78.199(4)
β (°)	90	97.606(2)	71.360(9)	76.926(4)
γ (°)	90	102.758(2)	72.926(9)	82.581(4)
V (Å^3), Z	4045.4(5), 8	1078.8(3), 2	1457.6(3), 2	1516.83(11), 2
ρ_{calcd} (g cm^{-3})	1.577	1.571	1.442	1.452
μ (mm^{-1})	1.069	1.011	0.722	5.708
Refl. collected	7685	10216	10048	10500
Refl. unique	3569	3792	5128	5709
Refl. [$I \geq 2\sigma(I)$]	2002	3687	4150	5056
Parameters	248	267	363	382
$R1$,$wR2$ [$I \geq 2\sigma(I)$]	0.0560, 0.0661	0.0415, 0.1041	0.0381, 0.0691	0.0384, 0.0950
$R1$, $wR2$ [all data]	0.1160, 0.0834	0.0430, 0.1050	0.0531, 0.0749	0.0450, 0.1005
GOF on F^2	0.961	1.246	1.024	1.048
Max./Min. $\Delta\rho$ (e Å^{-3})	0.593/–0.492	0.954/–0.566	0.381/–0.390	0.779/–0.731

Table 2.2. Selected crystallographic data for **5**, **6** and **7**

Complex	**5**	**6**	**7**
Chemicalformula	$C_{62}H_{60}N_4O_2P_2Pd$	$C_{64}H_{64}N_4O_4P_2Pd_2$	$C_{70}H_{64}N_4O_4P_2FePd$
Formula weight	1167.88	1227.93	1355.84
Crystal system	Triclinic	Triclinic	Triclinic
λ (Å)	0.71073	0.71073	0.71073
Space group	$P\bar{1}$	$P\bar{1}$	$P\bar{1}$
a (Å)	9.4748(10)	9.2761(19)	9.4603(8)
b (Å)	11.8957(12)	12.497(3)	10.9537(10)
c (Å)	12.6851(13)	12.821(3)	15.2313(13)
α (°)	84.284(2)	87.01(3)	98.929(1)
β (°)	72.879(2)	79.49(3)	95.113(1)
γ (°)	76.109(2)	76.29(3)	105.100(1)
V (Å^3), *Z*	1325.8(2), 1	1419.6(5), 1	1491.4(2), 1
ρ_{calcd} (g cm^{-3})	1.463	1.436	1.510
μ (mm^{-1})	0.787	0.741	0.944
Refl. collected	12823	13582	14415
Refl. unique	4648	4971	5229
Refl. [$I \geq 2\sigma(I)$]	4272	4268	4776
Parameters	327	345	379
*R*1,*wR*2 [$I \geq 2\sigma(I)$]	0.0259, 0.0698	0.0475, 0.1253	0.0274, 0.0720
*R*1, *wR*2 [all data]	0.0284, 0.0711	0.0550, 0.1327	0.0304, 0.0737
GOF on F^2	1.068	1.078	1.058
Max./Min. $\Delta\rho$ (eÅ^{-3})	0.420/–0.232	1.082/–0.366	0.407/–0.268

stronger (*vide infra*) and facilitates the formation of **3**–**7** via replacement of the labile chloride from the coordination environment by the phosphine P-atom. The elemental (CHN) analysis data of **1**–**7** are in good agreement with the corresponding molecular formulas. As expected for square-planar palladium(II) species all the complexes are diamagnetic in nature. Both **1** and **2** are highly soluble in dimethylformamide and dimethyl sulfoxide, while sparingly soluble in dichloromethane and chloroform. In contrast, **3**–**7** are highly soluble in dimethylformamide, dimethyl sulfoxide, dichloromethane and chloroform and moderately soluble in acetonitrile. The solution colors are light-yellow to yellow. All the complexes are electrically non-conducting in solution.

2.3.2. Spectroscopic characterization

2.3.2.1. Infrared spectra

Infrared spectra of the 4-R-*N′*-(mesitylidene)benzohydrazides (H_2L^n) and their complexes **1**–**7** in KBr pellets were recorded in the range 4000 to 400 cm^{-1}. Three representative spectra are illustrated in Figures 2.1–2.3. Each of these spectra shows several bands of various intensities. We have not tried to assign all the bands except for the following selected few. The spectra of H_2L^n display the N–H and the C=O stretches at ~3210 and ~1650 cm^{-1}, respectively. A medium intensity band observed at ~1605 cm^{-1} is assigned to the C=N stretching of the free H_2L^n. The chloropalladacycles **1** and **2** show a weak broad band at ~3186 cm^{-1} and a sharp strong band at 1606 cm^{-1}. These two bands are attributed to the N–H and the C=O stretches, respectively of the O-coordinated amide functionality of $(HL^n)^-$. In contrast, none of the phosphinopalladacycles **3**–**7** shows any such band. Absence of these bands indicates the deprotonation of the amide functionality of the corresponding ligands $(L^n)^{2-}$ in **3**–**7**. Both **1** and **2** display a sharp and strong band at 1562 cm^{-1} due to the metal coordinated

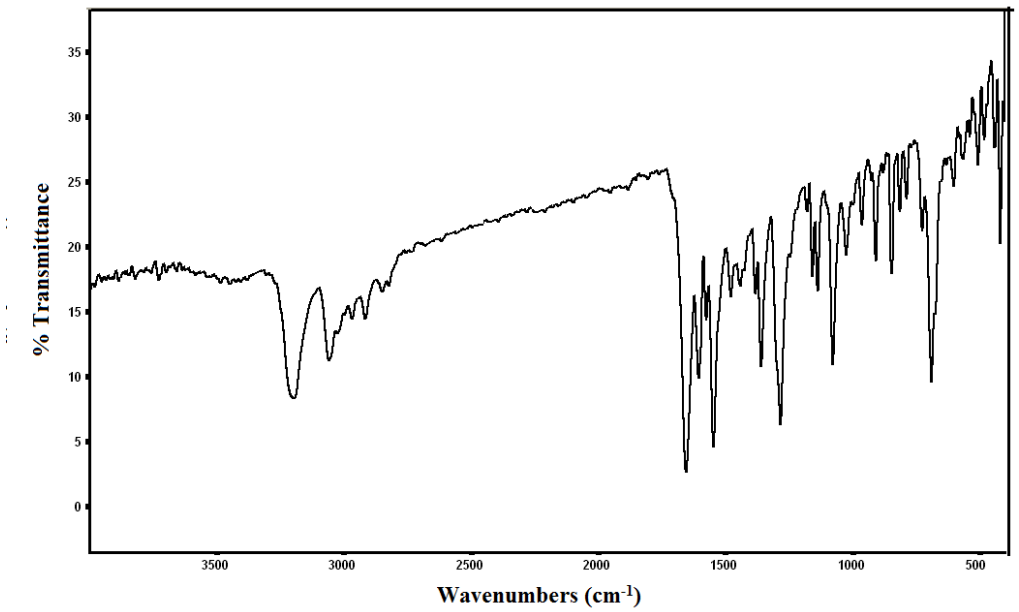

Figure 2.1. Infrared spectrum of H_2L^1

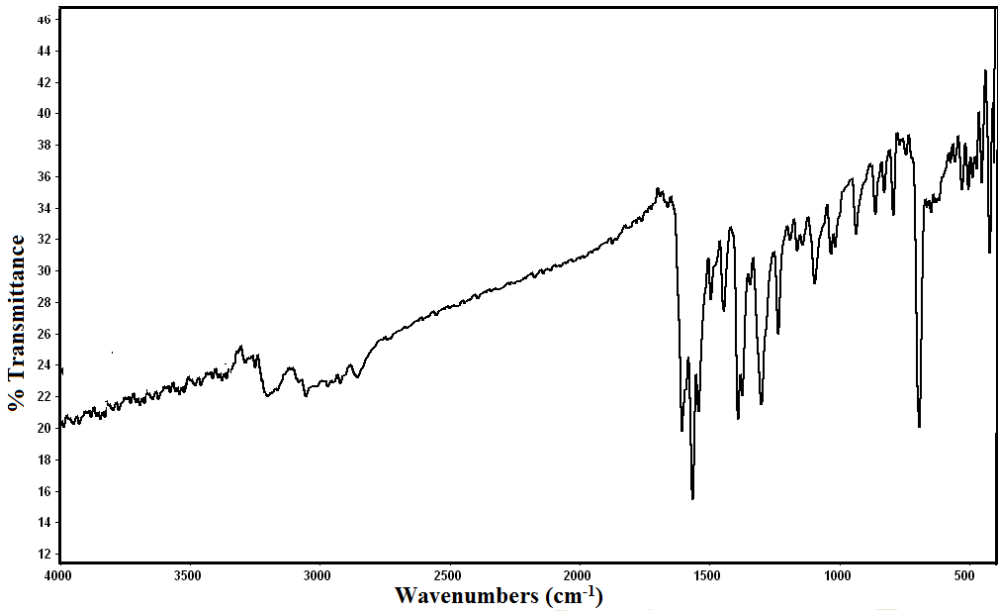

Figure 2.2. Infrared spectrum of [Pd(HL^1)Cl] (**1**)

C=N stretching. On the other hand, a broad band at 1594 cm^{-1} is observed for **5**, while the remaining phosphinopalladacycles (**3**, **4**, **6** and **7**) show two closely spaced sharp bands at ~1598 and ~1579 cm^{-1}. These bands are assigned to the one end coordinated conjugated C=N–N=C moiety of the ligand $(L^n)^{2-}$ in **3**–**7**. Three strong bands appeared in the ranges 752–732, 698–682 and 533–517 for **3**–**7** are most likely associated with the ancillary phosphine lig-

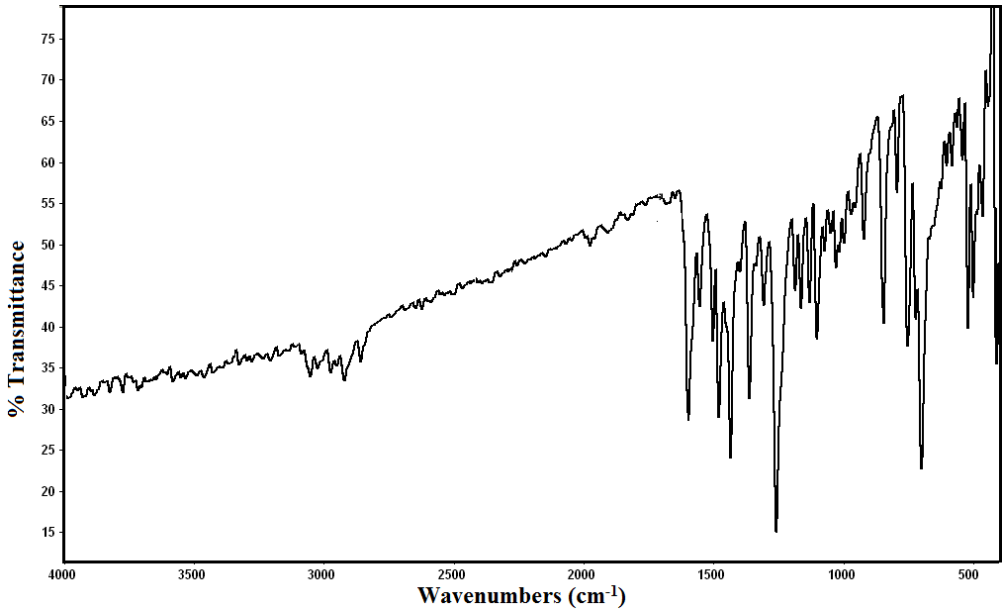

ands in them [1–4, 18].

Figure 2.3. Infrared spectrum of $[Pd_2(\mu\text{-dppf})(L^2)_2]$ (**7**)

2.3.2.2. Electronic spectra

Electronic spectra of H_2L^n and **1**–**7** were collected using their corresponding dimethylformamide solutions. Representative spectra are shown in Figure 2.4. A broad intense band centered at 300 nm appeared in the spectra of both H_2L^1 and H_2L^2. In contrast, the complexes (**1**–**7**) display an absorption peak at ~370 nm with a shoulder on the right side at ~395 nm. On the left side of this peak,

only **1**, **2** and **6** display another shoulder at ~356 nm. In the UV-range, **1** shows a broad shoulder centered at ~305 nm, while the remaining complexes (**2**–**7**) exhibit a strong absorption peak or shoulder centered within 328–314 nm and a second intense peak or shoulder in the range 290–278 nm. It is very likely that the absorptions centered at ~370 nm are associated with ligand to metal charge transfer transitions [18,19], while the remaining higher energy bands are due to predominantly ligand centered transitions.

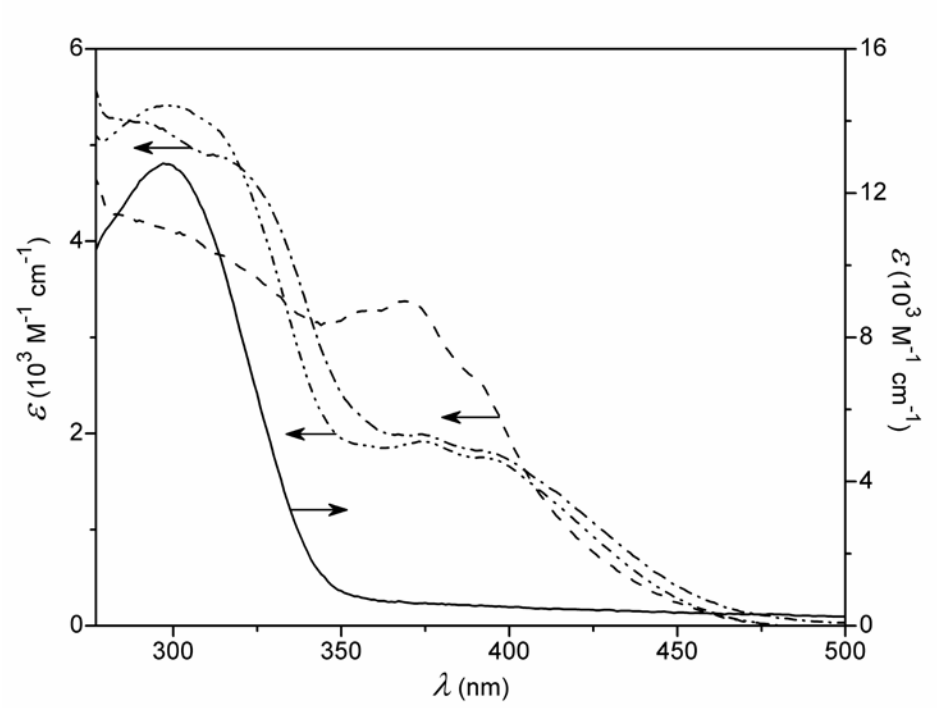

Figure 2.4. Electronic spectra of H_2L^1 (——), [Pd(HL^1)Cl] (**1**) (– – –), [Pd(L^2)(PPh_3)] (**4**) –(–··–), and [Pd $_2$(μ-dppb)(L^2)$_2$] (**6**) –(–···–) in dimethylformamide.

2.3.2.3. NMR spectra

The ^{1}H NMR spectra of the free Schiff bases (H_2L^1 and H_2L^2) and their complexes (**1**–**7**) were recorded in $(CD_3)_2SO$ and $CDCl_3$, respectively using

tetramethylsilane as the internal standard. Four representative ^{1}H NMR spectra are shown in Figures 2.5–2.8 and two $^{31}P\{^{1}H\}$ spectra are shown in Figures 2.9 and 2.10. The spectra of the dinuclear complexes **5**–**7** clearly indicate that in each complex both halves are equivalent as observed in the corresponding X-ray structures. The chemical shift data with the tentative assignments for each compound are listed in the experimental section. The amide N–H proton in H_2L^1 and H_2L^2 resonates as a sharp singlet at δ 11.72 and 11.62 ppm, respectively. A weak and broad signal observed at δ 11.68 and 11.59 ppm for **1** and **2**, respectively is assigned to the amide N–H proton of their corresponding ligands $(HL^n)^-$. Absence of any such signal for **3**–**7** is consistent with the deprotonated state of the amide functionalities of the ligands$(L^n)^{2-}$ in them. The azomethine (CH=N) proton of H_2L^1, H_2L^2 and the corresponding chloropalladacycles (**1** and **2**) appears as a sharp singlet in the range δ 8.75–8.80 ppm. In contrast, complexes **3**–**7** containing P-donor mono- or diphosphine ancillary ligands display the azomethine proton as a doublet within δ 8.68–8.75 ppm (J = 10–12 Hz) due to its coupling with ^{31}P. A two-proton doublet (J = 6–10 Hz) corresponding to the aroyl ring protons H^{13} and H^{17} appears at δ ~7.97 ppm for H_2L^1, H_2L^2 and the chloropalladacycles **1** and **2**, whereas the doublet resonance is somewhat downfield (δ 8.10–8.27 ppm) for the mono- or diphosphine containing **3**–**7**, perhaps due to deshielding by the neighboring phenyl rings of the phosphine ligands. The H^{14-16} in H_2L^1 and **5** are observed as a three-proton multiplet (δ 7.73–7.49 ppm), while for **3** the corresponding multiplet coincides with the multiplets (δ 7.73–7.39 ppm) due to the PPh_3 protons. However, for **1**, H^{15} appears as a broad singlet at δ 7.69 ppm and H^{14} and H^{16} resonate as a two-proton multiplet centered at δ ~7.61 ppm. The H^{14} and H^{16} in H_2L^2 and its complexes **4**, **6** and **7** appear as a two-proton doublet within δ 6.82–7.07 ppm (J ~ 8 Hz), whereas, due to overlap of the signals from these two protons and the mesityl

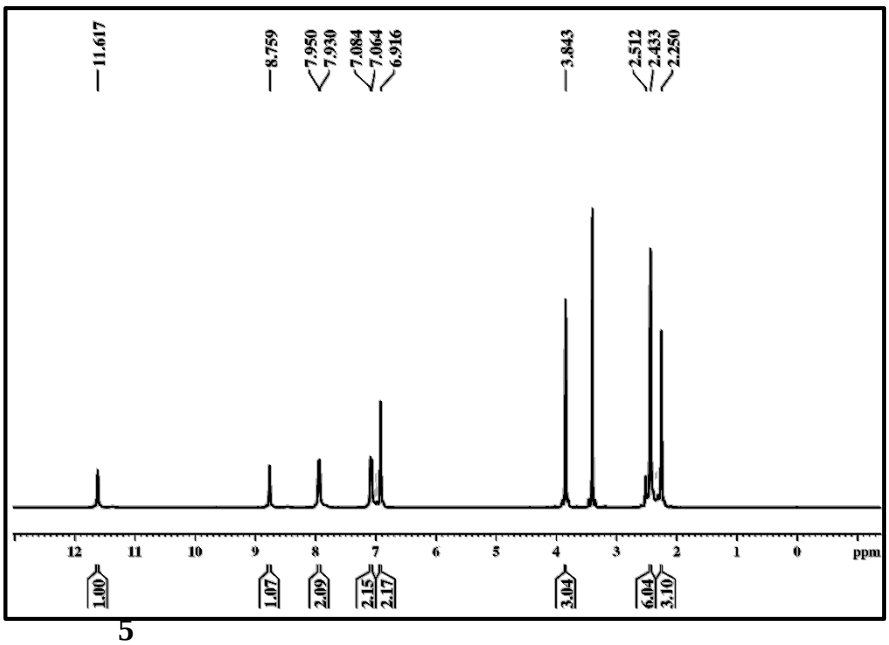

5

. ^{1}H-NMR spectrum of H_2L^2

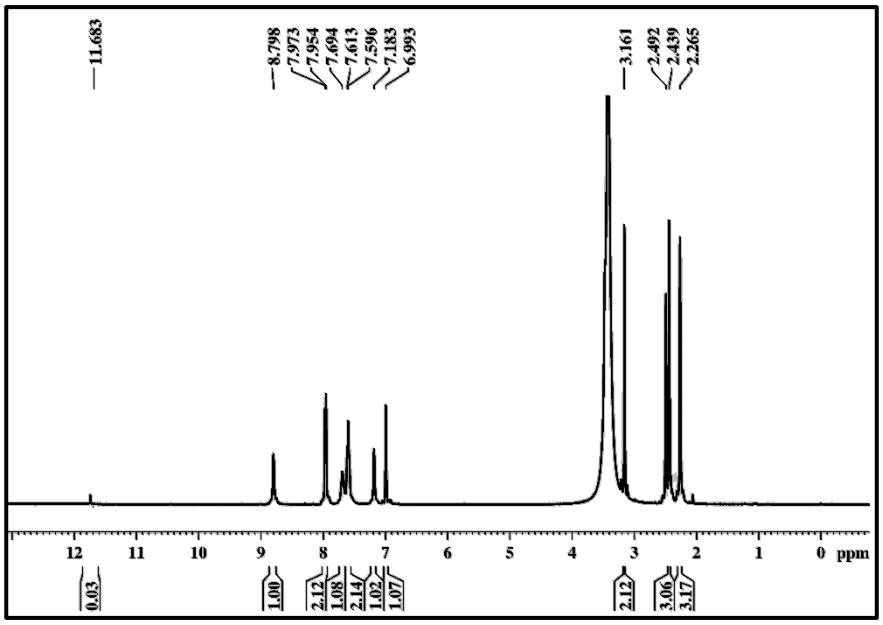

Figure 2.6. ^{1}H-NMR spectrum of [Pd(HL^{1})Cl] (**1**)

ring protons H^3 and H^5 a four-proton multiplet centered at δ ~7.61 ppm is observed for **2**. A three-proton singlet observed for H_2L^2, **2**, **4**, **6** and **7** within δ 3.80–3.90 ppm is assigned to the protons of the group of their *p*-anisoyl moiety. H_2L^1 and H_2L^2 exhibit a two-proton singlet at δ ~6.91 ppm due to the mesityl group ring protons H^3 and H^5. However, due to metallation of one of the mesityl *ortho*-methyl groups, H^3 and H^5 resonate separately as singlets in the ranges δ 7.18–6.81 and 6.99–6.44 ppm, respectively in all the complexes except for **2**, where these resonances overlap with that for H^{14} and H^{16} (*vide supra*). A six-proton singlet observed at δ ~2.42 ppm for H_2L^1 and H_2L^2 is assigned to the protons of the two *ortho*-methyl groups of their mesityl fragment. In contrast, in all the complexes (**1**–**7**) this signal splits into a two-proton signal for the metallated-CH_2 protons and a three-proton signal for the unchanged *ortho*-methyl protons. The metallated-CH_2 protons resonate as a singlet at δ ~3.17 ppm in the chloropalladacycles **1** and **2**, respectively, whereas they appear as a doublet within δ 2.84–3.05 ppm (J = 4–6 Hz) due to coupling with ^{31}P in the mono- and diphosphine coordinated complexes **3**–**7**. The unchanged *ortho*-methyl protons resonate as a singlet in the range δ 2.44–2.54 ppm for all the complexes. The three-proton singlet corresponding to the mesityl *para*-methyl protons of H_2L^1, H_2L^2 and complexes **1**–**7** appears within the narrow chemical shift range of δ 2.19–2.29 ppm. Two broad two-proton singlets observed at δ ~2.46 and ~1.92 ppm for the dppb bridged dinuclear complexes **5** and **6** are attributed to the P–CH_2–C and C–CH_2–C protons, respectively. In **7**, the *ortho*- and *meta*-protons of the ferrocene fragment appear as two broad two-proton singlets at δ 4.91 and 4.20 ppm, respectively. The ^{31}P NMR spectra of the complexes having PPh_3, dppb and dppf as ancillary ligands (**3**–**7**) have been also recorded using phosphoric acid as the external standard. A singlet resonance line is displayed by each of these complexes. The signal for the mononuclear complexes **3** and **4** containing

PPh_3 appears at δ 31.67 and 32.69 ppm, respectively, whereas for the dinuclear complexes (**5**–**7**) with the diphosphine ligands (dppb and dppf) it is observed in the relatively upfield chemical shift range of δ 23.81–26.92 ppm.

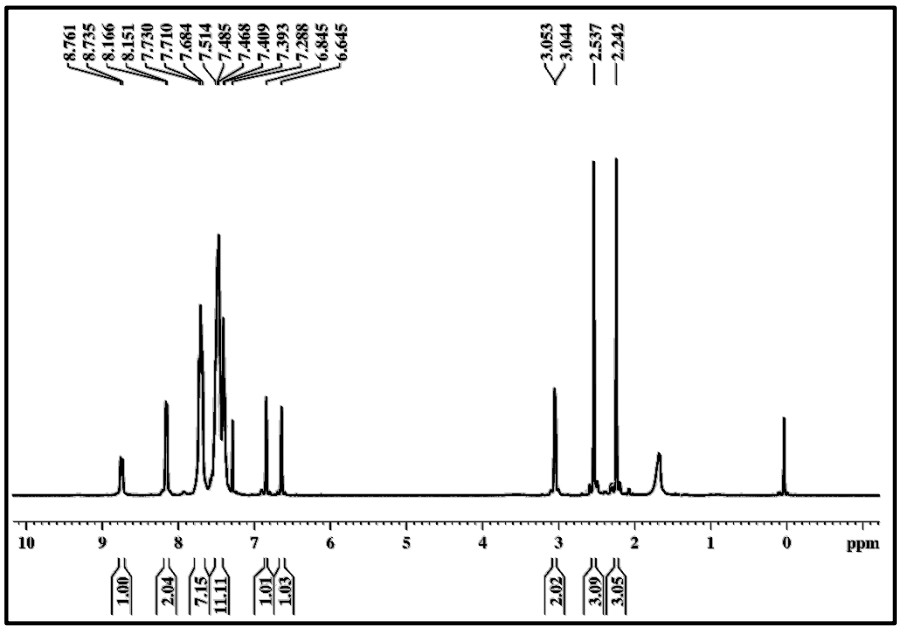

Figure 2.7. ^{1}H-NMR spectrum of [Pd(L^1)(PPh_3)] (**3**)

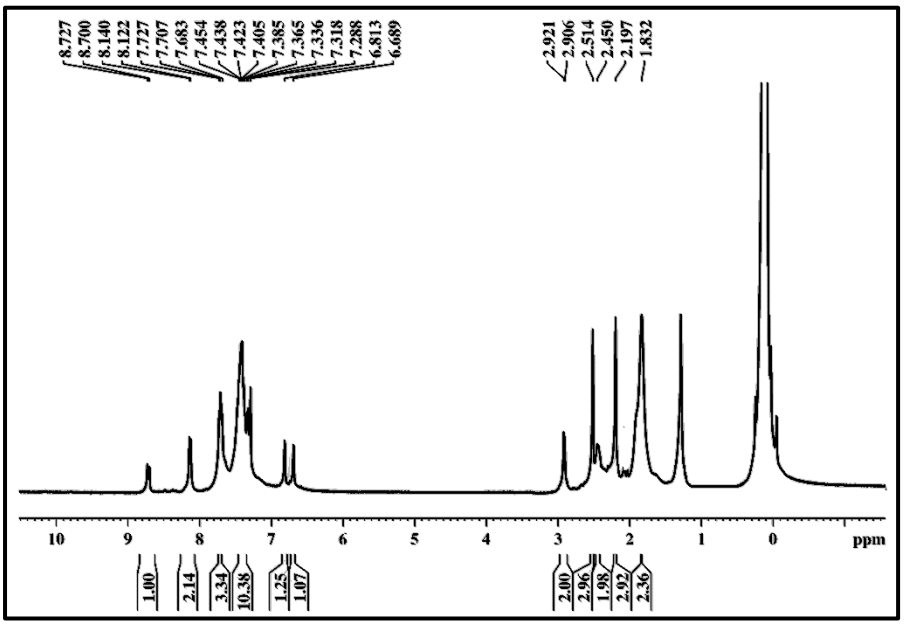

Figure 2.8. ^{1}H-NMR spectrum of [Pd_2(μ-dppb)(L^1)$_2$] (**5**)

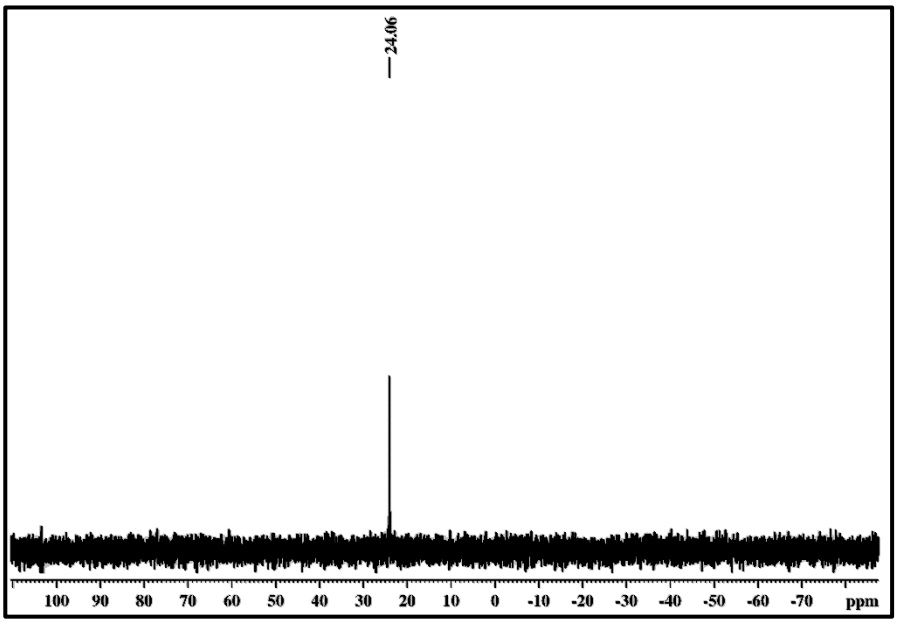

Figure 2.9. ^{31}P{^{1}H} -NMR spectrum of [Pd_2(μ-dppb)(L^1)$_2$] (**5**)

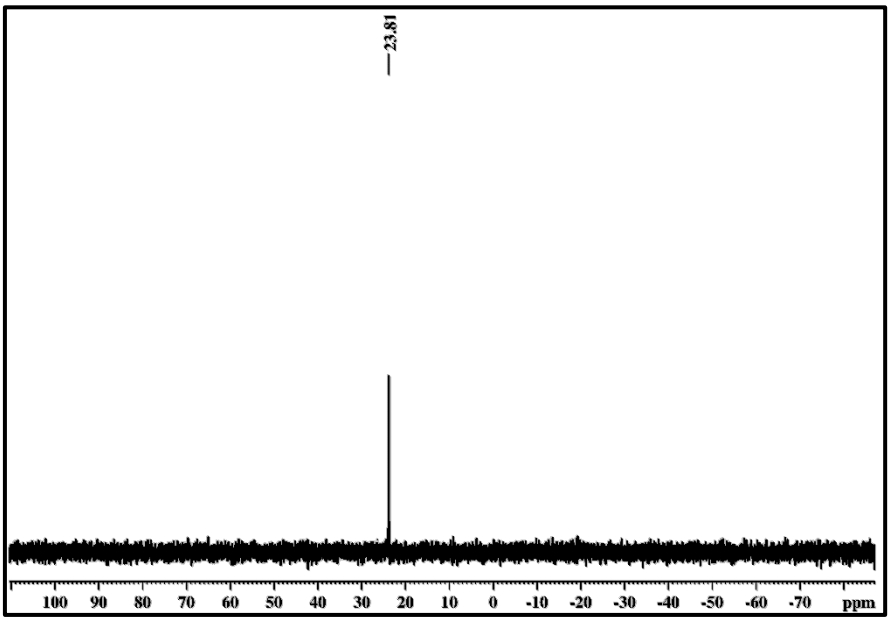

Figure 2.10. ^{31}P{^{1}H} -NMR spectrum of [Pd_2(μ-dppf)(L^2)$_2$] (**7**)

2.3.3. X-ray molecular structures

The structures of the solvated chloropalladacycles [Pd(HL^n)Cl]·Me_2NCHO (**1**·Me_2NCHO and **2**·Me_2NCHO) are illustrated in Figures 2.11 while Figures 2.12 depicts the structures of the triphenylphosphinopalladacycles [Pd(L^n)(PPh_3)] (**3** and **4**). Perspective views of the dinuclear complexes [Pd_2(μ-dppb)(L^n)$_2$] (**5** and **6**) and [Pd_2(μ-dppf)(L^2)$_2$] (**7**) obtained using the bridging diphosphine ligands 1,4-bis(diphenylphosphino)butane (dppb) and 1,1'-bis(diphenylphosphino)ferrocene (dppf) are shown in Figures 2.13 and 2.14, respectively. Selected bond lengths and bond angles are listed in Table 2.3. In each of **1**·Me_2NCHO and **2**·Me_2NCHO, the metal center is in a square-planar CNOCl coordination environment assembled by the 6,5-membered fused chelate rings forming methylene-C, azomethine-N and amide-O donor (HL^n)$^-$ and a chloride ion. In each of **3**–**7**, (L^n)$^{2-}$ acts as methylene-C, azomethine-N and amidate-O donor, whilst a phosphine-P atom completes a CNOP square-plane around the metal center. Two halves of each of the three dinuclear complex molecules (**5**–**7**) are related by an inversion center (Figures. 2.13 and 2.14). In [Pd(HL^n)Cl]·Me_2NCHO (**1**·Me_2NCHO and **2**·Me_2NCHO), the O-atom of the dimethylformamide molecule is hydrogen bonded with amide N–H group of the ligand (HL^n)$^-$ (Figures 2.11). The N(2)··O(2) distance and the N(2)–H···O(2) angle are 2.783(6) Å and 163º and 2.738(5) Å and 156° for **1**·Me_2NCHO and **2**·Me_2NCHO, respectively. The C(11)–O(1) and C(11)–N(2) bond lengths (Table 2.3) clearly indicate that the amide functionality of (HL^n)$^-$ is protonated in **1** and **2**, while that of (L^n)$^{2-}$ is deprotonated in **3**–**7**. It is expected that the amide-O is an inferior σ-donor than the amidate-O. Thus the longer Pd(1)–O(1) bond lengths in **1** and **2** (2.165(4) and 2.222(3) Å, respectively) than in **3**–**7** (2.107(2)–2.131(2) Å) al-

so corroborate the amide protonation state difference in $(HL^n)^-$ and $(L^n)^{2-}$. The metal to azomethine-N (Pd(1)–N(1)) bond

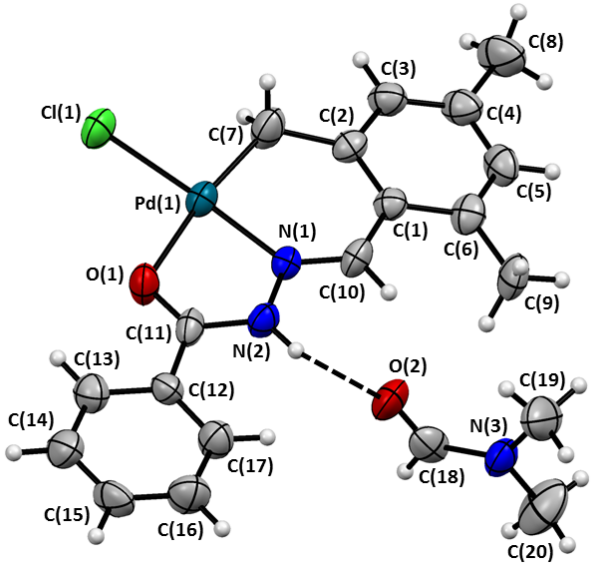

.

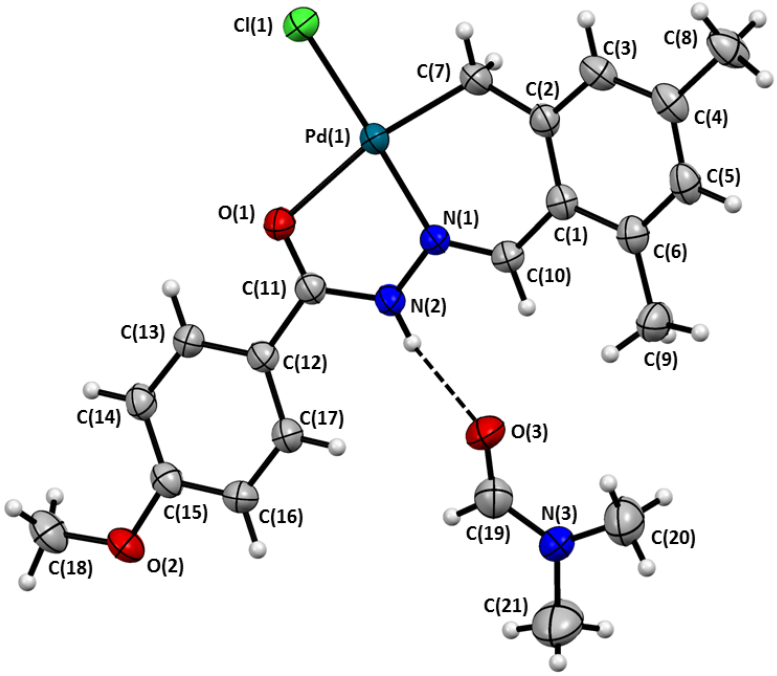

Figure 2.11. Molecular structures of $[Pd(HL^1)Cl]\cdot Me_2NCHO$ (**1**·Me_2NCHO) (top) and $[Pd(HL^2)Cl]\cdot Me_2NCHO$ (**2**·Me_2NCHO) (bottom) with the atom la-

beling schemes. In both structures, all non-hydrogen atoms are shown at their 40% probability thermal ellipsoids.

Table 2.3. Selected bond lengths (Å) and angles (°) for **1**·Me_2NCHO, **2**·Me_2NCHO and **3**–**7**

Complex	**1**·Me_2NCHO	**2**·Me_2NCHO	**3**	**4**	**5**	**6**	**7**
Pd(1)–C(7)	1.940(6)	1.984(4)	2.012(3)	2.045(3)	2.014(2)	2.028(4)	2.031(2)
Pd(1)–N(1)	1.961(4)	1.980(3)	2.003(3)	2.028(3)	2.0243(18)	2.034(3)	2.031(2)
Pd(1)–O(1)	2.165(4)	2.222(3)	2.1066(19)	2.131(2)	2.1134(16)	2.125(3)	2.1065(17)
Pd(1)–Cl(1)/P(1)	2.2910(16)	2.2975(12)	2.2393(9)	2.2582(8)	2.2492(6)	2.2468(12)	2.2502(7)
C(11)–O(1)	1.229(6)	1.233(5)	1.272(4)	1.289(4)	1.284(3)	1.283(5)	1.285(3)
C(11)–N(2)	1.332(7)	1.346(5)	1.318(4)	1.312(5)	1.312(3)	1.310(5)	1.315(3)
C(7)–Pd(1)–N(1)	92.7(2)	90.37(15)	90.35(11)	89.21(12)	90.71(9)	89.17(15)	89.02(9)
C(7)–Pd(1)–O(1)	170.6(2)	165.00(16)	166.43(11)	163.92(13)	165.47(10)	161.55(15)	164.11(9)
C(7)–Pd(1)–Cl(1)/P(1)	90.52(18)	91.09(13)	91.59(10)	94.16(10)	91.94(8)	92.64(12)	93.68(8)
N(1)–Pd(1)–O(1)	78.35(18)	77.63(11)	77.84(9)	77.12(10)	77.87(7)	77.16(12)	77.11(7)
N(1)–Pd(1)–Cl(1)/P(1)	176.79(15)	176.87(9)	175.01(7)	175.98(8)	176.30(5)	176.40(8)	174.57(6)
O(1)–Pd(1)–Cl(1)P(1)	98.44(12)	101.35(8)	100.73(7)	99.85(7)	99.91(5)	101.72(8)	100.79(5)

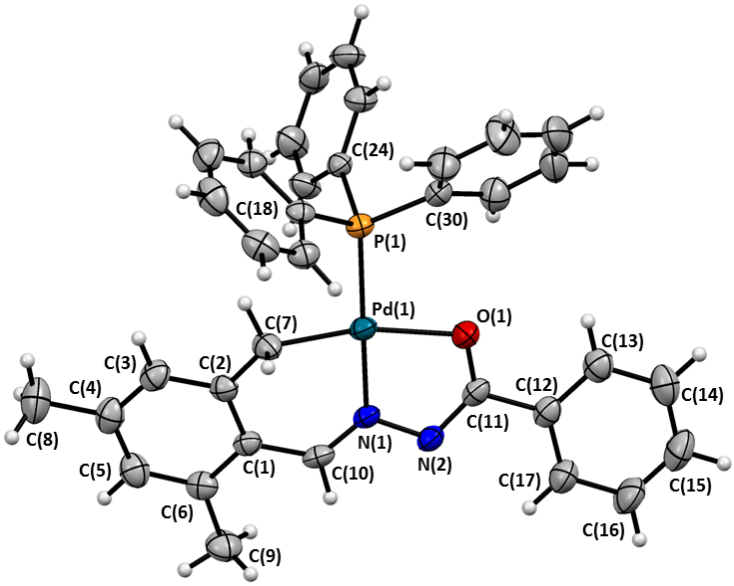
C(24)
C(18)
C(30)
P(1)
Pd(1)
O(1)
C(7)
C(13)
C(3)
C(2)
C(12)
C(4)
C(14)
C(11)
C(8)
N(1)
N(2)
C(5)
C(1)
C(10)
C(17)
C(15)
C(6)
C(16)
C(9)

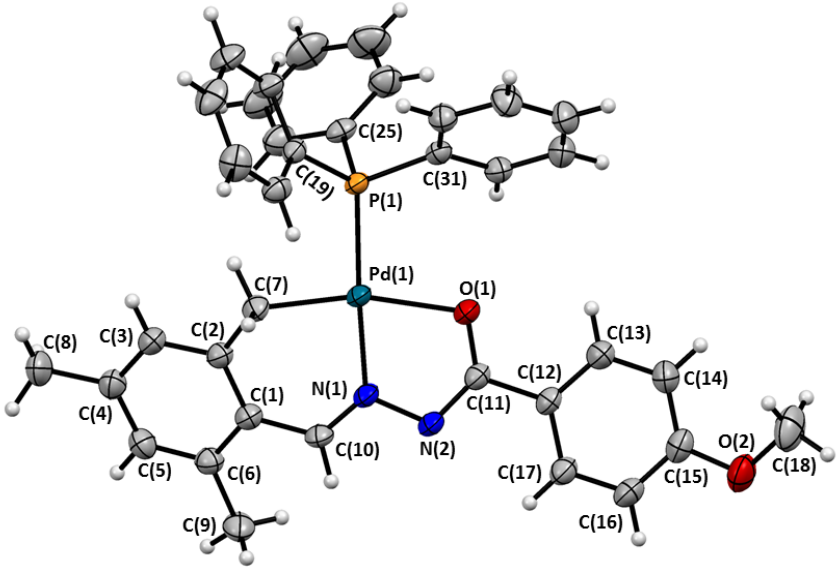
C(25)
C(19)
C(31)
P(1)
Pd(1)
C(7)
O(1)
C(8)
C(3)
C(2)
C(13)
C(12)
C(14)
C(1)
N(1)
C(11)
C(4)
C(10)
N(2)
O(2)
C(18)
C(5)
C(6)
C(17)
C(15)
C(9)
C(16)

Figure 2.12. Molecular structures of [Pd(L^1)(PPh_3)] (**3**) (top) and [Pd(L^2)(PPh_3)] (**4**) (bottom) with the atom labeling schemes. In both structures, all non-hydrogen atoms are shown at their 40% probability thermal ellipsoids.

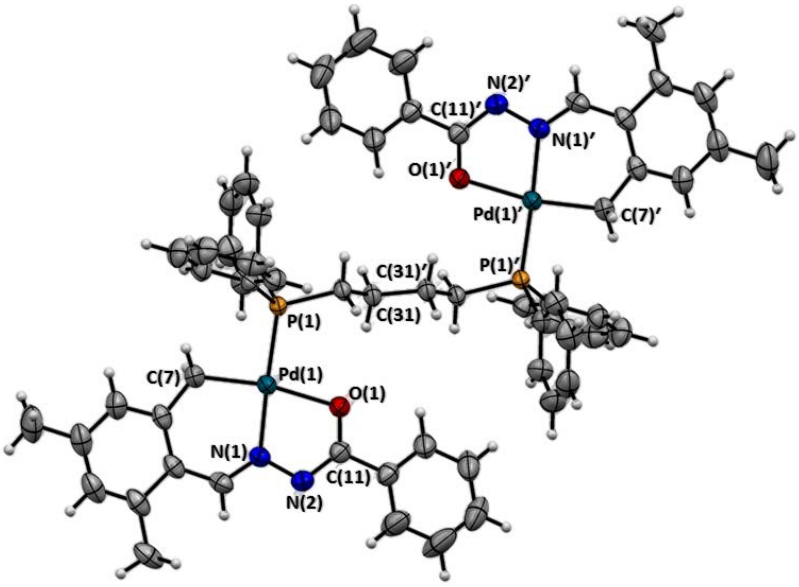

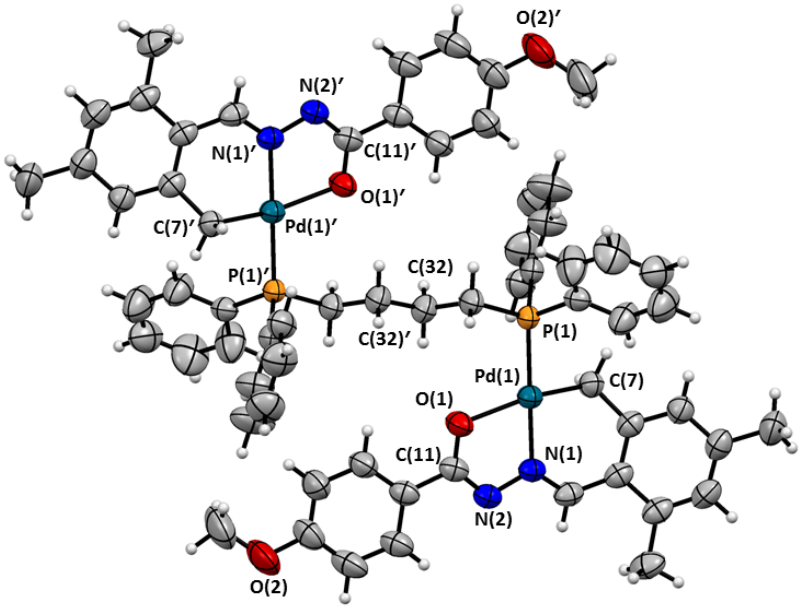

Figure 2.13. Molecular structures of $[Pd_2(\mu\text{-dppb})(L^1)_2]$ (**5**) (top) and $[Pd_2(\mu\text{-dppb})(L^2)_2]$ (**6**) (bottom) with the atom labeling schemes. In both structures, all non-hydrogen atoms are shown at their 40% probability thermal ellipsoids.

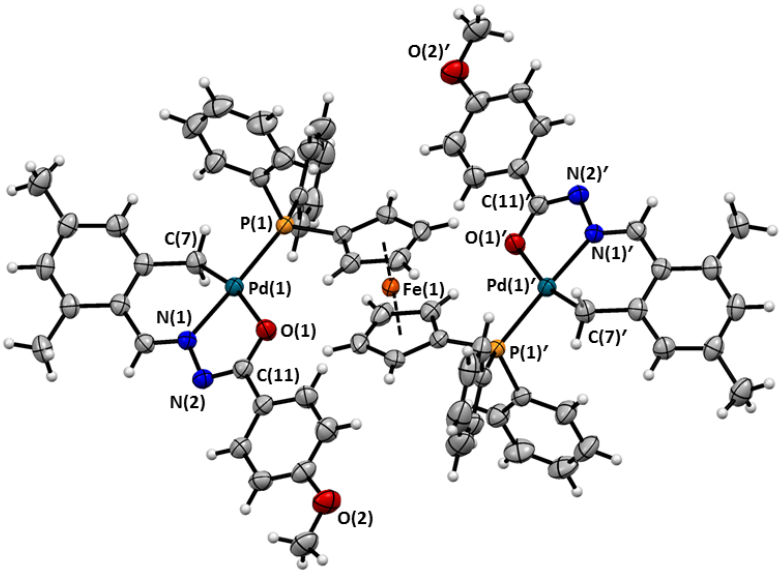

Figure 2.14. Molecular structure of $[Pd_2(\mu\text{-dppf})(L^2)_2]$ (**7**) with the atom labeling schemes. All non-hydrogen atoms are shown at their 40% probability thermal ellipsoids.

lengths in **1** and **2** (1.961(4) and 1.980(3) Å, respectively) are significantly smaller than the corresponding bond lengths in **3**–**7** (2.003(3)–2.034(3) Å). This difference is due to the better *trans*-effect of the phosphine ligand in **3**–**7** than that of the chloride in **1** and **2**. The Fe–C distances in the ferrocene fragment of **7** are unexceptional. In general, the bond lengths associated with the metal ions in all the complexes are comparable with the corresponding bond

lengths observed for palladium(II) complexes having comparable coordinating atoms [2,3,15–17].

2.4. Conclusions

Cylopalladation chemistry of 4-R-*N'*-(mesitylidene)benzohydrazides (H_2L^n) has been investigated. It has been found that the NO-chelating benzohydrazone scaffold of the Schiff base system H_2L^n is able to facilitate the activation of an *ortho*-methyl C(sp^3)–H bond of the pendant mesityl fragment and produce cyclopalladated complexes. A series of mononuclear palladacycles with chloride and triphenyl phosphine as ancillary ligands ([Pd(HL^n)Cl] and [Pd(L^n)(PPh_3)]) and dinuclear palladacycles with bridging diphosphines ([Pd_2(μ-diphos)(L^n)$_2$], diphos = diphosphines) have been isolated. In these palladium(II) complexes, $(HL^n)^-$ and $(L^n)^{2-}$ behave as 6,5-membered fused chelate rings forming methylene-C, azomethine-N and amide- or amidate-O coordinating ligands. The molecular structures of all the complexes have been authenticated by X-ray crystallography. The spectroscopic characteristics of the complexes complement very well the corresponding X-ray molecular structures.

2.5. References

[1] K. Nagaraju, S. Pal, *J. Organomet. Chem*. 745-746 (2013) 404–408.

[2] A.R.B. Rao, S. Pal, *J. Organomet. Chem*. 762 (2014) 58–66.

[3] A.R.B. Rao, S. Pal, *J. Organomet. Chem*. 797 (2015) 96–100.

[4] R.N. Prabhu, S. Pal, *J. Chem. Sci*. 127 (2015) 589–596, and references there in.

[5] D.N. Neogi, A.N. Biswas, P. Das, R. Bhawmick, P. Bandyopadhyay, *J. Organomet. Chem*. 724 (2013) 147–154.

[6] L. Cuesta, E.P. Urriolabeitia, *Comments Inorg. Chem*. 33 (2012) 55–85.

[7] D.D. Perrin, W.L.F. Armarego, D.P. Perrin, Purification of Laboratory Chemicals, second ed. Pergamon, Oxford, 1983.

[8] CrysAlisPro version 1.171.37.34i, Agilent Technologies, Yarnton, Oxfordshire, UK, 2014.

[9] SMART version 5.630 and SAINT-plus version 6.45, Bruker-Nonius Analytical X-ray Systems Inc. Madison, WI, USA, 2003.

[10] G.M. Sheldrick, SADABS, Program for Area Detector Absorption Correction, University of Göttingen, Göttingen, Germany, 1997.

[11] G.M. Sheldrick, *Acta Crystallogr., Sect. A*, 64 (2008) 112–122.

[12] L.J. Farrugia, *J. Appl. Crystallogr*. 45 (2012) 849−854.

[13] A.L. Spek, Platon, A Multipurpose Crystallographic Tool, Utrecht Uni versity, Utrecht, The Netherlands, 2002.

[14] C.F. Macrae, I.J. Bruno, J.A. Chisholm, P.R. Edgington, P. McCabe, E. Pidcock, L. Rodriguez-Monge, R. Taylor, J. van de Streek, P.A. Wood, *J. Appl. Crystallogr*. 41 (2008) 466−470.

[15] A.A. Musaev, B.T. Usubaliev, A.A. Guliev, V.V. Bashilov, V.I. Sokolov, *J. Struct. Chem*. 26 (1985) 643–647.

[16] J. Albert, J. Granell, J. Sales, *Organometallics* 5 (1986) 2567–2568.

[17] J. Nicasio-Collazo, E. Álvarez, J.C. Alvarado-Monzón, G. Andreu-de-Riquer, J.O.C. Jimenez-Halla, L.M. De León-Rodríguez, G. Merino, U. Morales, O. Serrano, J.A. López, *Dalton Trans*. 40 (2011) 12450–12453.

[18] S. Halder, M.G.B. Drew, S. Bhattacharya, *J. Chem. Sci*. 120 (2008) 441–446.

[19] Y.–G. Sun, Y. Guo, D. Sun, M.–C. Zhu, F. Ding, Y.–N. Liu, E.–J. Gao, S.–J. Wang, G. Xiong, I. Dragutan, V. Dragutan, *Eur. J. Inorg. Chem.* (2014) 5741–5751.

Chapter 3

Mono- and dinuclear cyclopalladated complexes as catalysts for Suzuki–Miyaura cross-coupling reactions in predominantly aqueous media[§]

Suzuki–Miyaura cross-coupling reactions of aryl halides with arylboronic acids were performed in predominantly aqueous media employing two mono- and two dinuclear cyclopalladated complexes as catalysts. These complexes are [Pd(HL)Cl] (**I**), [Pd(L)(PPh_3)] (**II**), [Pd_2(μ-dppb)($L)_2$] (**III**) and [Pd_2(μ-dppf)($L)_2$] (**IV**); where H_2L, dppb and dppf represent 4-methoxy-*N*′-(mesitylidene)benzohydrazide, 1,4-bis(diphenylphosphino)butane and 1,1′-bis(diphenylphosphino)ferrocene, respectively. The reactions were conducted using potassium carbonate as base in presence of tetrabutylammonium bromide (TBAB) at 70/90 °C in dimethylformamide–water (1:20) mixture. Among the four catalysts used, the dinuclear complex **IV** turned out to be the most effective and afforded moderate to excellent yields with broad substrate scope.

3.1. Introduction

Since the discovery of Suzuki–Miyaura cross coupling reaction, there is a continuous effort to develop new catalyst systems which will be effective for a wide range of products. Generally organic media are more common for this coupling reaction. However, due to the environmental concerns necessity for the use of the benign solvent water as the medium for chemical reactions is

[§] This work has been published in *Tetrahedron Letters* 58 (2017) 1000–1005.

continuously growing. Thus, in recent times, there is a particular emphasis on the development of catalyst systems that will

be effective for Suzuki–Miyaura cross-coupling reactions in aqueous media [1–6]. So far, among the various catalyst systems used for Suzuki–Miyaura reaction in aqueous or aqueous-organic media, very few are based on cyclopalladated complexes [7–12]. These complexes are either water soluble for use in homogeneous reactions or anchored to silica or nano-particles for applications in heterogeneous reactions. Our group has been working on coordination [13–17] and cyclometallated [18,19] complexes of transition metal ions with Schiff bases and reduced Schiff bases and their applications as catalysts in synthetic organic reactions for the past couple of years.

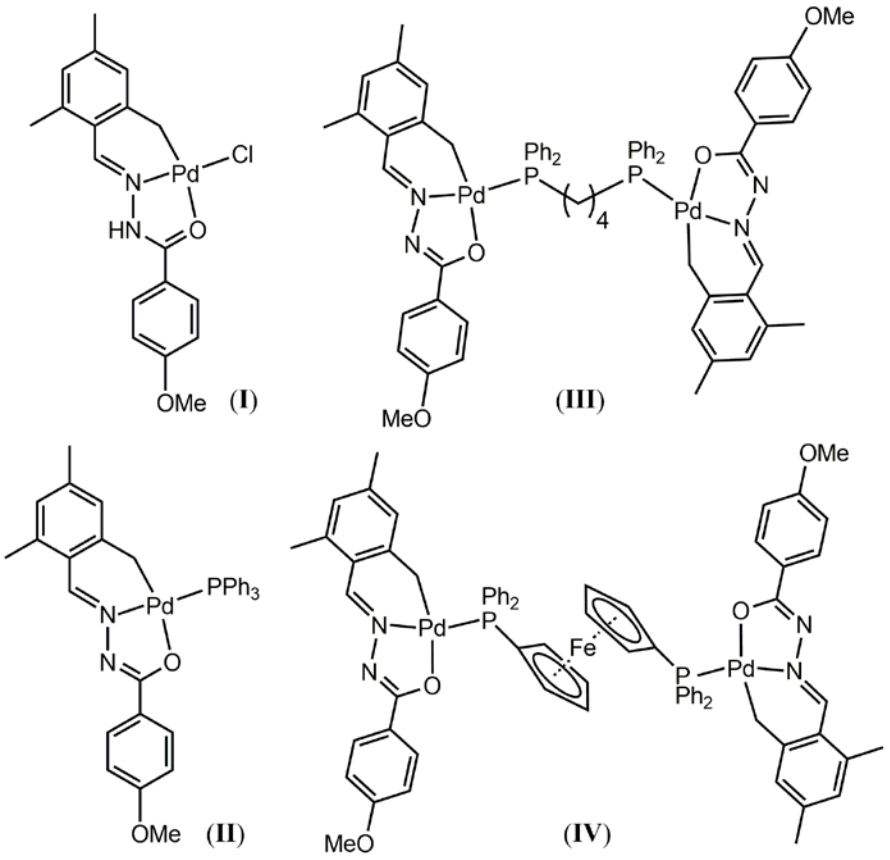

Chart 3.1. Chemical structures of **I–IV**.

In the previous chapter

r, we have reported a series of mononuclear and dinuclear cyclometallated palladium(II) complexes with the Schiff base 4-methoxy-*N*′-(mesitylidene)benzohydrazide (H_2L) [20]. In these complexes having the formulas [Pd(HL)Cl] (**I**), [Pd(L)(PPh_3)] (**II**), [Pd_2(μ-dppb)$(L)_2$] (**III**) and [Pd_2(μ-dppf)$(L)_2$] (**IV**) (dppb = 1,4-bis(diphenylphosphino)butane and dppf = 1,1′-bis(diphenylphosphino)ferrocene); the ligands ($(HL)^-$ and $(L)^{2-}$) have the 5,6-membered fused chelate rings forming pincer-like ONC-coordinating mode (Chart 3.1). In the present chapter, we have examined the catalytic properties of these four complexes in Suzuki–Miyaura cross-coupling reactions of phenyl- and 2-naphthylboronic acids with electronically diverse types of aryl halides in predominantly aqueous media.

3.2. Experimental

3.2.1. Physical measurements

A Shimadzu GCMS-QP2010 gas chromatograph mass spectrometer was used for GC-MS analysis. High resolution mass spectra were recorded with a Bruker Maxis (ESI-TOF analyzer) spectrometer. The ^1H (400 MHz) and ^{13}C (100 MHz) NMR spectra were collected with the help of a Bruker NMR spectrometer.

3.2.2. General procedure for the Suzuki–Miyaura reaction

An oven-dried round bottom flask (10 ml) was charged with 0.1 ml dimethylformamide solution of complex **IV** (0.1 mol % for aryl bromides and 0.2 mol% for aryl chlorides), aryl boronic acid (1.2 mmol), aryl halide (1.0 mmol), K_2CO_3 (1.5 mmol), TBAB (1.0 mmol) and 2 ml water. The reaction mixture was then heated (to 70 °C for aryl bromides and 90 °C for aryl chlorides) with stirring under aerobic conditions for the required time. At the end of the reaction, the reaction mixture was cooled to room temperature and

extracted with ethyl acetate (2 x 5 ml). The combined extract was washed with water (2 x 10 ml), dried over anhydrous sodium sulfate and then subjected to GC-MS analysis for identification and yield determination (from the areas under the peaks) of the products. In the case of reactions with 2-naphthylboronic acid, the combined extract was evaporated to dryness under reduced pressure and the residue was purified by column chromatography (silica gel, ethyl acetate/*n*-hexane) to afford the coupling products. The products were identified by ^{1}H and ^{13}C NMR and HR-MS analysis.

3.3. Results and discussion

4-bromobenzaldehyde and phenylboronic acid were chosen as the model substrates for optimization of the reaction conditions. The reactions were performed in water (2 ml) under aerobic conditions at 70 °C in presence of tetrabutylammonium bromide (TBAB) by varying the catalyst (**I**–**IV**) (taken in 0.1 ml of dimethylformamide (DMF)), catalyst loading (mol% of the metal complex), base, and the amounts of base and TBAB (Table 3.1). Among the four catalysts **I**–**IV** assessed (entries 1–4), catalyst **IV** provided the highest yield in shortest reaction time (entry 4). Decrease in the mol% of **IV** resulted into significant decrease in the yield and increase in the reaction time (entries 5–7). Considering the dinuclearity of **IV**, it is expected to be more productive than either of the two mononuclear complexes (**I** and **II**). But, the performances of **IV** with significantly lower loadings of 0.01–0.0001 mol% were better than the performances of 0.1 mol% of both **I** and **II** (entries 1 and 2). Variation of temperature (entries 8–10) showed that at elevated reaction temperature (90 °C) though same yield was obtained but there was no significant decrease in the reaction time (entry 10). K_2CO_3 turned out to be the best base when compared with the other inorganic bases and triethylamine (entries 11–16). Lowering of

Table 3.1. Optimization of reaction conditions[a]

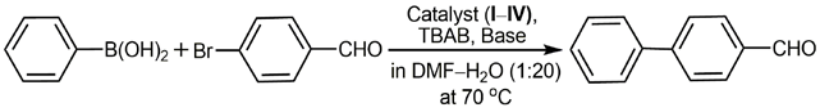

Entry	Catalyst	Base	TBAB	Time (h)	Yield[b]
1	**I** (0.1)	K_2CO_3 (2)	1	12	63
2	**II** (0.1)	K_2CO_3 (2)	1	8	77
3	**III** (0.1)	K_2CO_3 (2)	1	8	95
4	**IV** (0.1)	K_2CO_3 (2)	1	5	99
5	**IV** (0.01)	K_2CO_3 (2)	1	6	84
6	**IV** (0.001)	K_2CO_3 (2)	1	6	71
7	**IV** (0.0001)	K_2CO_3 (2)	1	10	59
8	**IV** (0.1)	K_2CO_3 (2)	1	24	76[c]
9	**IV** (0.1)	K_2CO_3 (2)	1	18	88[d]
10	**IV** (0.1)	K_2CO_3 (2)	1	4.5	99[e]
11	**IV** (0.1)	NaOH (2)	1	12	92
12	**IV** (0.1)	KOH (2)	1	12	93
13	**IV** (0.1)	K_3PO_4 (2)	1	12	84
14	**IV** (0.1)	CS_2CO_3 (2)	1	12	86
15	**IV** (0.1)	Et_3N (2)	1	12	75
16	**IV** (0.1)	Na_2CO_3 (2)	1	6	94
17	**IV** (0.1)	K_2CO_3 (1.5)	1	6	99
18	**IV** (0.1)	K_2CO_3 (1)	1	6	82
19	**IV** (0.1)	K_2CO_3 (0.5)	1	6	71
20	**IV** (0.1)	K_2CO_3 (1.5)	0.5	12	80
21	**IV** (0.1)	K_2CO_3 (1.5)	0.2	12	64
22	**IV** (0.1)	K_2CO_3 (1.5)	–	12	49
23	–	K_2CO_3 (1.5)	1	24	–
24	**IV** (0.1)	–	1	24	29
25	**IV** (0.1)	–	–	24	21

[a] 4-Bromobenzaldehyde (1.0 mmol), phenylboronic acid (1.2 mmol), catalyst (**I**–**IV**) in 0.1 ml of dimethylformamide, tetrabutylammonium bromide (TBAB) (1.0 mmol), H_2O (2 ml).

[b] GC-MS yield (based on 4-bromobenzaldehyde).

[c] At 25 °C.

[d] At 50 °C.

[e] At 90 °C.

the amount of K_2CO_3 from 2 mmol to 1.5 mmol increased the reaction time by 1 h for the same yield (99%) (entry 17). However, further lowering resulted into significant decrease in the yields (entries 18 and 19). Similarly decrease in the amount of TBAB or its absence resulted into significantly reduced yields in longer durations of the reactions (entries 20–22). The requirement of TBAB is perhaps due to the formation of $[Bu_4N][BPh(OH)_3]$ which helps to increase the rate of the reaction and hence more yield of the cross-coupling product [8,21]. The control experiments showed no detectable product formation without catalyst (entry 23), while yields were 29 or 21% in presence of catalyst but without base (entry 24) or both base and TBAB (entry 25), respectively. Thus the conditions used for entry 17 were found to be optimal and used for subsequent reactions with various substrates.

The optimized conditions as described above were then employed for Suzuki–Miyaura cross-coupling reactions of substituted phenyl bromides with phenylboronic acid. The products [22–26] obtained with required reaction times and the yields are listed in Table 3.2. Phenyl bromides bearing electron withdrawing groups at *para* position were more reactive and provided excellent yields (≥ 98%) in 6 h (entries 1, 4 and 5). In comparison, reactions involving phenyl bromides containing electron withdrawing groups at *meta* position produced slightly lower yields (~93%) in the same reaction time of 6 h (entries 3 and 6). In contrast, due to steric effect *ortho*-bromobenzaldehyde gave a relatively modest yield of 82% in 6 h and 91% when the reaction was allowed for longer time of 8 h (entry 2). In contrast, phenyl bromides containing electron donating groups showed somewhat low reactivities and gave moderate to excellent yields in longer reaction durations (entries 7–14).

In the cases of *para*- and *meta*-bromoanisoles, yields of coupling products were ≥ 90%, while the

Table 3.2. Suzuki–Miyaura reactions of aryl bromides with phenylboronic acid[a]

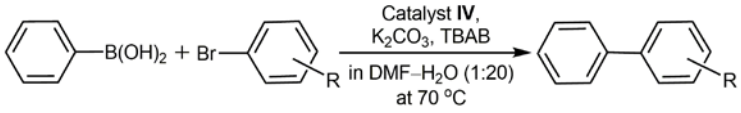

Entry	R	Product	Time (h)	Yield[b] (%)
1	*p*-CHO		6	99
2	*o*-CHO		6, 8	82, 91
3	*m*-CHO		6	92
4	*p*-NO_2		5	99
5	*p*-COOH		6	98
6	*m*-COOH		6	94
7	*p*-OMe		8	94
8	*m*-OMe		8	90
9	*o*-OMe		8	84
10	*p*-OH		8	91
11	*m*-OH		8	85
12	*o*-OH		8	78
13	*p*-NH_2		8	86
14	*o*-NH_2		8	74

[a] Aryl bromide (1.0 mmol), phenylboronic acid (1.2 mmol), catalyst **IV** (0.1 mol%) in 0.1 ml of dimethylformamide, K_2CO_3 (1.5 mmol), TBAB (1.0 mmol), H_2O (2 ml).

[b] GC-MS yield (based on aryl bromide).

yield was 84% for *ortho*-anisole in 8 h of reaction time for each (entries 7–9). Similarly, in 8 h, yields were 85–91% for both *para*- and *meta*-bromophenols and *para*-bromoaniline (entries 10, 11 and 13). However, because of steric effect both *ortho*-bromophenol and *ortho*-bromoaniline provided the corresponding coupling products in lower yields of 78 and 74%, respectively in 8 h (entries 12 and 14). Thus, in general, presence of electron withdrawing substituents enhances the reactivities of the aryl bromides in comparison to the electron donating substituents, as reported earlier [27–29].

The same approach as described above for phenylboronic acid was employed for the cross-coupling reactions of 2-naphthylboronic acid with a variety of aryl bromides using the catalyst **IV**. Table 3.3 lists the products [30–36] isolated with the corresponding reaction times and the yields. Results were very similar to those observed for phenylboronic acid. Excellent yields (96%) of the coupling products were obtained in 6 h for phenyl bromides having electron withdrawing groups at *para* position (entries 1 and 2). On the other hand, yields were relatively less (91 and 86%) even in longer reaction time (8 h) for phenyl bromides having electron donating groups at the same *para* position (entries 3 and 4). Similar or even less yields of 88 and 80% were obtained in 8 h for two electron donating atoms/groups containing aryl bromides such as 5-bromo-1,3-benzodioxole and 4-bromo-1,2-dimethoxybenzene, respectively (entries 5 and 6). Interestingly, among all the aryl bromides, 5-bromo-2-hydroxybenzaldehyde having an electron donating group as well as an electron withdrawing group was least reactive and

provided comparatively very low yields of 62 and 80% yields in significantly longer reaction durations of 10 and 16 h, respectively (entry 7). Furthermore, catalyst **IV** was also very effective for heteroaryl bromides such as 2-bromothiophene, 2-acetyl-5-bromothiophene and 2-bromopyrimidine, and the reactions afforded > 90% yields of the corresponding aryl-heteroaryl cross-coupling products in 6–10 h (entries 8, 9

Table 3.3. Coupling reactions of aryl bromides with 2-naphthylboronic acid[a]

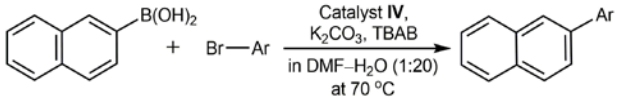

Entry	Aryl bromide	Product	Time (h)	Yield[b] (%)
1			6	96
2			6	96
3			8	91
4			8	86
5			8	88
6			8	80
7			10, 16	62, 80
8			10	90

9	6	92
10	8	94

[a] Aryl bromide (1.0 mmol), 2-naphthylboronic acid (1.2 mmol), catalyst **IV** (0.1 mol%) in 0.1 ml of dimethylformamide, K_2CO_3 (1.5 mmol), TBAB (1.0 mmol), H_2O (2 ml).
[b] Np represents the 2-naphthyl group. [c] Isolated yield.

and 10). Here also presence of electron withdrawing substituent on the heteroaryl bromide enhances its reactivity (entries 8 and 9).

The aryl chlorides are less reactive than the aryl bromides because of the stronger C–Cl bond than the C–Br bond [37]. Hence, previously reported cyclopalladate catalyzed Suzuki–Miyaura coupling reactions involving aryl chlorides in water or water-organic mixed solvents were generally performed at rather higher temperatures (≥ 100 °C) [7–12]. However, somewhat related complexes of $\{Pd(CH_3)(PR_3)\}^+$ with NN-coordinating β-dikitiminate ligands were shown to effectively catalyze coupling of aryl chlorides with arylboronic acids in ethanol–water (1:1) mixture at lower temperatures ranging from 50–80 °C [38]. We also examined the catalytic effectiveness of complex **IV** in the cross-coupling reactions of phenylboronic acid with a range of aryl chlorides. The products [22–26,39,40] formed, reaction durations and the yields are summarized in Table 3.4. Under the same optimized conditions as used for aryl bromides (Table 3.1, entry 17), the yields were 63 and 74% in reaction times of 10 and 18 h, respectively for *para*-nitrochlorobenzene. Increase of reaction temperature from 70 to 90 °C led to the improved yields of 71 and 82% in 10 and 18 h, respectively. The yield improved further to 98% in 10 h reaction time when the catalyst loading was also increased from 0.1 to 0.2 mol% with the increase of temperature to 90 °C. Thus the conditions used for entry 1 in Table 3.4 were found to be the best and applied for the

remaining aryl chloride substrates. Chlorobenzenes substituted at *para* position by electron withdrawing groups provided excellent yields (95–99%) of the corresponding coupling products in 10 h (entries 1–3). In slightly longer reaction time of 12 h, chlorobenzenes with electron withdrawing substituents at *meta* position also gave very good yields (91 and 94%) (entries 4 and 5). Whereas, a comparatively moderate yield of 84% was obtained for *ortho*-chlorobenzonitrile in 12 h (entry 6). In contrast, the coupling reactions of chlorobenzenes having electron

Table 3.4. Suzuki–Miyaura reactions of aryl chlorides and phenylboronic

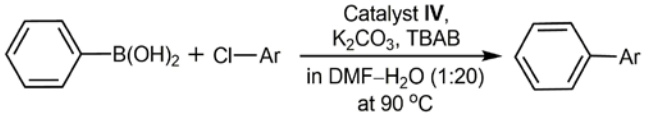

acid[a]

Entry	Aryl chloride	Product	Time (h)	Yield[b] (%)
1			10	98
2			10	99
3			10	95
4			12	91
5			12	94
6			12	84
7			14	83
8			14	87
9			14	91
10			12	85

[a] Aryl chloride (1.0 mmol), phenylboronic acid (1.2 mmol), catalyst **IV** (0.2 mol%) in 0.1 ml of dimethylformamide, K_2CO_3 (1.5 mmol), TBAB (1.0 mmol), H_2O (2 ml).

[b] GC-MS yield (based on aryl chloride).

donating groups at the *para* position required somewhat longer reaction time (14 h) for moderate to very good yields (83–91%) (entries 7–9). The reaction with the heteroaryl chloride 2-chloropyrimidine was also successful and a yield of 85% was obtained in a reaction time of 12 h. Not surprisingly, as observed before [7–12] here also the aryl chlorides required higher reaction temperature as well as higher catalyst loading and longer reaction durations for moderate to excellent yields of the cross-coupling products in comparison to the aryl bromides due to the difference in the C–Cl and C–Br bond strengths [37].

3.4. Conclusions

The catalytic properties of a series of mono- and dinuclear cyclometallated palladium(II) complexes having the pincer-like ONC-donor $(L)^{2-}$ (H_2L = 4-methoxy-*N*′-(mesitylidene)benz-ohydrazide) as primary and monodentate chloride or monophosphine or bidentate bridging diphosphines as ancillary ligands in Suzuki–Miyaura cross-coupling reactions of a diverse range of aryl bromides and chlorides with arylboronic acids in predominantly aqueous media were investigated. Out of the four complexes evaluated, the dinuclear $[Pd_2(\mu\text{-dppf})(L)_2]$ containing the 1,1′-bis(diphenylphosphino)ferrocene (dppf) as the bridging ligand turned out to be the best performing catalyst. The

catalytic reactions exhibited a broad substrate scope and afforded a wide variety of biaryl and aryl-heteroaryl products. The yields were moderate to excellent in reasonably short duration reactions.

3.5. References

[1] V. Polshettiwar, A. Decottignies, C. Len, A. Fihri, *Chem. Sus. Chem*. 3 (2010) 502–522.

[2] S. Liu, M. Lv, D. Xiao, X. Li, X. Zhou, M. Guo, *Org. Biomol. Chem*. 12 (2014) 4511–4516.

[3] Y. Liu, N. Gu, P. Liu, X. Ma, J. Xie, B. Dai, *Tetrahedron*. 71 (2015) 7985–7989.

[4] S. Wang, R. Guo, J. Li, D. Zou, Y. Wu, Y. Wu, *Tetrahedron Lett*. 56 (2015) 3750–3753.

[5] A. Dewan, P. Bharali, U. Bora, A. Thakur, *J. RSC Adv*. 6 (2016) 11758–11762.

[6] A. Chatterjee, T. R. Ward, *Catal. Lett*. 146 (2016) 820–840.

[7] D.A. Alonso, C. Nájera, M.C. Pacheco, *J. Org. Chem*. 67 (2002) 5588–5594.

[8] L. Botella, C. Nájera, *Angew. Chem. Int. Ed*. 41 (2002) 179–181.

[9] C.–L. Chen, Y.–H. Liu, S.–M. Peng, S.–T. Liu, *Tetrahedron Lett*. 46 (2005) 521–523.

[10] R. Huang, K. H. Shaughnessy, *Organometallics* 25 (2006) 4105–4112.

[11] H. Li, Y. Wu, *Appl. Organomet. Chem*. 22 (2008) 233–236.

[12] G. Zhang, W. Zhang, Y. Luan, X. Han, C. Ding, *Chin. J. Chem*. 33 (2015) 705–710.

[13] S. K. Kurapati, S. Maloth, S. Pal, *Inorg. Chim. Acta* 430 (2015) 66–73.

[14] R. N. Prabhu, S. Pal, *Tetrahedron Lett*. 56 (2015) 5252–5256.

[15] S. K. Kurapati, S. Pal, *Appl. Organomet. Chem*. 30 (2016) 116–124.

[16] R. N. Prabhu, G. N. Babu, S. Pal, *Appl. Organomet. Chem*. 31 (2017) e3544.

[17] S. Ghosh, S. K. Kurapati, S. Pal, *Polyhedron* 125 (2017) 26–33.

[18] G. N. Babu, S. Pal, *J. Organomet. Chem*. 824 (2016) 42–47.

[19] S. Keesara, G. N. Babu, S. Pal, *Appl. Organomet. Chem*. In press

[20] G. N. Babu, S. Pal, *J. Organomet. Chem*. 805 (2016) 19–26.

[21] D. Badone, M. Baroni, R. Cardamone, A. Ielmini, U. Guzzi, *J. Org. Chem*. 62 (1997) 7170–7173.

[22] T. Mino, Y. Shirae, M. Sakamoto, T. Fujita, *J. Org. Chem*. 70 (2005) 2191–2194.

[23] D. Srimani, A. Sarkar, *Tetrahedron Lett*. 49 (2008) 6304–6307.

[24] L. Li, T. Wu, J. Wang, R. Wang, *ChemPlusChem* 79 (2014) 257–265.

[25] K. Okamoto, R. Akiyama, S. Kobayashi, *Org. Lett*. 6 (2004) 1987−1990.

[26] Z. Li, C. Gelbaum, W. L. Heaner, J. Fisk, A. Jaganathan, B. Holden,; P. Pollet, C. L. Liotta, *Org. Process Res. Dev*. 20 (2016) 1489−1499.

[27] S. Saito, S. Oh-tani, N. Miyaura, *J. Org. Chem*. 62 (1997) 8024–8030.

[28] H. Weissman, D. Milstein, *Chem. Commun*. (1999) 1901–1902.

[29] D. Zim, A. S. Gruber, G. Ebeling, J. Dupont, A. L. Monteiro, *Org. Lett*. 2 (2000) 2881–2884.

[30] N. Mase, T. Ando, F. Shibagaki, A. Sugita, T. Narumi, M. Toda, N. Watanabe, F. Tanaka, *Tetrahedron Lett*. 55 (2014) 1946–1948.

[31] T. Sultana, B. H. Mandal, Md. L. Rahman, S. M. Sarkar, *ChemistrySelect* 1 (2016) 4108–4112.

[32] J. L. Bolligera, C. M. Frecha, *Adv. Synth. Catal*. 352 (2010) 1075–1080.

[33] X. Bei, H. W. Turner, W. H. Weinberg, A. S. Guram, *J. Org. Chem*. 64 (1999) 6797–6803.

[34] A. D. Zotto, F. Amoroso, W. Baratta, P. Rigo, *Eur. J. Org. Chem*. 1 (2009) 110–116.

[35] T. T. Dang, M. Bonneau, J. A. G. Williams, H. L. Bozec, H. Doucet, V. Guerchais, *Eur. J. Inorg. Chem*. 18 (2015) 2956–2964.

[36] S. Bhadra, C. Matheis, D. Katayev, L. J. Gooßen, *Angew. Chem. Int. Ed*. 52 (2013) 9279–9283.

[37] Y.–R. Luo, Handbook of Bond Dissociation Energies in Organic Compounds, CRC Press LLC: Boca Raton, 2003.

[38] D.–H. Lee, M.–J. Jin, *Org. Lett*. 13 (2011) 252–255.

[39] G. K. Rao, A. Kumar, J. Ahmedz, A. K. Singh, *Chem. Commun*., 46 (2010) 5954–5956.

[40] H. Ke, X. Chen, G. Zou, *Appl. Organomet. Chem*. 28 (2014) 54–60.

Chapter 4

Syntheses, structures and catalytic applications of Mono- and tetranuclear cyclopalladated complexes with *N′*-(9-anthracenylidene)benzothiohydrazide[§]

Reaction of $PdCl_2$, LiCl, N′-(9-anthracenylidene)benzothiohydrazide (H_2L, 2 Hs represent the thioamide NH proton and the 9-anthracenyl *peri* proton) and $NaOAc{\cdot}3H_2O$ in 1:2:1:1 mole ratio in methanol produced $[Pd_4(L)_4]$ (**1**) in 75 % yield. Treatment of **1** with PPh_3 (1:4.5 mole ratio) in acetone provided $[Pd(L)(PPh_3)]$ (**2**) in 72% yield. The molecular formulas of the diamagnetic and non-electrolytic **1** and **2** were established by elemental analyses. Molecular structures of **1** and **2** were determined by single crystal X-ray diffraction studies. In the tetranuclear **1**, the palladium(II) centers are in distorted square-planar CNS_2 coordination environments created by four $(L)^{2-}$, each of which acts as 5,6-membered fused chelate rings forming thioamidate-S, azomethine-N and 9-anthracenyl *peri*-C donor to one metal center and uses the thioamidate-S atom to bridge a second metal center. In the mononuclear **2**, $(L)^{2-}$ and PPh_3 assemble a distorted square-planar CNSP coordination environment around the palladium(II) center. Spectroscopic (IR, NMR and UV-Vis) measurements were also used to characterize **1** and **2**. The catalytic properties of both complexes in the oxidative phenylacetylene homocoupling reaction were examined.

[§] This work has been published in *J. Organomet. Chem*. 824 (2016) 42–47.

4.1. Introduction

Our group has been working on cyclometallates of platinum metal ions with aroylhydrazones and thiosemicarbazones of various mono- and polycyclic aromatic aldehydes over the past several years [10–16]. It has been found that five-membered ring forming azomethine-N and amidate-O or thioamidate-S chelation by aroylhydrazonates or thiosemicarbazonates facilitates cyclometallation via not only C(sp^2)–H [1–6] but also C(sp^3)–H [7] activation. The aroylhydrazonates or the thiosemicarbazonates act as pincer-like CNO- or CNS-donor in the final cyclometallated complexes formed. In the present chapter, to examine whether N′-(9-anthracenylidene)benzothiohydrazide (H_2L) behaves in the same way or not we have explored its chemistry with palladium(II) and isolated a mononuclear cyclopalladate and a teranuclear cyclopalladate (Scheme 4.1). Herein we report the syntheses, crystal structures and spectroscopic properties of these two complexes and their catalytic applications in oxidative homocoupling of phenylacetylene.

4.2. Experimental

4.2.1. Materials

The Schiff base N′-(9-anthracenylidene)benzothiohydrazide (H_2L) was synthesized from equimolar amounts of 9-anthraldehyde and thiobenzhydrazide by following a slightly modified (using methanol instead of ethanol as solvent) reported procedure [8]. All other chemicals used in this work were of reagent grade available commercially and were used as received without any further purification. Standard methods [9] were employed for purification of the solvents used.

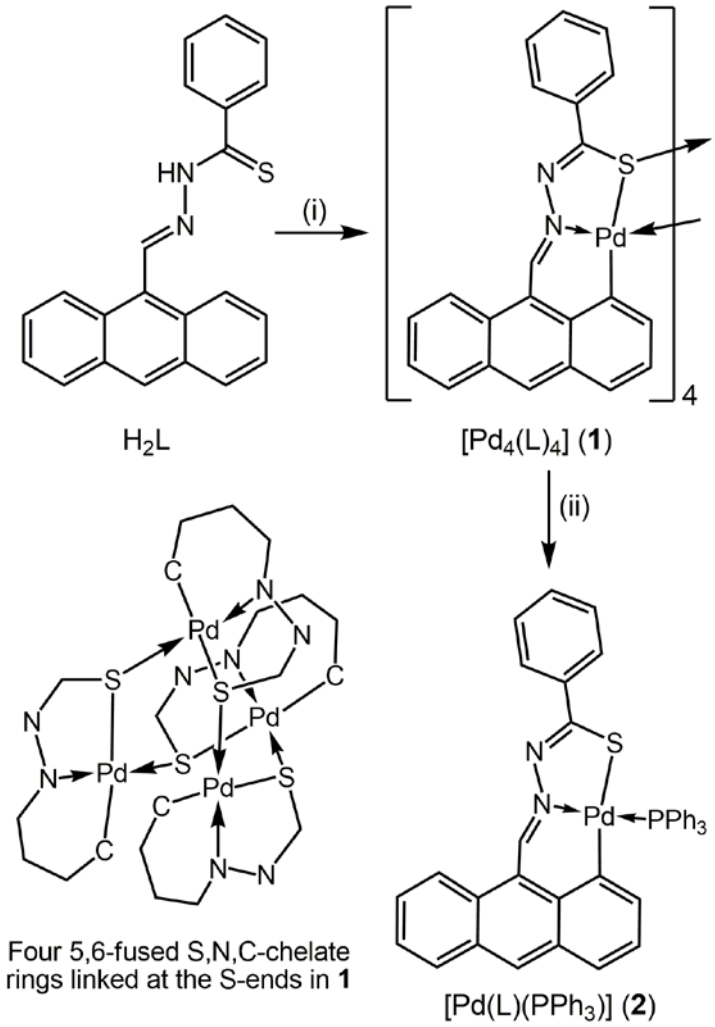

Scheme 4.1. (i) $PdCl_2$, LiCl and $NaOAc{\cdot}3H_2O$ (1:2:1 mole ratio) in methanol at 298 K. (ii) PPh_3 (4.5 mole equivalents) in acetone at 298 K.

4.2.2. Physical measurements

Elemental (CHN) analysis data were obtained using a Thermo Finnigan Flash EA1112 series elemental analyzer. A Shimadzu LCMS 2010 liquid chromatograph mass spectrometer was used to verify the purity of H_2L. Magnetic susceptibility measurements at room temperature were performed

with a Sherwood scientific balance. A Thermo Scientific Nicolet 380 FT-IR spectrophotometer was employed to collect the infrared spectra. A Digisun DI-909 conductivity meter was used for solution electrical conductivity measurements. Electronic spectra were recorded on a Shimadzu UV3600 UV-Vis-NIR spectrophotometer. The ^{1}H (400 MHz, $SiMe_4$ as an internal standard) and $^{31}P\{^{1}H\}$ (160 MHz, 85% H_3PO_4 as an external standard) NMR spectra were recorded on a Bruker NMR spectrometer. A Shimadzu GCMS-QP2010 gas chromatograph mass spectrometer was used for GC-MS analysis.

4.2.3. Synthesis of [Pd$_4$(L)$_4$] (1)

A mixture of $PdCl_2$ (90 mg, 0.5 mmol), LiCl (43 mg, 1 mmol), H_2L (171 mg, 0.5 mmol) and NaOAc·3H$_2$O (69 mg, 0.5 mmol) in 40 ml methanol was stirred at room temperature (298 K) for 2 days. The brick red solid separated was collected by filtration, dissolved in minimum amount of dichloromethane and added to a silica gel column (packed with a *n*-hexane slurry of silica gel). Elution with *n*-hexane–ethylacetate (3:7) mixture initially provided a light yellow band which was discarded. The following brick red band containing **1** was collected and evaporated to dryness. Yield: 170 mg (75%). Anal. Calcd for $C_{88}H_{56}N_8S_4Pd_4$: C, 59.40; H, 3.17; N, 6.30. Found: C, 59.27; H, 3.23; N, 6.38. Selected IR data: ν (cm^{-1}) = 1594 & 1581 (N=C–C=N), 945 (C–S). UV-Vis in CH_2Cl_2: λ_{max} (nm) (10^4 x ε (M^{-1} cm^{-1})) = 562 (0.93), 525 (1.10), 490 (1.04), 392 (1.33), 376 (1.19). ^{1}H NMR in $CDCl_3$: δ (ppm) (J (Hz)) = 9.37 (s, 1H), 8.87 (s, 1H), 8.47 (7) (d, 2H), 7.96 (9) (d, 1H), 7.77 (s, 1H), 7.75 (2) (d, 1H), 7.63 (s, 1H), 7.43 (4) (d, 2H), 7.21–7.13 (m, 3H), 6.57 (8) (t, 1H).

4.2.4. Synthesis of [Pd(L)(PPh$_3$)] (2)

To a suspension of [$Pd_4(L)_4$] (**1**) (135 mg, 0.076 mmol) in acetone (20 ml) solid PPh_3 (90 mg, 0.34 mmol) was added. The resulting mixture was stirred at room temperature (298 K) for one day. The orange red solid obtained was filtered off, dissolved in minimum amount of dichloromethane and transferred to a silica gel column (packed with a silica gel slurry in *n*-hexane). Elution with *n*-hexane–ethylacetate (9:1) gave an orange red band containing **2**. This band was collected and evaporated to dryness. Yield: 155 mg (72%). Anal. Calcd for $C_{40}H_{29}N_2SPPd$: C, 67.94; H, 4.13; N, 3.96. Found: C, 67.85; H, 4.18; N, 4.07. Selected IR data: ν (cm^{-1}) = 1596 & 1581 (N=C–C=N), 941 (C–S), 742, 691 and 536 (PPh_3). UV-Vis in CH_2Cl_2: λ_{max} (nm) (10^4 x ε (M^{-1} cm^{-1}) = 550^{sh} (0.73), 511 (1.27), 485^{sh} (1.14), 390 (0.65), 370 (0.56). ^{1}H NMR in $CDCl_3$: δ (ppm) (J (Hz)) = 9.99 (10) (d, 1H), 8.69 (s, 1H), 8.66 (9) (d, 1H), 8.17 (8) (d, 2H), 8.11 (8) (d, 1H), 7.70–7.65 (m, 8H), 7.59–7.56 (m, 2H), 7.46–7.42 (m, 3H), 7.39–7.35 (m, 9H), 6.72 (8) (t, 1H). $^{31}P\{^1H\}$ NMR in $CDCl_3$: δ (ppm) = 36.26.

4.2.5. X-ray crystallography

Single crystals of [$Pd_4(L)_4$] (**1**) were grown by slow evaporation of its solution in chloroform-acetonitrile (1:1), while slow evaporation of an acetonitrile solution of [Pd(L)(PPh_3)] (**2**) provided its single crystals. Both **1** and **2** crystallized as solvates – **1**·$CHCl_3$ and **2**·CH_3CN, respectively. Unit cell determination and intensity data collection for both crystals were performed at 298 K on an Oxford Diffraction Xcalibur Gemini single crystal X-ray diffractometer using graphite monochromated Mo $K\alpha$ radiation (λ = 0.71073 Å). The CrysAlisPro software [10] was used for data collection, reduction and absorption correction. The structures of both **1**·$CHCl_3$ and **2**·CH_3CN were solved by direct methods and refined on F^2 by full-matrix least-squares

procedures In the case of **1**, the phenyl rings of the thiobenzoyl moieties of two

Table 4.1. Selected crystal data and structure refinement summary

Complex	**1**·$CHCl_3$	**2**·CH_3CN
Chemical formula	$C_{89}H_{57}Cl_3N_8S_4Pd_4$	$C_{42}H_{32}N_3PSPd$
Formula weight	1898.62	748.14
Crystal system	Tetragonal	Monoclinic
Space group	$I4_1/a$	$P2_1/n$
a (Å)	44.5189(10)	12.4885(18)
b (Å)	44.5189(10)	12.9202(19)
c (Å)	15.3784(5)	21.517(3)
α (°)	90	90
β (°)	90	105.596(9)
γ (°)	90	90
V (Å^3), Z	30478.9(14), 16	3344.0(8), 4
ρ_{calcd} (g cm^{-3})	1.655	1.486
μ (mm^{-1})	1.198	0.701
Refl. collected	29976	12756
Refl. unique	13418	5880
Refl. [$I \geq 2\sigma(I)$]	8547	4324
Parameters	973	434
$R1$, $wR2$ [$I \geq 2\sigma(I)$]	0.0688, 0.1369	0.0417, 0.0841
$R1$, $wR2$ [all data]	0.1143, 0.1531	0.0656, 0.0944
GOF on F^2	1.062	1.026
Max./Min. $\Delta\rho$ (e Å^{-3})	0.769/–0.509	0.502/–0.439

$(L)^{2-}$ were refined with geometric restraints. A few additional significant residual electron density peaks (38 e^- per unit cell in a total potential solvent-accessible void volume of 1940.2 Å^3) which could not be refined as disordered

solvent molecules were dealt with SQUEEZE procedure [11] as implemented in the Platon package [12]. In both structures, all non-hydrogen atoms were refined anisotropically. The hydrogen atoms were placed in geometrically idealized positions and refined by using a riding model. SHELX-97 programs [13] used for structure solution and refinement were accessed through the WinGX package [14]. Thermal ellipsoid plots were prepared using the Mercury [15] package. Crystallographic data for both structures have been deposited with the Cambridge Crystallographic Data Centre. The deposition numbers are CCDC 1497686 and 1497687 for **1**·$CHCl_3$ and **2**·CH_3CN, respectively. Selected crystallographic data for both structures are summarized in Table 4.1.

4.2.6. Procedure for the homocoupling of phenyl acetylene

To a mixture of phenylacetylene (1 mmol), K_3PO_4 (1.5 mmol) and cocatalyst CuI (0.5 mol%) in acetonitrile (1 ml) a dimethylformamide solution (0.1 ml) of catalyst (**1** or **2**) (0.1 mol%) was added. The reaction mixture was stirred at 60 ^oC for the required time and then cooled to room temperature. It was transferred to a separating funnel containing water (20 ml) and extracted with ethylacetate (20 ml). The ethylacetate extract was washed with water (2 x 10 ml), dried over anhydrous Na_2SO_4 and finally subjected to GC-MS analysis for confirmation of the product and determination of its yield.

4.3. Results and discussion

4.3.1. Synthesis and characterization

The Schiff base N′-(9-anthracenylidene)benzothiohydrazide (H_2L) was synthesized in *ca.* 90% yield by the condensation reaction of equimolar amounts of benzothiohydrazide and 9-anthraldehyde in methanol in presence of a few drops of acetic acid [8]. The identity and purity of H_2L were

confirmed by elemental analysis, LC-MS and spectroscopic (IR and ^{1}H NMR) measurements. Reaction of Li_2PdCl_4 (prepared in situ), H_2L and $NaOAc{\cdot}3H_2O$ in 1:1:1 mole ratio in methanol afforded a tetranuclear palladium(II) complex of molecular formula $[Pd_4(L)_4]$ (**1**) in 75% yield. Treatment of **1** with *ca.* 4.5 molar equivalent of PPh_3 in acetone produced the mononuclear palladium(II) complex having the molecular formula $[Pd(L)(PPh_3)]$ (**2**) in 72% yield (Scheme 4.1). Elemental analysis data of **1** and **2** are in good agreement with their corresponding molecular formulas. Both complexes are diamagnetic. Thus the palladium centers in them are bivalent and they are in square-planar coordination environment. The tetranuclear complex (**1**) is brick-red, while the mononuclear complex (**2**) is orange-red in color. They are highly soluble in dichloromethane, chloroform, dimethylsulfoxide and dimethylformamide; sparingly soluble in acetonitrile, methanol and toluene and insoluble in *n*-hexane. The electrically non-conducting behavior of both **1** and **2** in solution is consistent with them being neutral molecular species.

4.3.2. Spectroscopic properties

4.3.2.1. Infrared spectra

Infrared spectra of H_2L and the complexes **1** and **2** were recorded in the range 4000–400 cm^{-1} using KBr pellets. Spectra of **1** and **2** are shown in Figures 4.1 and 4.2, respectively. Each compound displayed a large number of bands of various intensities. Except for the following few selected bands no attempt was made to assign the other bands. The spectrum of the free Schiff base H_2L showed the thioamide N–H and C=S stretches as a broad strong band at 3183 cm^{-1} and as a sharp strong band at 954 cm^{-1}, respectively [8,17,20]. The disappearance of the N–H stretching band and appearance of the C=S stretching

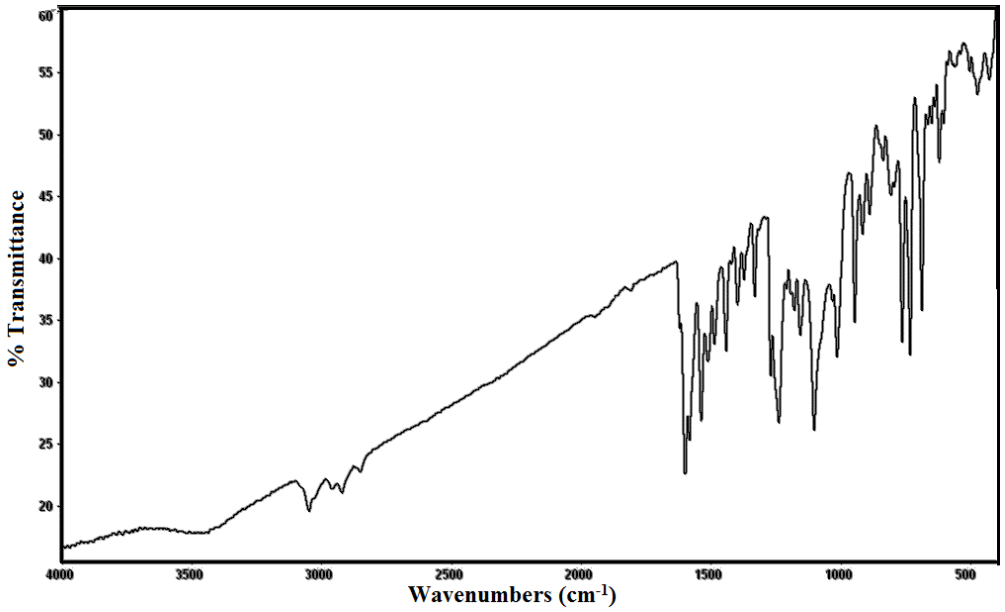

Figure 4.1. IR-spectrum of $[Pd_4(L)_4]$ (**1**)

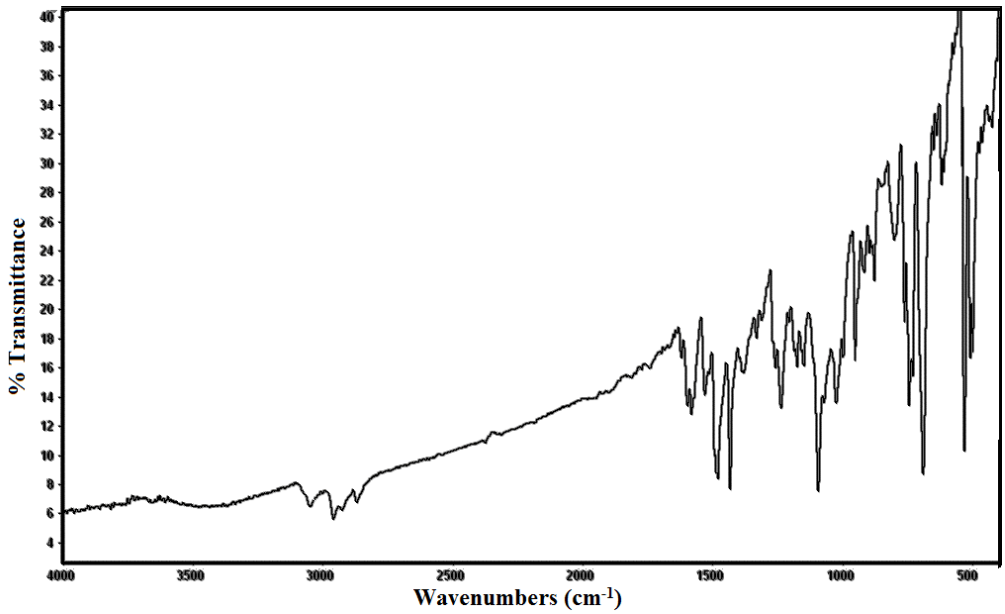

Figure 4.2. IR-spectrum of $[Pd(L)(PPh_3)]$ (**2**)

band at lower frequency (*ca.* 943 cm^{-1}) with less intensity in the spectra of **1** and **2** indicate the thioamidate-S coordination to the metal center in both complexes. A medium intensity band observed for H_2L at 1594 cm^{-1} is attributed to the C=N stretching. On the other hand, both **1** and **2** displayed two closely spaced medium to strong bands at *ca.* 1595 and 1581 cm^{-1}. These bands are most likely associated with the one end coordinated conjugated –N=C–C=N– moiety of the ligand $(L)^{2-}$ (Scheme 4.1). The presence of the coordinated PPh_3 in the mononuclear **2** is indicated by the characteristic three strong bands at 742, 691 and 536 cm^{-1} [6,7,18].

4.3.2.2. Electronic spectra

Electronic absorption spectra of **1** and **2** were recorded in dichloromethane. Both complexes exhibited a strong band in the visible region (*ca.* 518 nm) flanked on both sides by two shoulders and two more strong bands in the ultraviolet region (*ca.* 391 and 373 nm) (Figure 4.3). It may be noted that the spectrum of the free Schiff base (H_2L) displayed a shoulder at 435 nm and a group of four rather closely spaced strong bands in the range 395–335 nm followed by a very strong absorption at 257 nm [8]. This spectral profile of H_2L is very similar to that of anthracene containing Schiff bases and free anthracene [2,21,22]. Except for the red shift, the visible region absorption profiles of **1** and **2** are somewhat similar to the spectral profile observed for H_2L [8]. Thus it is very likely that the structured visible region absorption as well as the couple of higher energy absorptions displayed by the complexes **1** and **2** are largely due to ligand centered transitions only [2,4–6]. Further, metallation of the aromatic ring is also known to cause red shift of absorption bands related to π–π^* transitions [2,4–6,19,23].

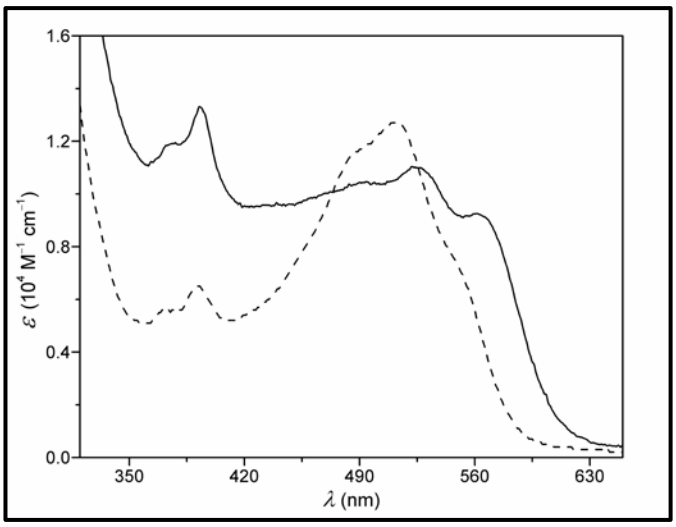

Figure 4.3. Electronic spectra of $[Pd_4(L)_4]$ (**1**) (——) and $[Pd(L)(PPh_3)]$ (**2**) (– – –) in dichloromethane.

4.3.2.3. NMR spectra

The ^1H NMR spectra of **1** and **2** were recorded in $CDCl_3$. The spectrum of **1** indicated that its four {Pd(L)} units are equivalent to each other. None of the two complexes displayed the singlet resonance of the thioamide N–H proton observed for the free H_2L at δ 13.45 ppm [8]. Thus in each of **1** and **2** the thioamide fragment is deprotonated. The azomethine proton of H_2L resonates as a singlet at δ 9.96 ppm. A singlet observed at δ 9.37 ppm for **1** is attributed to the proton of the azomethine group that is coordinated to the metal via the N-atom. In contrast, the azomethine proton in **2** appeared as a doublet (J = 10 Hz) at δ 9.99 ppm (Figure 4.4) due to coupling with the PPh_3 P-atom at the coordination site *trans* to the azomethine-N. The chemical shift ranges and the intensities of the signals corresponding to the aromatic protons of both **1** (δ 8.87–6.57 ppm) and **2** (δ 8.69–6.7 ppm) are unexceptional and as expected. The $^{31}P\{^1H\}$ NMR spectrum of **2** exhibited a singlet at δ 36.26 ppm, corresponding to the PPh_3 ligand present in it.

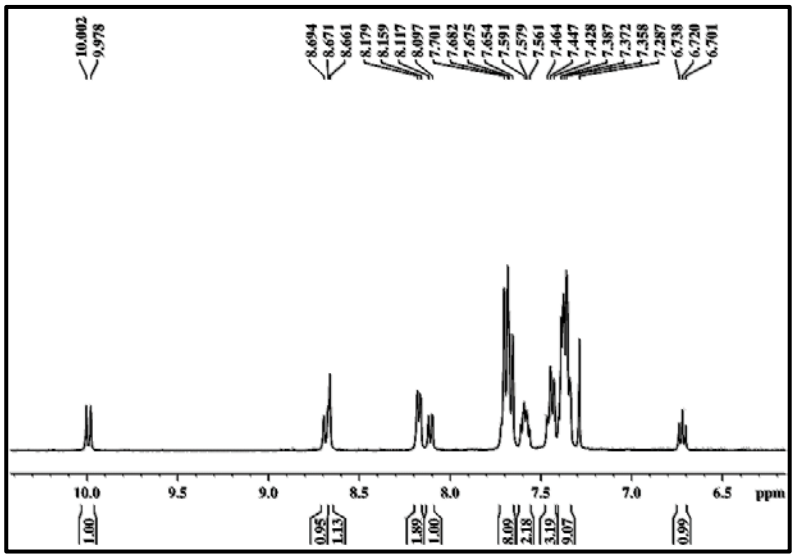

Figure 4.4. ^{1}H-NMR spectrum of [Pd(L)(PPh_3)] (**2**)

4.3.2.4. X-ray molecular structures

The molecular structures of **1** and **2** are illustrated in Figures. 4.5 and 4.6, respectively. The bond lengths and angles related to the metal centers are listed in Tables 4.2 and 4.3. In both complexes, the metal centers are in distorted square-planar coordination environments. In the tetranuclear **1**, each $(L)^{2-}$ binds one palladium atom through the thioamidate-S, the azomethine-N and the 9-anthracenyl *peri*-C atoms to form a 5,6-membered fused chelate rings motif and uses the thioamidate-S again to coordinate a second palladium atom (Scheme 4.1 and Figure 4.5). As a result, all four palladium centers are in planar CNS_2 (rms deviations from the mean plane are in the range 0.03–0.06 Å) environments. The {$Pd_4(\mu$-S$)_4$} core has a cradle-like structure (Figure. 4.5, inset). The metal···metal distances in the four Pd–S–Pd fragments are in the

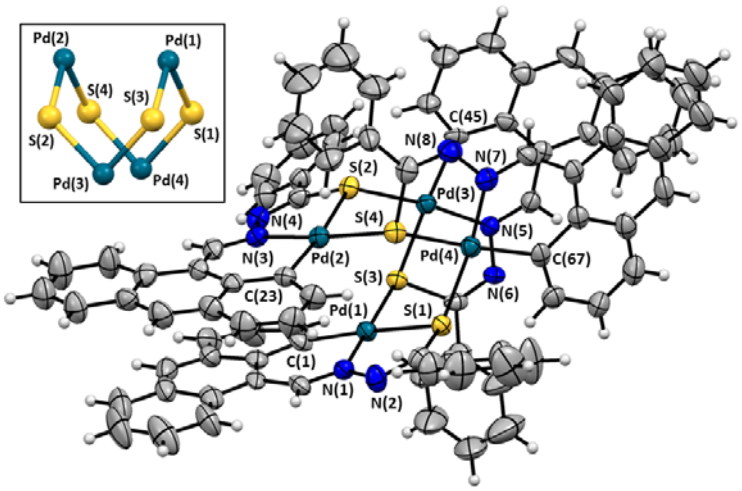

Figure 4.5. ORTEP representation of $[Pd_4(L)_4]$ (**1**) and the cradle-like $\{Pd_4(\mu\text{-}S)_4\}$ core (inset). All non-hydrogen atoms are shown at their 40% probability thermal ellipsoids. All non-carbon atoms and only the metallated carbons are labeled for clarity.

.

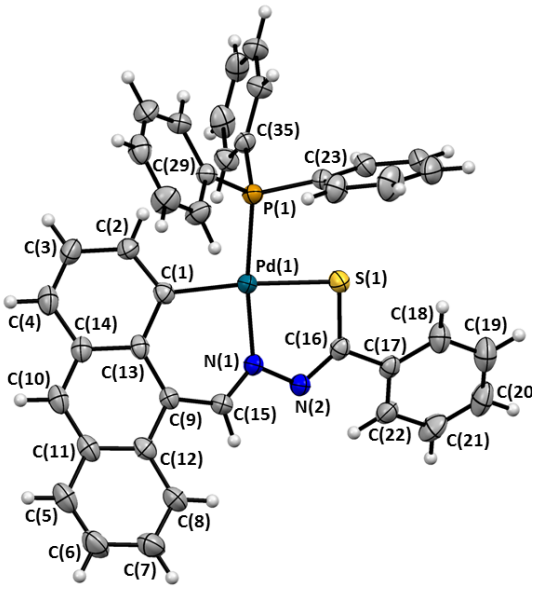

Figure 4.6. ORTEP representation of $[Pd(L)(PPh_3)]$ (**2**) with the atom labeling scheme. The thermal ellipsoids of all non-hydrogen atoms are drawn at the 40% probability level.

Table 4.2. Selected bond lengths (Å) and angles (°) for **1**·$CHCl_3$

Pd(1)–C(1)	2.026(7)	Pd(3)–C(45)	2.044(7)
Pd(1)–N(1)	1.995(6)	Pd(3)–N(5)	1.994(6)
Pd(1)–S(1)	2.3376(19)	Pd(3)–S(3)	2.319(2)
Pd(1)–S(3)	2.312(2)	Pd(3)–S(2)	2.345(2)
Pd(2)–C(23)	2.028(8)	Pd(4)–C(67)	2.035(8)
Pd(2)–N(3)	2.001(6)	Pd(4)–N(7)	1.987(7)
Pd(2)–S(2)	2.329(2)	Pd(4)–S(4)	2.331(2)
Pd(2)–S(4)	2.338(2)	Pd(4)–S(1)	2.357(2)
C(1)–Pd(1)–N(1)	91.7(3)	C(45)–Pd(3)–N(5)	91.6(3)
C(1)–Pd(1)–S(1)	175.4(2)	C(45)–Pd(3)–S(3)	174.2(2)
C(1)–Pd(1)–S(3)	93.1(2)	C(45)–Pd(3)–S(2)	94.6(2)
N(1)–Pd(1)–S(1)	84.16(17)	N(5)–Pd(3)–S(3)	83.73(19)
N(1)–Pd(1)–S(3)	173.33(19)	N(5)–Pd(3)–S(2)	173.37(19)
S(3)–Pd(1)–S(1)	91.18(7)	S(3)–Pd(3)–S(2)	90.25(7)
C(23)–Pd(2)–N(3)	91.7(3)	C(67)–Pd(4)–N(7)	91.4(3)
C(23)–Pd(2)–S(2)	173.5(2)	C(67)–Pd(4)–S(4)	173.0(3)
C(23)–Pd(2)–S(4)	94.2(2)	C(67)–Pd(4)–S(1)	96.0(3)
N(3)–Pd(2)–S(2)	82.95(19)	N(7)–Pd(4)–S(4)	82.9(2)
N(3)–Pd(2)–S(4)	174.1(2)	N(7)–Pd(4)–S(1)	172.6(2)
S(2)–Pd(2)–S(4)	91.14(7)	S(4)–Pd(4)–S(1)	89.70(7)

Table 4.3. Selected bond lengths (Å) and angles (°) for **2**·CH_3CN

Pd(1)–C(1)	2.021(3)	Pd(1)–S(1)	2.3126(9)
Pd(1)–N(1)	2.005(3)	Pd(1)–P(1)	2.2659(10)
C(1)–Pd(1)–N(1)	90.43(12)	N(1)–Pd(1)–S(1)	82.61(8)
C(1)–Pd(1)–S(1)	169.77(11)	N(1)–Pd(1)–P(1)	170.91(9)
C(1)–Pd(1)–P(1)	96.37(10)	S(1)–Pd(1)–P(1)	91.39(3)

3.8859(9)–4.0912(8) Å, while those in the two pairs of unbridged palladium centers are comparatively much shorter (Pd(1)···Pd(2), 3.3636(9) Å and Pd(3)···Pd(4), 3.2592(9) Å). It may be noted that a tetrapalladium(II) complex with a CNS-donor thiosemicarbazonate ligand [16] also has the molecular structure very similar to that of **1**. In the mononuclear **2**, $(L)^{2-}$ acts as CNS-donor and the P-atom of PPh_3 occupies the fourth coordination site (Figure. 4.6). The CNSP coordination environment around the metal center in **2** is not so planar (rms deviation from the mean plane is 0.13 Å) as that of the CNS_2 environment in **1**. This slight non-planarity is perhaps due to the steric effect of the PPh_3. Overall, the metal centered bond lengths in **1** and **2** are comparable with those observed for palladium(II) complexes having similar coordinating atoms [16–19].

4.3.2.5. Catalytic activities

Conjugated 1,3-diynes derived via cross coupling of sp-hybridized carbons have been found to be very useful and effective synthons for a variety of biologically active natural products, pharmaceuticals and also functional materials [24–29]. The first oxidative homocoupling reaction of the terminal alkyne phenylacetylene using CuCl in ammoniacal ethanol medium in presence of air was reported way back in 1869 by Glaser [30,31]. Since then the original procedure has been modified every now and then by varying the catalyst composition, base, oxidant and solvent to broaden its applications. Among various catalysts employed so far, quite a few were copper/palladium based [24–29]. Majority of the palladium cocatalysts used were either palladium(II) salts or palladium(0/II) coordination complexes. To the best of our knowledge

there are only two reports on the use of cyclopalladated complexes as catalysts [32,33]. Hence, we examined the catalytic properties of the present cyclometallted complexes **1** and **2** in the homocoupling of phenylacetylene.

Table 4.4. Optimization of reaction conditions[a]

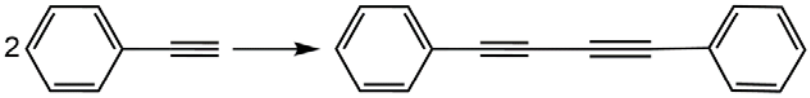

Entry	Base	Solvent	Temp. (°C)	Time (h)	Yield (%)
1	No Base	CH_3CN	60	24	23
2	K_2CO_3 (2 mmol)	CH_3CN	60	16	47
3	Na_2CO_3 (2 mmol)	CH_3CN	60	16	43
4	NaOAc (2 mmol)	CH_3CN	60	18	55
5	$NaHCO_3$ (2 mmol)	CH_3CN	60	24	37
6	NaOH (2 mmol)	CH_3CN	60	24	31
7	DBU (2 mmol)	CH_3CN	60	10	82
8	DABCO (2 mmol)	CH_3CN	60	12	72
9	Et_3N (2 mmol)	CH_3CN	60	12	66
10	PPh_3 (2 mmol)	CH_3CN	60	24	74
11	K_3PO_4 (2 mmol)	CH_3CN	60	04	94
12	K_3PO_4 (1.5 mmol)	CH_3CN	60	04	93
13	K_3PO_4 (1.0 mmol)	CH_3CN	60	10	81
14	K_3PO_4 (0.5 mmol)	CH_3CN	60	12	66
15	K_3PO_4 (1.5 mmol)	$(CH_3)_2NCHO$	60	04	88
16	K_3PO_4 (1.5 mmol)	$C_6H_5CH_3$	60	04	80
17	K_3PO_4 (1.5 mmol)	H_2O	60	12	68
18	K_3PO_4 (1.5 mmol)	CH_3OH	60	04	79
19	K_3PO_4 (1.5 mmol)	$(CH_2)_4O$	60	04	85
20	K_3PO_4 (1.5 mmol)	CH_3CN	25	24	62
21	K_3PO_4 (1.5 mmol)	CH_3CN	40	16	78
22	K_3PO_4 (1.5 mmol)	CH_3CN	80	04	94
23[b]	K_3PO_4 (1.5 mmol)	CH_3CN	60	04	48
24[c]	K_3PO_4 (1.5 mmol)	CH_3CN	60	04	29

[a] Phenylacetylene (1 mmol), **2** (0.1 mol%) in $(CH_3)_2NCHO$ (0.1 ml), CuI (0.5 mol%), base, solvent (1 ml).

[b] Without **2**. [c] Without CuI.

Optimization of the reaction conditions was performed by varying the base and its amount, solvent (1 ml) and temperature using 1 mmol of the substrate phenylacetylene and **2** (0.1 mol% in 0.1 ml dimethylformamide) with CuI (0.5 mol%) as the catalyst system in presence of air (Table 4.4). In each attempt, the reaction was considered complete when there was no change of the substrate concentration. The best condition was found to be the use of K_3PO_4 (1.5 mmol) as the base and acetonitrile as the solvent at a temperature of 60 °C (entry 12). Under this condition in 4 h the reaction was complete and 93% yield was obtained. In the control experiments, 48% yield was obtained without **2** (entry 23) and 29% yield was obtained in the absence of CuI (entry 24). In the previously reported first instance of cyclopalladate catalyzed homocoupling of terminal alkynes, a dinuclear *ortho*-metallated complex $[Pd_2(\mu\text{-}Cl)_2(L')_2]$ (0.05 mol%) (HL′ = 4,4'-dichlorobenzophenone oxime) and CuI (5 mol%) were used

as the catalyst mixture [32]. The reactions performed in N-methylpyrrolidinone solvent in presence of pyrrolidine or Bu_4NOAc as base provided 90–99% yields of the coupled products in 2–3 h, but at a much higher temperature of 110 °C. While in the second such example, both the dinuclear $[Pd_2(\mu\text{-}Cl)_2(L'')_2]$ and the mononuclear $[Pd(L'')(PPh_3)Cl]$ (HL″ = 4-methyl-*N*-(ferrocenylidene)aniline) cyclopalladates (1 mol%) along with CuI (2.5 mol%) were examined as the catalyst systems in presence of KOAc as the base for the terminal alkyne homocoupling reactions in dimethylformamide solvent at 40 °C [42]. The reaction showed a broad substrate scope with yields in the range of 42–96%, but the reaction time varied from 2 to 44 h. The reaction time also increases significantly with the decrease of the catalyst

loading from 1 mol% to 0.1 mol%. It was also found that the mononuclear complex was more active and efficient than the dinuclear complex. In the present study, change of the catalyst from the mononuclear **2** to the teranuclear **1** keeping the same loading (0.1 mol%) did not affect the reaction time and the yield in any significant way (Table 4.5, entries 1 and 2). Further, the extents of the increase in the reaction time and the decrease in the yield with the decrease of the catalyst loading were very similar for both complexes (entries 3–8). The reaction time increased 2.5-fold and the yield decreased by about 20% for both **1** and **2** with the decrease of the catalyst loading from 0.1 to 0.001 mol%. Although both **1** and **2** displayed very similar catalytic activities, but the difference in the nuclearities of **1** and **2** suggests that **2** is a better performing catalyst than **1**.

Table 4.5. Variation of catalyst and its loading[a]

Entry	Catalyst	Mol%	Time (h)	Yield (%)
1	**1**	0.1	4 h	96
2	**2**	0.1	4 h	93
3	**1**	0.05	5 h	91
4	**2**	0.05	5 h	91
5	**1**	0.01	6 h	86
6	**2**	0.01	6 h	88
7	**1**	0.001	10 h	78
8	**2**	0.001	10 h	73

[a]Reaction conditions: Phenylacetylene (1 mmol), catalyst in $(CH_3)_2NCHO$ (0.1 ml), CuI (0.5 mol%), K_3PO_4 (1.5 mmol), CH3CN (1 ml), 60 ^{o} C.

4.4. Conclusions

The capability of N′-(9-anthracenylidene)benzothiohydrazide (H_2L) to produce cyclometallated species has been demonstrated. The cyclopalladated complexes isolated were characterized as the tetranuclear $[Pd_4(L)_4]$ (**1**) and the mononuclear $[Pd(L)(PPh_3)]$ (**2**). X-ray crystal structures of **1** and **2** revealed the pincer-like 5,6-membered fused chelate rings forming thioamidate-S, azomethine-N and 9-anthracenyl *peri*-C coordination mode of $(L)^{2-}$ and its additional ability to bridge a second metal atom via the thioamidate-S in **1**, leading to a cradle-like $\{Pd_4(\mu\text{-}S)_4\}$ core. The spectroscopic characteristics of **1** and **2** are consistent with the corresponding molecular structures. Both complexes exhibited comparable and decent catalytic activities in the oxidative homocoupling reaction of phenylacetylene.

4.5. References

[1] S. Das, S. Pal, *J. Organomet. Chem*. 689 (2004) 352–360.

[2] A.R.B. Rao, S. Pal, *J. Organomet. Chem*. 731 (2013) 67–72.

[3] K. Nagaraju, S. Pal, *J. Organomet. Chem*. 745-746 (2013) 404–408.

[4] A.R.B. Rao, S. Pal, *J. Organomet. Chem*. 762 (2014) 58–66.

[5] A.R.B. Rao, S. Pal, *J. Organomet. Chem*. 797 (2015) 96–100.

[6] R.N. Prabhu, S. Pal, *J. Chem. Sci*. 127 (2015) 589–596.

[7] G.N. Babu, S. Pal, *J. Organomet. Chem*. 805 (2016) 19–26.

[8] K. Nagaraju, S. Pal, *Inorg. Chim. Acta* 413 (2014) 102–108.

[9] D.D. Perrin, W.L.F. Armarego, D.P. Perrin, Purification of Laboratory Chemicals, 2nd ed., Pergamon, Oxford, 1983.

[10] CrysAlisPro version 1.171.37.34i, Agilent Technologies, Yarnton, Oxfordshire, UK, 2014.

[11] P. van der Sluis, A.L. Spek, *Acta Crystallogr. Sect. A* 46 (1990) 194–201.

[12] A.L. Spek, Platon, A Multipurpose Crystallographic Tool, Utrecht University, Utrecht, The Netherlands, 2002.

[13] G.M. Sheldrick, *Acta Crystallogr. Sect. A* 64 (2008) 112–122.

[14] L.J. Farrugia, *J. Appl. Crystallogr*. 45 (2012) 849−854.

[15] C.F. Macrae, I.J. Bruno, J.A. Chisholm, P.R. Edgington, P. McCabe, E. Pidcock, L. Rodriguez-Monge, R. Taylor, J. van de Streek, P.A. Wood, *J. Appl. Crystallogr*. 41 (2008) 466−470.

[16] J.M. Antelo, L. Adrio, M.T. Pereira, J.M. Ortigueira, J.J. Fernández, J.M. Vila, *Cryst. Growth Des*. 10 (2010) 700−708.

[17] P. Pelagatti, A. Venturini, A. Leporati, M. Carcelli, M. Costa, A. Bacchi, G. Pelizzia, C. Pelizzi, *J. Chem. Soc., Dalton Trans*. (1998) 2715–2721.

[18] P. Paul, S. Bhattacharya, *J. Chem. Sci*. 126 (2014) 1547–1555.

[19] S. Lentijo, J.A. Miguel, P. Espinet, *Dalton Trans*., 40 (2011) 7602–7609.

[20] D. Nin-Vien, N.B. Clothup, W.G. Fateley, J.G. Grasselli, The Handbook of Infrared and Raman Characteristic Frequencies of Organic Molecules, Academic Press, London, 1991, pp. 236–238.

[21] H. Du, R.A. Fuh, J. Li, L.A. Corkan, J.S. Lindsey, *Photochem. Photobiol*. 68 (1998) 141−142.

[22] Z. Bedlovicová, J. Imrich, P. Kristian, I. Danihel, S. Böhm, D. Sabolová, M. Kozurková, H. Paulíková, K.D. Klika, *Heterocycles* 80 (2010) 1047−1066.

[23] S. Lentijo, J.A. Miguel, P. Espinet, *Organometallics*. 30 (2011) 1059−1066.

[24] P. Siemens, R.C. Livingston, F. Diederich, *Angew. Chem. Int. Ed*. 39 (2000) 2632−2657.

[25] A.L.K.S. Shun, R.R. Tykwinski, *Angew. Chem. Int. Ed*. 45 (2006) 1034–1057.

[26] H.A. Stefani, A.S. Guarezemini, R. Cella, *Tetrahedron* 66 (2010) 7871–7918.

[27] W. Shi, A. Lei, *Tetrahedron Lett*. 55 (2014) 2763–2772.

[28] W. Shei, *Curr. Organocatal*. 2 (2015) 2–13.

[29] K.S. Sindhu, A.P. Thankachan, P.S. Sajitha, G. Anilkumar, *Org. Biomol. Chem*. 13 (2015) 6891–6905.

[30] C. Glaser, *Ber. Dtsch.Chem. Ges*. 2 (1869) 422–424.

[31] C. Glaser, *Ann. Chem. Pharm*. 154 (1870) 137–171.

[32] D.A. Alonso, C. Nájera, M.A. Pacheco, *Adv. Synth. Catal*. 345 (2003) 1146–1158.

[33] F. Yang, X. Cui, Y. Li, J. Zhang, G. Rena, Y. Wu, *Tetrahedron* 63 (2007) 1963–1969.

Chapter 5

Syntheses, Characterization and Catalytic properties of two cyclopalladated complexes with *N′*-(2-naphthaldimine)benzohydrazide

Condensation reaction of 2-naphthaldehyde with one equivalent of benzohydrazide in presence of acetic acid in refluxing methanol yielded the Schiff base *N′*-(2-naphthaldimine)benzohydrazide (H_2L) in 86% yield. Reaction of equimolar amounts of Li_2PdCl_4 (generated in situ from $PdCl_2$ and LiCl taken in 1:2 mole ratio), H_2L and $NaOAc{\cdot}3H_2O$ in methanol at room temperature provided the complex [Pd(HL)Cl] (**1**) in 82% yield. Treatment of one mole equivalent of **1** with two mole equivalents of PPh_3 in acetone at room temperature produced the complex [Pd(L)(PPh_3)] (**2**) in 72% yield. The Schiff base and the two complexes were characterized by elemental analysis, mass spectrometric and various spectroscopic (IR, UV-Vis and ^{1}H-NMR) measurements. The molecular structures of both complexes (**1** and **2**) were determined by single crystal X-ray crystallography. In each square-planar complex, the tridentate ligand (HL^- in **1** and L^{2-} in **2**) acts as pincer-like CNO-donor. The fourth coordination site is occupied by chloride in **1**, while that in **2** is satisfied by the P-atom of PPh_3. The 2-naphthyl fragment of both $(HL)^-$ and $(L)^{2-}$ is palladated at the 3-position. Complex **2** was found to be an effective catalyst for one-pot Suzuki-Miyaura double cross-coupling reactions of 3,5-dihalosalicylaldehydes with a variety of arylboronic acids to provide the corresponding triaryl products in moderate to excellent yields.

5.1. Introduction

Regioselective cyclometallation reaction is an important tool in organic

synthesis reactions as it can assist in functionalization of a specific site among

several available. The Schiff base *N'*-(2-naphthaldimine)benzohydrazide (H_2L,

2 Hs represent the amide-H and the H-atom at the 1- or 3-position of the 2-

naphthyl group) is one such Schiff base (Scheme 5.1). It is expected that the

chelation of the Schiff base via the azomethine-N and the amide-O atom will

bring the 2-naphthyl moiety in close proximity of the metal center for the activation of its C–H bond either at the 1- or 3-position both being *ortho* to the azomethine group and eventual cyclometallation at one of the two C-atoms.

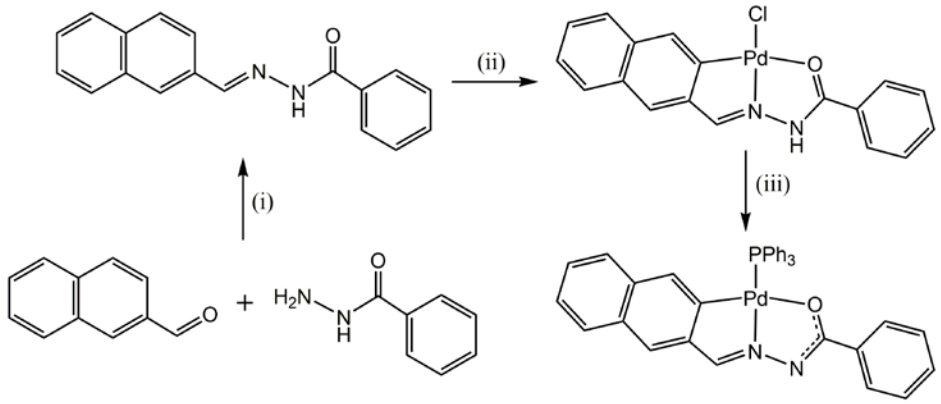

There are very few reports on cyclometallated 2-naphthyl containing chelating ligands [1–4]. As observed in the previous reports, generally 3-position gets regioselectively metallated when both 1- and 3-positions of the 2-naphthyl fragment are available [1–3]. In such cases, it is thought that the 1-position is not accessible for metallation due to steric hindrance caused by the H-atom at the *peri*-C (8-position). However, it has been shown that the 1-position of the 2-naphthyl group can be metallated when the 3-position is blocked by a substituent [4]. In the present chapter, we have studied the palladium(II) coordination chemistry of H_2L to examine how the cyclopalladation of the 2-naphthyl fragment occurs. In this effort, two complexes, [Pd(HL)Cl] (**1**) and [Pd(L)(PPh_3)] (**2**), have been isolated. In these complexes, the 3-position of the 2-naphthyl fragment of each of the two pincer-like tridentate ligands (HL^- and L^{2-}) is regioselectively metallated (Scheme 5.1). In the following sections, syntheses, X-ray crystal structures and spectroscopic properties of these two complexes have been described. The catalytic activities of both complexes in the one-pot Suzuki-Miyaura double cross-coupling reactions of 3,5-dihalosalicylaldehydes with various arylboronic acids have been also evaluated.

Scheme 5.1. (i) CH_3COOH (few drops) in methanol boiled under reflux. (ii) $PdCl_2$, LiCl and NaOAc·3H $_2O$ (1:2:1 mole ratio) in methanol at 298 K. (iii) PPh_3 (2 molar equivalents) in acetone at 298 K.

5.2. Experimental

5.2.1. Materials

All chemicals used in this work were of analytical grade available commercially and were used as received without any further purification. All solvents used were purified by standard procedures [5].

5.2.2. Physical measurements

Elemental (CHN) analysis measurements were performed using a Thermo Finnigan Flash EA1112 series elemental analyzer. High resolution mass spectra were recorded with a Bruker Maxis (ESI-TOF analyzer) spectrometer. A Sherwood Scientific balance was used for room temperature magnetic susceptibility measurements. The solution electrical conductivities were measured with the help of a Digisun DI-909 conductivity meter. A Thermo Scientific Nicolet 380 FT-IR spectrophotometer was used to collect the infrared spectra. The electronic absorption spectra were recorded by employing a Shimadzu UV3600 UV-Vis-NIR spectrophotometer. A Bruker spectrometer was used to record the ^1H (400 MHz, $SiMe_4$ as an internal standard) and $^{31}P\{^1H\}$ (160 MHz, 85% H_3PO_4 as an external standard) NMR spectra.

5.2.3. Synthesis of H_2L

Few drops of acetic acid were added to a methanol solution (40 ml) of benzohydrazide (681 mg, 5 mmol) and 2-naphthaldehyde (786 mg, 5 mmol) and the resulting mixture was refluxed for 5 h. The reaction mixture was then

cooled to room temperature. The white solid precipitated was filtered, washed with methanol (2 x 15 ml) and finally dried in vacuum. Yield: 1.18 gm (86%). Anal. Calcd for $C_{18}H_{14}N_2O$ (%): C, 78.81; H, 5.14; N, 10.21. Found (%): C, 78.65; H, 5.21; N, 10.12. HRMS in $CHCl_3$ m/z found (calcd) for $[M+H]^+$: 275.1187 (275.1184). Selected IR bands: ν (cm^{-1}) = 3199 (N–H), 1638 (C=O), 1605 (C=N). UV-Vis in Me_2NCHO: λ_{max} (nm) (ε (10^4 M^{-1} cm^{-1})) = 347^{sh} (0.65), 333^{sh} (1.74), 315 (2.48), 282 (2.01), 274 (1.86). ^{1}H NMR in $(CD_3)_2SO$: δ (ppm) = 11.99 (s, 1H), 8.64 (s, 1H), 8.16 (s, 1H), 8.03–7.93 (m, 6H), 7.63–7.53 (m, 5H).

5.2.4. Synthesis of [Pd(HL)Cl] (1)

To a methanol (30 ml) solution of $Li_2[PdCl_4]$ (generated in situ from $PdCl_2$ (178 mg, 1 mmol) and LiCl (85 mg, 2 mmol)) were added H_2L (275 mg, 1 mmol) and $NaOAc{\cdot}3H_2O$ (137 mg, 1 mmol) and the mixture was stirred at room temperature (298 K) for 24 h. The yellow solid separated was collected by filtration, washed with methanol (2 x 10 ml) and then dried in vacuum. Yield: 340 mg (82%). Anal. Calcd for $C_{18}H_{13}N_2OClPd$ (%): C, 52.07; H, 3.16; N, 6.75. Found (%): C, 52.21; H, 3.09; N, 6.87. HRMS in $CHCl_3$-MeCN (1:1) m/z found (calcd) for $[M–Cl+MeCN]^+$: 420.0407 (420.0328). Selected IR bands: ν (cm^{-1}) = 3178 (N–H), 1612 (C=O), 1596 (C=N). UV-Vis in Me_2NCHO: λ_{max} (nm) (ε (10^4 M^{-1} cm^{-1})) = 442 (0.44), 419^{sh} (0.57), 394 (1.21), 374 (1.17), 356 (0.95). ^{1}H NMR in $(CD_3)_2SO$: δ (ppm) = 12.32 (br s, 1H), 8.85 (s, 1H), 8.33 (s, 1H), 8.11–7.99 (m, 2H), 7.83–7.33 (m, 6H), 7.25–7.16 (m, 1H), 7.01–6.94 (m, 1H).

5.2.5. Synthesis of [Pd(L)(PPh_3)] (2)

Solid PPh_3 (263 mg, 1 mmol) was added to a suspension of [Pd(HL)Cl] (**1**) (208 mg, 0.5 mmol) in acetone (25 ml) and the mixture was stirred at room

temperature (298 K) for 24 h. The light yellow solid precipitated was collected by filtration, washed with acetone (2 x 10 ml) and finally dried in air. Yield: (230 mg, 72%). Anal. Calcd for $C_{36}H_{27}N_2OPPd$ (%): C, 67.45; H, 4.25; N, 4.37. Found (%): C, 67.31; H, 4.18; N, 4.46. HRMS in $CHCl_3$ m/z found (calcd) for $[M+H]^+$: 641.0971 (641.0974). Selected IR bands: ν (cm^{-1}) = 1587 (C=N). UV-Vis in Me_2NCHO: λ_{max} (nm) (ε (10^4 M^{-1} cm^{-1})) = 448 (0.63), 422 (0.78), 393 (1.26), 374 (1.18), 357 (0.84). ^1H NMR in $CDCl_3$: δ (ppm) (J (Hz)) = 8.04 (s, 1H), 8.02 (s, 1H), 7.91 (7) (d, 1H), 7.79–7.75 (m, 6H), 7.59 (6) (d, 1H), 7.56–7.52 (m, 4H), 7.49–7.46 (m, 6H), 7.42 (6) (d, 1H), 7.37 (6) (t, 2H), 7.26 (6) (t, 1H), 7.19 (6) (t, 1H), 6.80 (6) (d, 1H), 6.32 (3) (d, 1H). $^{31}P\{^1H\}$ NMR in $CDCl_3$: δ (ppm) = 34.06.

5.2.6. General procedure for double cross-coupling reactions

In a 10 ml round bottom flask, 3,5-dihalosalicylaldehyde (1 mmol), arylboronic acid (2.2 mmol for diiodo precursor or 2.5 mmol for dibromo precursor), $LiOH{\cdot}H_2O$ (2 mmol) and complex **2** (0.01 mol% for diiodo precursor or 0.05 mol% for dibromo precursor) in 0.1 ml dimethylformamide were taken in 2 ml of water-methanol (1:1) mixture. The reaction mixture was then heated at 80 °C under aerobic condition. Progress of the reaction was monitored by TLC. On completion, the reaction mixture was cooled to room temperature and extracted with two 10 ml portions of ethyl acetate. The combined extract was washed with water (2 x 10 ml), dried over anhydrous Na_2SO_4 and finally the solvent was removed under reduced pressure. The solid obtained was subjected to column chromatography over silica gel using ethyl acetate and hexane mixture as the eluent to afford the pure product. All the functionalized triaryl products obtained were characterized by ^1H-NMR spectroscopy and high resolution mass spectrometry.

5.2.7. X-ray crystallography

Single crystals of [Pd(HL)Cl] (**1**) were grown by diethyl ether vapor diffusion into its dimethylformamide solution, whereas single crystals of [Pd(L)(PPh_3)] (**2)** were obtained by slow evaporation of its chloroform-methanol (1:1) solution. **1** crystallizes as **1**·Me_2NCHO and **2** crystallizes as it is without any solvent molecule. Unit cell determination and intensity data collection for **1**·Me_2NCHO were performed on an Oxford Diffraction Xcalibur Gemini single crystal X-ray diffractometer using graphite monochromated Mo *K*α radiation (λ = 0.71073 Å) at 298 K. Data collection, reduction and absorption correction were performed using the CrysAlisPro software [6]. In the case of **2**, a Bruker D8 QUEST diffractometer equipped with a PHOTON 100 CMOS area detector and an INCOATEC microfocus source for graphite-monochromated Mo *K*α radiation (λ = 0.71073 Å) was used for determination of the unit cell and intensity data collection at 298 K. The APEX3 software package [7] was used for data collection, data integration, reduction and absorption correction. The structures of both complexes were solved by direct method and refined on F^2 by full-matrix least-squares procedures. The structure of **2** was refined as an inversion twin using the TWIN/BASF procedure [8]. The non-hydrogen atoms of both structures were refined anisotropically. In the case of **2**, four carbon atoms (two from benzoyl phenyl ring and two from PPh_3 phenyl ring) were

Table 5.1. Selected crystallographic data for **1**·Me_2NCHO and **2**

Complex	**1**·Me_2NCHO	**2**
Chemical formula	$C_{21}H_{20}ClN_3O_2Pd$	$C_{36}H_{27}N_2OPPd$
Formula weight	488.25	640.97
Crystal system	Monoclinic	Monoclinic
Space group	*C*2/c	$P2_1$
a (Å)	21.2070(12)	10.7825(4)

b (Å)	7.8317(4)	25.5879(9)
c (Å)	25.7759(15)	11.1205(4)
β (°)	108.187(6)	106.426(2)
V (Å^3), Z	4067.2(4), 8	2942.94(18), 4
ρ_{calcd} (g cm^{-3})	1.595	1.447
μ (mm^{-1})	1.065	0.717
Refl. collected	8212	54013
Refl. unique	4161	12071
Refl. [$I \geq 2\sigma(I)$]	2872	10725
Data/Restraints/Parameters	4161/0/255	12071/3/740
$R1$, $wR2$ [$I \geq 2\sigma(I)$]	0.0483, 0.0740	0.0392, 0.0948
$R1$, $wR2$ [all data]	0.0825, 0.0853	0.0478, 0.0986
GOF on F^2	1.031	1.080
Max./Min. $\Delta\rho$ (e Å^{-3})	0.481/–0.434	0.945/–0.510

refined with restraints on anisotropic displacement parameters. All hydrogen atoms were included in the structure factor calculation at idealized positions using a riding model. The SHELX-97 programs [8] available in the WinGX software suite [9] were used for structure solution and refinement. The Mercury package [10] was used to prepare the molecular illustrations. Crystallographic data for both structures have been deposited with the Cambridge Crystallographic Data Centre. The deposition numbers are CCDC 1553122 and 1553123 for **1**·Me_2NCHO and **2**, respectively. Selected crystal data and structure refinement summary are given in Table 5.1.

5.3. Results and discussion

5.3.1. Synthesis and characterization

The Schiff base *N'*-(2-naphthaldimine)benzohydrazide (H_2L) was prepared in good yield (86%) by condensation reaction of equimolar amounts of 2-naphthaldehyde and benzohydrazide in methanol in presence of a few drops of acetic acid (Scheme 5.1). The purity and the identity of H_2L have been confirmed by elemental analysis, mass spectrometric and spectroscopic (IR, UV-Vis and ^{1}H NMR) measurements. The palladium(II) complex [Pd(HL)Cl] (**1**) was synthesized in 77% yield by reacting in situ generated Li_2PdCl_4, $NaOAc{\cdot}3H_2O$ and H_2L in 1:1:1 mole ratio in methanol at room temperature. The second complex [Pd(L)(PPh_3)] (**2**) was synthesized in 73% yield by treating **1** with two equivalents of PPh_3 in acetone (Scheme 5.1). The excess PPh_3 is expected to facilitate the deprotonation of the amide functionality of HL^- in **1**. The elemental analyses data of **1** and **2** are in good agreement with their corresponding molecular formulas. In chloroform and dichloromethane, **2** is highly soluble but **1** is sparingly soluble. Both complexes are highly soluble in dimethylformamide and dimethylsulfoxide, sparingly soluble in acetonitrile and methanol and insoluble in hexane and toluene. Due to solvent restrictions and the solubility problem the positive ion ESI mass spectrum of **1** was collected in $CHCl_3$-MeCN (1:1) mixture, where its solubility is slightly better when compared with that in the pure solvents. The spectrum shows the base peak at 420.0407 corresponding to the cation where the chloride is replaced by acetonitrile, i.e., $[\mathbf{1}–Cl+MeCN]^+$. On the other hand, the spectrum of **2** in pure $CHCl_3$ displays the usual $[\mathbf{2}+H]^+$ as the base peak at 641.0971. As expected for square-planar complexes of palladium(II), both **1** and **2** are diamagnetic. The electrically non-conducting nature of **1** and **2** in solution is consistent with their molecular formulas as neutral species.

5.3.2. Spectroscopic properties

5.3.2.1. Infrared spectra

Infrared spectra of the Schiff base (H_2L) and the complexes (**1** and **2**) were recorded by employing KBr pellets in the range 4000–400 cm^{-1}. The spectra of H_2L and [Pd(HL)Cl] (**1**) are shown in Figures 5.1 and 5.2, respectively. A large number of bands have been observed in all three spectra. Except for few characteristic bands we have not attempted to assign the remaining bands. The free Schiff base (H_2L) displays the typical bands for the amide N–H and C=O stretching vibrations at 3199 and 1638 cm^{-1}, respectively. A medium intensity band observed at 1605 cm^{-1} has been assigned to the azomethine C=N stretching vibration. The spectrum of **1** displays the amide N–H stretch at 3178 cm^{-1}. Two medium intensity bands observed at 1612 and 1596 cm^{-1} are assigned to the amide C=O and the azomethine C=N stretching frequencies, respectively. Appearance of these two bands at lower frequencies compared to those of the free Schiff base is consistent with the coordination of both amide-O and azomethine-N to the metal center in **1**. On the other hand, the spectrum of **2** does not display the amide N–H and C=O stretching bands due to deprotonation of the amide functionality. A strong band observed at 1587 cm^{-1} is most likely associated with the one end coordinated diazine (C=N–N=C) like fragment of $(L)^{2-}$ in **2**.

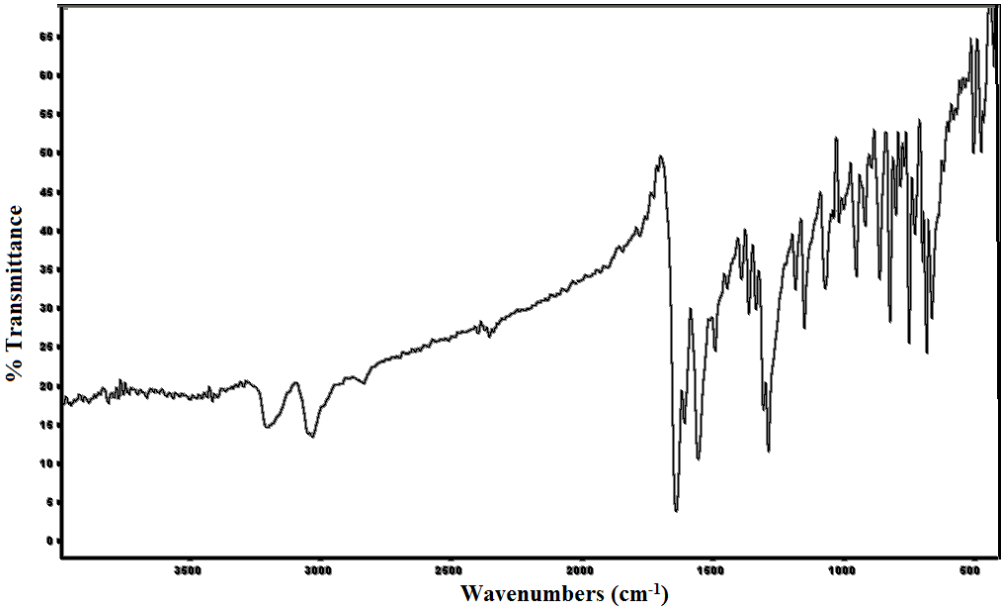

Figure 5.1. IR-spectrum of H_2L

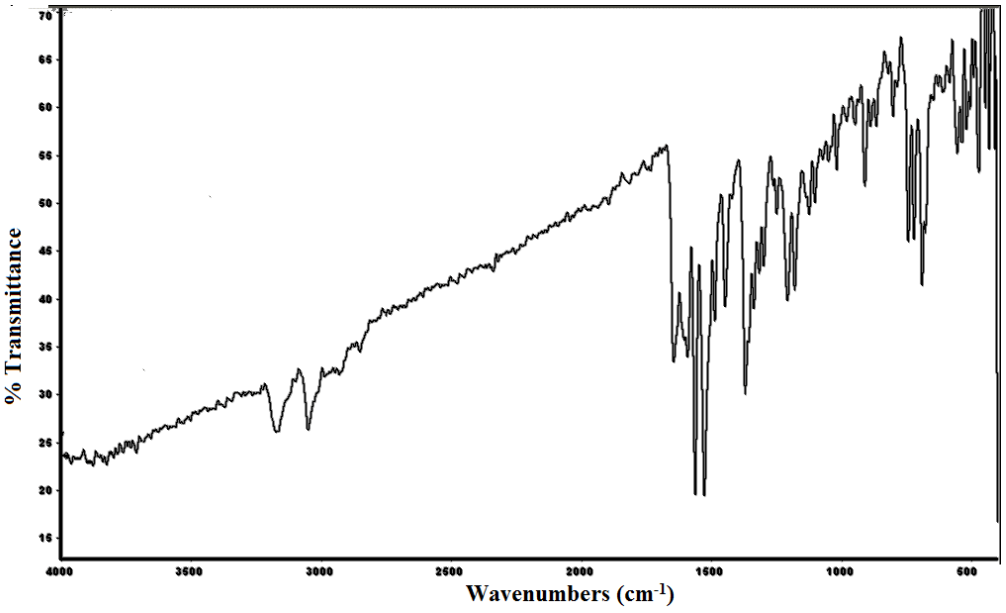

Figure 5.2. IR-spectrum of [Pd(HL)Cl] (**1**)

5.3.2.2. Electronic spectra

Electronic absorption spectra of H_2L, **1** and **2** were recorded in dimethylformamide. The spectrum of H_2L displays a broad band centered at 315 nm preceded by a couple of shoulders and followed by a relatively narrow band at 282 nm and a shoulder (Figure 5.3). This type of spectral profile is typical of organic compounds containing naphthyl group [11-13]. Pure naphthalene is known to display similar absorptions at higher energy region with more pronounced vibrational structure [14,15]. The spectral profile of naphthalene consists of a group of absorption bands centered at ~275 nm. The absorption profiles of the two complexes **1** and **2** are very similar to that of the naphthalene except for a large red-shift. A group of five bands are observed in the range 448–356 nm for both **1** and **2**. The spectrum of **2** is illustrated in Figure 5.3. Thus the absorption bands observed for H_2L as well as its complexes **1** and **2** are attributed to transitions predominantly centered at their corresponding 2-naphthyl fragments.

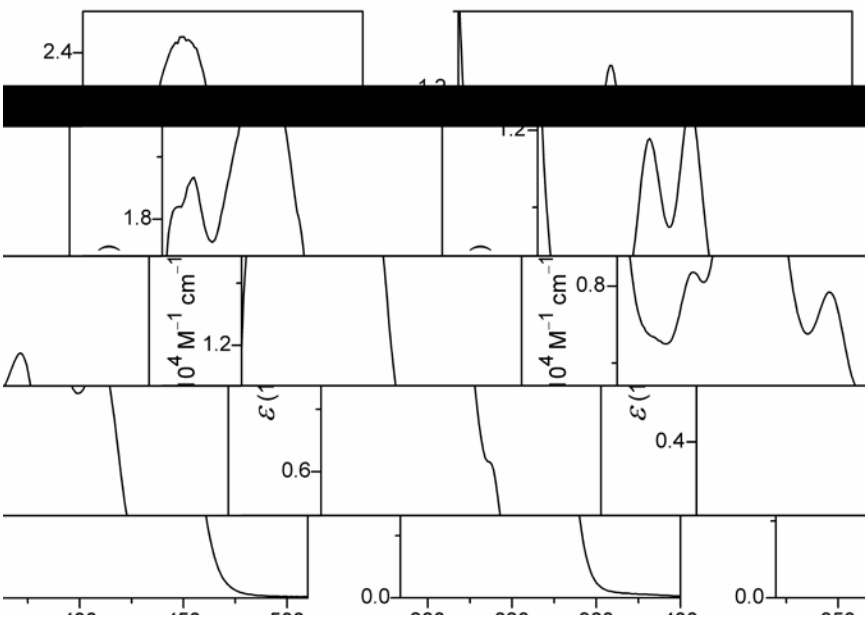

Figure 5.3. Electronic spectra of H_2L (left) and [Pd(L)(PPh_3)] (**2**) (right) in dimethylformamide.

5.3.2.3. NMR spectra

^1H NMR spectra of H_2L and **1** were recorded in $(CD_3)_2SO$ solution and the ^1H and $^{31}P\{^1H\}$ spectra of **2** were recorded in $CDCl_3$ solution. The ^1H NMR spectra of H_2L and **2** are illustrated in Figures 5.4 and 5.5, respectively. The amide N–H proton of H_2L resonates as a singlet at δ 11.99 ppm. The azomethine proton and the proton at the 1-position of the 2-naphthyl fragment of H_2L appear as two one-proton singlets at δ 8.64 and 8.16 ppm, respectively. The remaining aromatic protons are observed as a six-proton multiplet and another five-proton multiplet having the chemical shifts centered at δ ~7.98 and ~7.58 ppm, respectively. A broad singlet at δ 12.32 ppm due to the amide N–H proton of the ligand HL^- is observed in the spectrum of **1**. As in the free Schiff base, here also two one-proton singlets corresponding to the azomethine proton and the proton at the 1-position of the 2-naphthyl fragment of HL^- are observed at δ 8.85 and 8.33 ppm, respectively. Slight downfield shifts of these three resonances in **1** when compared with those in free H_2L are not unusual considering the deshielding caused by coordination of the amide-O and the azomethine-N to the palladium(II) center. The remaining ten aromatic protons belonging to the 2-naphthyl and the phenyl rings of HL^- appear as four multiplets centered at δ ~8.05, ~7.58, ~7.21 and ~6.98 ppm. As expected the spectrum of **2** does not display the signal corresponding to the amide N–H due to deprotonation. The spectrum shows two closely spaced one-proton singlets at δ 8.04 and 8.02 ppm followed by a one-proton doublet at δ 7.91 ppm. The singlets are very likely to be due to the protons at the 1- and 4-positions of the 2-naphthyl fragment of L^{2-}. The one-proton doublet is assigned to the azomethine proton. The doublet splitting is attributed to the PPh_3 P-atom coordinated at the *trans*-position with respect to the azomethine-N. There is a

significant upfield shift of the azomethine proton in **2** compared to that in H_2L

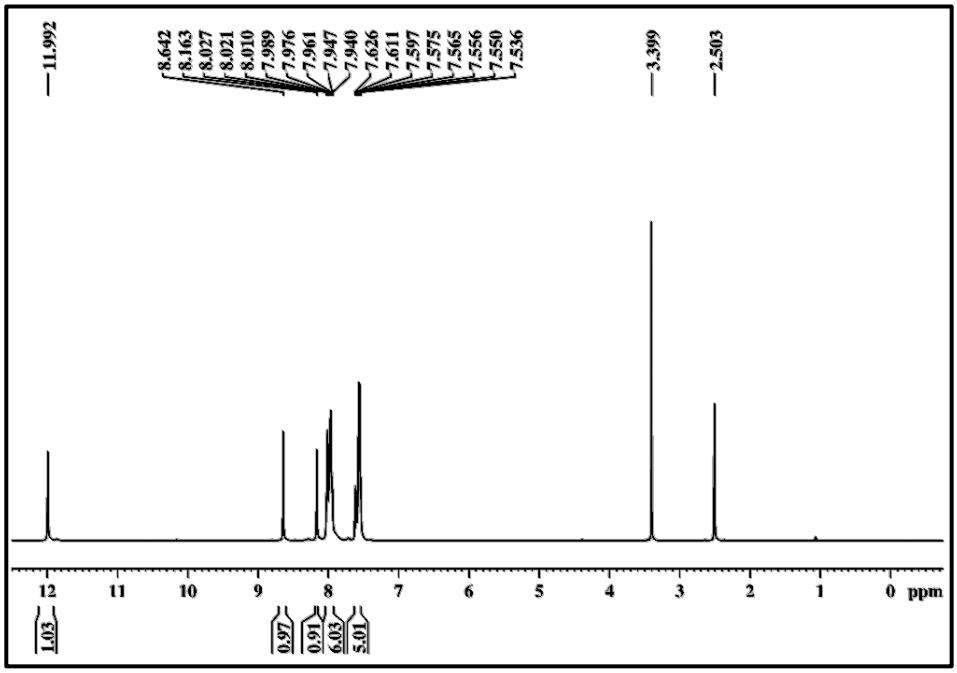

and **1**. It is very likely that the stronger σ-donor PPh_3 facilitates better π-

Figure 5.4. ^{1}H-NMR spectrum of H_2L

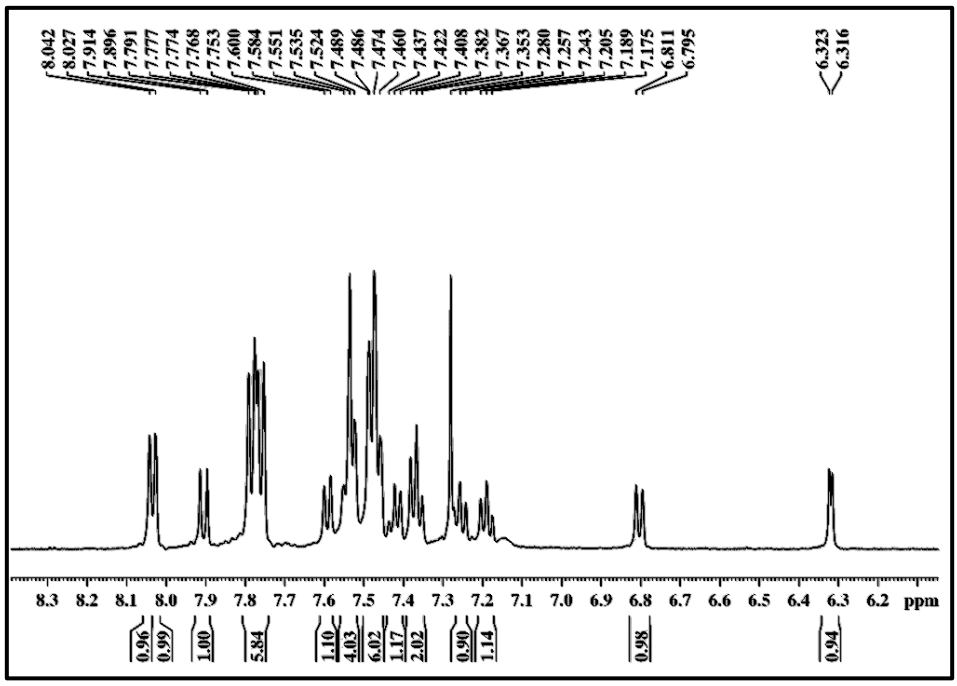

Figure 5.5. ^{1}H-NMR spectrum of [Pd(L)(PPh_3)] (**2**)

backdonation from metal to azomethine in **2** and hence causes the upfield shift of the azomethine proton. The remaining nine aromatic protons of L^{2-} and fifteen protons of the PPh_3 phenyl rings appear in the range δ 7.79–6.32 ppm with various splitting patterns such as doublet, triplet and multiplet. In general, the aromatic protons in the complexes are observed over a broader chemical shift range than in the free Schiff base due to shielding/deshielding caused by metal coordination and presence of the monodentate ancillary ligands. The singlet observed at δ 34.06 ppm in the $^{31}P\{^{1}H\}$ NMR spectrum of **2** confirms the presence of PPh_3 as the ancillary ligand.

4.3.2.4. X-ray molecular structures

The structures of **1**·Me_2NCHO and **2** have been solved in the monoclinic space groups *C*2/c and $P2_1$, respectively. The asymmetric unit of **1**·Me_2NCHO consists of one molecule each of the complex and the solvent dimethylformamide, while that of **2** contains two complex molecules. In **1**·Me_2NCHO, the solvent molecule is hydrogen bonded with the complex molecule. The structure of the solvated species is illustrated in Figure 5.6. The O-atom of the solvent molecule and the amide-NH of the ligand HL^- are involved in this hydrogen bonding. The N(2)···O(2) distance and the N(2)–H···O(2) angle are 2.734(5) Å and 165°, respectively. In contrast, there is no significant interaction between the two complex molecules present in the asymmetric unit of **2**. Both molecules are very similar with respect to intramolecular bond lengths and bond angles. Thus the structure of one of these two independent molecules of **2** is depicted in Figure 5.7. Selected bond parameters for **1**·Me_2NCHO and **2** are listed in Table 5.2. In each complex, the tridentate ligand (HL^- in **1** and L^{2-} in **2**) acts as pincer-like CNO-donor

and forms fused 5,5-membered chelate rings. The structures reveal that the 2-naphthyl fragment of each of HL^- and L^{2-} is palladated at the 3-position instead of the 1-position. In the amide functionality (–C(=O)NH–) of HL^- in **1**, the C(12)–N(2) and the C(12)–O(1) bond lengths are 1.358 (5) and 1.246 (5) Å, respectively. These values are consistent with the neutral keto form of the amide functionality [18–20,22,23]. On the other hand, for **2** the average of C(12/12′)–N(2/2′) bond lengths and that of C(12/12′)–O(1/1′) bond lengths are 1.335(6) and 1.285(6) Å, respectively (Table 5.2). The shorter C(12/12′)–N(2/2′) and longer C(12/12′)–O(1/1′) bond lengths in **2** compared to the corresponding bond lengths in **1** clearly indicate that the amide functionality of L^{2-} in **2** is deprotonated and their values suggest that the negative charge is delocalized over the amidate fragment [16–24]. The HL^- and the chloride constitute a CNOCl square-plane around the metal center in **1**, while the L^{2-} and the PPh_3 assemble a square-planar CNOP coordination environment for the metal center in **2**. In both complexes, the metal center has no deviation from the square-plane formed by the four coordinating atoms. The rms deviations from the mean plane constituted by the metal and the four coordinating atoms are within 0.01–0.02 Å. The amidate-O is expected to be a better σ-donor than the amide-O. As a consequence, the Pd–O(amidate) bond length in **2** is significantly shorter (by ~0.1 Å) than the Pd–O(amide) bond length in **1**. In contrast, the Pd–C bond length in **1** is shorter by ~0.05 Å than that in **2**. This lengthening of the Pd–C bond in **2** is very likely due to the better *trans*-directing ability of the amidate-O than the amide-O (Figures. 5.6 and 5.7). Similarly the stronger *trans*-effect of PPh_3 than Cl^- causes a longer (by ~0.02 Å) Pd–N(azomethine) bond length in **2** compared to that in **1** (Table 5.2). Overall, all the bond lengths and the bond angles associated with the metal centers in **1** and **2** are within the ranges observed for palladium(II) complexes with similar ligands [16,18–20,22-23].

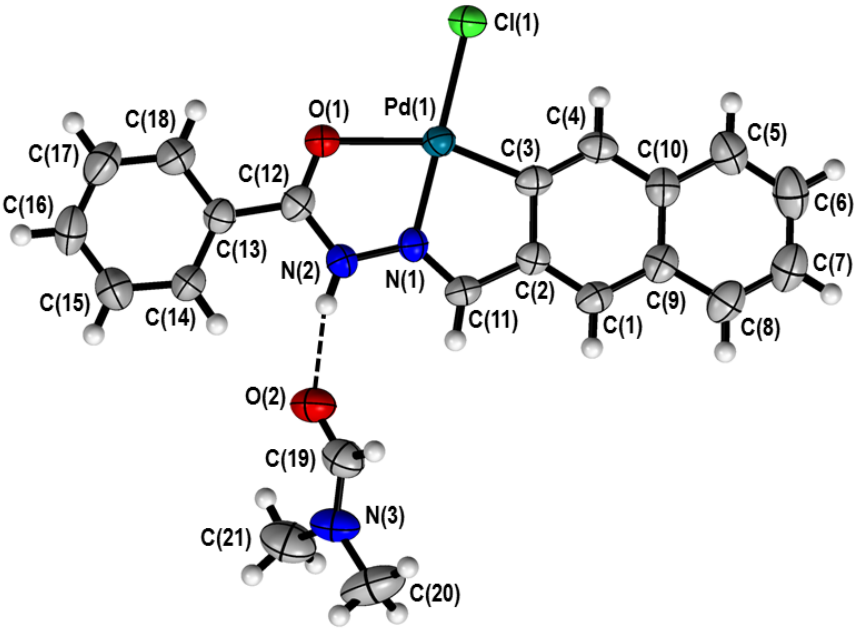

Figure 5.6. ORTEP representation of [Pd(HL)Cl]·Me_2NCHO (**1**·Me_2NCHO) with the atom numbering scheme. All non-hydrogen atoms are shown by their 50% probability thermal ellipsoids.

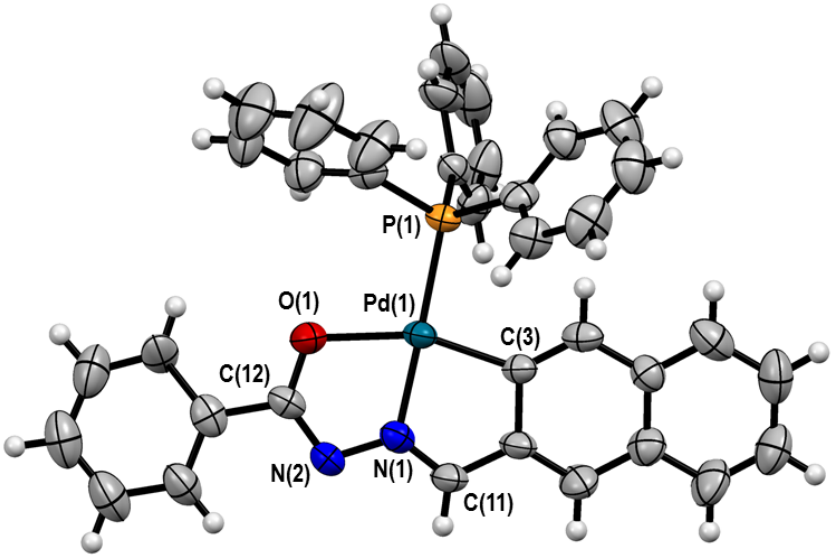

Figure 5.7. ORTEP representation of one of the two molecules of [Pd(L)(PPh_3)] (**2**) present in the asymmetric unit. The thermal ellipsoids for the non-hydrogen atoms are drawn at the 50% probability level. All non-carbon atoms and a few selected carbon atoms are labeled for clarity.

Table 5.2. Selected bond lengths (Å) and angles (°) for **1**·Me_2NCHO and **2**

[Pd(HL)Cl]·Me_2NCHO (**1**·Me_2NCHO)			
Pd(1)–C(3)	1.953(4)	Pd(1)–N(1)	1.977(3)
Pd(1)–O(1)	2.208(3)	Pd(1)–Cl(1)	2.2929(12)
C(12)–N(2)	1.358(5)	C(12)–O(1)	1.246(5)
C(3)–Pd(1)–N(1)	81.89(15)	C(3)–Pd(1)–O(1)	158.13(14)
C(3)–Pd(1)–Cl(1)	98.89(13)	N(1)–Pd(1)–O(1)	76.26(12)
N(1)–Pd(1)–Cl(1)	178.89(9)	O(1)–Pd(1)–Cl(1)	102.97(8)
[Pd(L)(PPh_3)] (**2**)			
Molecule 1			
Pd(1)–C(3)	2.008(5)	Pd(1)–N(1)	1.996(4)
Pd(1)–O(1)	2.107(3)	Pd(1)–P(1)	2.2594(11)
C(12)–N(2)	1.333(6)	C(12)–O(1)	1.288(6)
C(3)–Pd(1)–N(1)	82.25(18)	C(3)–Pd(1)–O(1)	158.52(15)
C(3)–Pd(1)–P(1)	98.94(13)	N(1)–Pd(1)–O(1)	76.40(15)
N(1)–Pd(1)–P(1)	178.55(13)	O(1)–Pd(1)–P(1)	102.38(10)
Molecule 2			
Pd(1′)–C(3′)	2.005(5)	Pd(1′)–N(1′)	2.002(4)
Pd(1′)–O(1′)	2.113(3)	Pd(1′)–P(1′)	2.2586(11)
C(12′)–N(2′)	1.337(6)	C(12′)–O(1′)	1.282(6)
C(3′)–Pd(1′)–N(1′)	82.62(19)	C(3′)–Pd(1′)–O(1′)	158.62(16)
C(3′)–Pd(1′)–P(1′)	98.61(15)	N(1′)–Pd(1′)–O(1′)	76.17(16)
N(1′)–Pd(1′)–P(1′)	178.18(14)	O(1′)–Pd(1′)–P(1′)	102.53(9)

5.3.2.5. Catalytic activities

Functionalized polyaryls and polyheteroaryls are of considerable interest because of their potential applications in natural products, biological, agrochemical, pharmaceutical and materials research [25–29]. Hence, there has been a continuous effort to develop new and efficient methods for the synthesis of such species [30–33]. Among the various strategies used so far, the simplest and most versatile approach is the palladium catalyzed Suzuki-Miyaura poly cross-coupling reactions of polyhaloaromatic compounds with arylboronic acids [34–37]. In the present work, we have attempted the one-pot synthesis of functionalized triaryls via double cross-coupling reactions of 3,5-dihalosalicylaldehydes with various arylboronic acids using the cyclopalladated complexes **1** and **2** as catalysts. The reaction of 3,5-diiodosalicylaldehyde and phenylboronic acid in presence of **2** as catalyst was chosen as the model reaction to screen the bases and the solvents (Table 5.3). Among the various inorganic bases used in water-methanol (1:1) as the reaction solvent (entries 1–6), $LiOH \cdot H_2O$ was found to provide the best yield (94 %) of the double cross-coupling product 3,5-diphenylsalicylaldehyde at a reaction temperature of 80 °C (entry 4). No coupling product was detected in the absence of base (entry 7). Using $LiOH \cdot H_2O$ as the base the reaction was then performed in various water-solvent (1:1) mixtures (entries 8–13). In all these reaction solvents, no yield to very poor yields were observed. Subsequently the reaction was conducted under the identical conditions as described in entry 4 except for the use of **1** instead of

2 as catalyst (entry 14). The change of the catalyst caused a significantly low yield (80%) of the coupled product and indicated that **2** is a better catalyst than **1**. Thus the optimal reaction conditions were found to be the use of 3,5-diiodosalicylaldehyde (1 mmol), phenylboronic acid (2.2 mmol), $LiOH \cdot H_2O$

(2 mmol) and **2** (0.01 mol%) in water-methanol (1:1) at 80 °C for 15 h (entry 4).

Table 5.3. Optimization of reaction conditions[a]

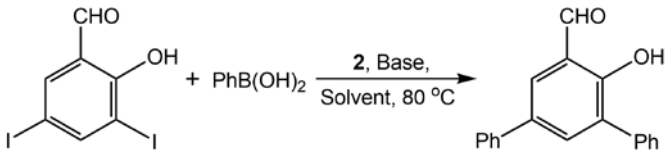

Entry	Base	Solvent	Time (h)	Yield[b] (%)
1	K_2CO_3	H_2O-MeOH	15	90
2	Na_2CO_3	H_2O-MeOH	15	86
3	$NaHCO_3$	H_2O-MeOH	24	70
4	$LiOH·H_2O$	H_2O-MeOH	15	94
5	K_3PO_4	H_2O-MeOH	24	N.R.[c]
6	$NaOAc·3H_2O$	H_2O-MeOH	24	N.R.[c]
7	–	H_2O-MeOH	24	N.R.[c]
8	$LiOH·H_2O$	H_2O-thf	24	N.R.[c]
9	$LiOH·H_2O$	H_2O-dioxane	24	10
10	$LiOH·H_2O$	H_2O-dcm	24	12
11	$LiOH·H_2O$	H_2O-nmp	24	24
12	$LiOH·H_2O$	H_2O-dmso	24	28
13	$LiOH·H_2O$	H_2O-dmf	24	30
14	$LiOH·H_2O$	H_2O-MeOH	15	80[d]

[a] 3,5-Diiodosalicylaldehyde (1 mmol), phenylboronic acid (2.2 mmol), base (2 mmol), **2** (0.01 mol%) in 0.1 ml of dimethylformamide, H_2O-solvent in 1:1 volume ratio (2 ml), 80 °C.

[b] Isolated yield.

[c] No reaction.

[d] Using **1** (0.01 mol%) instead of **2** as catalyst.

Table 5.4. Reactions of 3,5-diiodosalicylaldehyde with arylboronic acids[a]

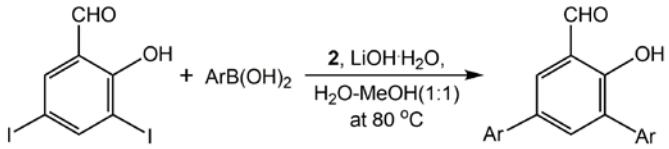

Entry	Ar	Time (h)	Yield[b] (%)
1	phenyl	15	94
2	*p*-anisolyl	24	88
3	*p*-fluorophenyl	20	90
4	*m*-chlorophenyl	24	92
5	2-naphthyl	24	90
6	*o*-anisolyl	24	74

[a] Conditions: 3,5-Diiodosalicylaldehyde (1 mmol), arylboronic acid (2.2 mmol), $LiOH·H_2O$ (2 mmol), **2** (0.01 mol%) in 0.1 ml of dimethylformamide, H_2O-MeOH in 1:1 volume ratio (2 ml), 80°C.

[b] Isolated yield.

To examine the substrate scope of the catalyst **2**, one-pot double cross-coupling reactions of 3,5-diiodosalicylaldehyde with various arylboronic acids were performed under the above mentioned optimal conditions. The results are summarized in Table 5.4. As observed with phenylboronic acid (entry 1), high yields (88–92%) of the double cross-coupled products were also obtained with *p*-methoxy-, *p*-fluoro-, and *m*-chlorophenylboronic acids and 2-naphthylboronic acid but in 5 to 9 h longer reaction times (entries 2–5). Comparatively rather low yield (74%) was obtained with *o*-anisolylboronic

acid even in longer reaction duration (entry 6). The scope of the catalyst **2** was further extended to double cross-coupling reactions of 3,5-dibromosalicylaldehyde with the same group of arylboronic acids which was used for 3,5-diiodosalicylaldehyde. The reaction of 3,5-dibromosalicylaldehyde with phenylboronic acid under the same optimal conditions described above for the diiodo precursor provided the product 3,5-diphenylsalicylaldehyde but in significantly low yield (40%). However, increase of the catalyst loading from 0.01 to 0.05 mol% and the amount of the phenylboronic acid doubled the yield to 82% in 24 h of reaction time (Table 5.5, entry 1). The reactions with the remaining arylboronic acids were then performed with the higher (0.05 mol%) catalyst loading and arylboronic acid to dibromo precursor mole ratio (2.5:1) (entries 2–6). The corresponding double cross-coupled products were isolated

Table 5.5. Reactions of 3,5-dibromosalicylaldehyde with arylboronic acids[a]

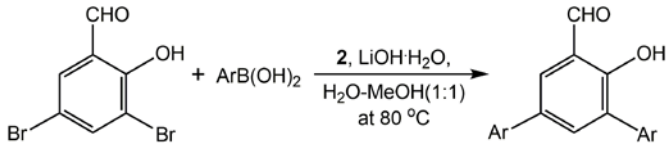

Entry	Ar	Time (h)	Yield[b] (%)
1	phenyl	24	82
2	*p*-anisolyl	24	80
3	*p*-fluorophenyl	24	84
4	*m*-chlorophenyl	30	60
5	2-naphthyl	30	62
6	*o*-anisolyl	24	83

[a] Conditions: 3,5-Dibromosalicylaldehyde (1 mmol), arylboronic acid (2.5 mmol), $LiOH \cdot H_2O$ (2 mmol), **2** (0.05 mol%) in 0.1 ml of dimethylformamide, H_2O-MeOH in 1:1 volume ratio (2 ml), 80^oC.
[b] Isolated yield.

were isolated in moderate to good yields (60–83%). In general, despite the use of higher catalyst loading and mole ratio of the reactants and comparable or longer reaction times, the yields of the coupled products from the dibromo precursor are less (Table 5.5) than the yields obtained in the case of the diiodo precursor (Table 5.4). This difference in the reactivities is attributable to the fact that the C–Br bond is stronger than the C–I bond [38].

5.4. Conclusions

Synthesis, characterization and spectroscopic properties of the Schiff base *N'*-(2-naphthaldimine)benzohydrazide (H_2L) and the cyclometallated palladium(II) complexes ([Pd(HL)Cl] and [Pd(L)(PPh_3)]) with it have been described. The X-ray molecular structures of the two complexes reveal pincer-like CNO coordination mode of both $(HL)^-$ and $(L)^{2-}$and regioselective cyclopalladation at the 3-position of the 2-naphthyl group of each ligand. The spectroscopic characteristics of the two complexes are consistent with their molecular structures. Catalytic properties of both complexes in one-pot Suzuki-Miyaura double cross-coupling reactions of 3,5-dihalosalicylaldehydes with a variety of arylboronic acids have been investigated. Between the two complexes, [Pd(L)(PPh_3)] has been found to be the better perfoming catalyst . The catalytic reactions exhibited reasonable substrate scope and provided moderate to excellent yields of the functionalized triaryls.

5.5. References

[1] J.–M. Valk, F. Maassarani, P. van der Sluis, A.L. Spek, J. Boersma, G. van Koten, *Organometallics* 13 (1994) 2320–2329.

[2] M. Crespo, M. Font-Bardía, S. Pérez, X. Solans, *J. Organomet. Chem*. 642 (2002) 171–178.

[3] S. Fuertes, H. García, M. Perálvarez, W. Hertog, J. Carreras, V. Sicilia, *Chem. Eur. J*. 21 (2015) 1620–1631.

[4] J.–M. Valk, R. van Belzen, J. Boersma, A.L. Spek, G. van Koten, *J. Chem. Soc. Dalton Trans*. (1994) 2293–2302.

[5] D.D. Perrin, W.L.F. Armarego, D.P. Perrin, Purification of Laboratory Chemicals, second ed., Pergamon, Oxford, 1983.

[6] CrysAlisPro Version 1.171.36.28, Agilent Technologies, Yarnton, Oxfordshire, UK, 2013.

[7] Bruker (2016). APEX3, SAINT-Plus and SADABS. Bruker AXS Inc., Madison, Wisconsin, USA.

[8] G.M. Sheldrick, *Acta Crystallogr. Sect. A* 64 (2008) 112–122.

[9] L.J. Farrugia, *J. Appl. Crystallogr*. 45 (2012) 849–854.

[10] F. Macrae, I.J. Bruno, J.A. Chisholm, P.R. Edgington, P. M. Cabe, E. Pidcock, L. Rodriguez-Monge, R. Taylor, J. van de Streek, P.A. Wood, *J. Appl. Crystallogr*. 41 (2008) 466–470.

[11] J.R. Cardinal, P. Mukerjee, *J. Phys. Chem*. 82 (1978) 1614–1620.

[12] P.K. Lekha, T. Ghosh, E. Prasad, *J. Chem. Sci*. 123 (2011) 919–926.

[13] R.N. Prabhu, S. Pal, *J. Chem. Sci*. 127 (2015) 589–596.

[14] J.M. Dixon, M. Taniguchi, J.S. Lindsey, *Photochem. Photobiol*. 81 (2005) 212–213.

[15] J. Krausko, J.K. Malongwe, G. Bičanová, P. Klán, D. Nachtigallová, D. Heger, *J. Phys. Chem. A* 119 (2015) 8565−8578.

[16] S. Das, S. Pal, *J. Organomet. Chem*. 689 (2004) 352–360.

[17] R. Raveendran, S. Pal, *J. Organomet. Chem*. 692 (2007) 824–830.

[18] A.R.B. Rao, S. Pal, *J. Organomet. Chem*. 696 (2011) 2660–2664.

[19] A.R.B. Rao, S. Pal, *J. Organomet. Chem*. 701 (2012) 62–67.

[20] A.R.B. Rao, S. Pal, *J. Organomet. Chem*. 731 (2013) 67–72.

[21] K. Nagaraju, S. Pal, *J. Organomet. Chem*. 737 (2013) 7–11.

[22] A.R.B. Rao, S. Pal, *J. Organomet. Chem*. 762 (2014) 58–66.

[23] G.N. Babu, S. Pal, *J. Organomet. Chem*. 805 (2016) 19–26.

[24] G.N. Babu, S. Pal, *J. Organomet. Chem*. 824 (2016) 42–47.

[25] J.–K. Liu, *Chem. Rev*. 106 (2006) 2209–2223.

[26] F. Bellina, R. Rossi, *Tetrahedron* 62 (2006) 7213–7256.

[27] G. Hervé, C. Len, *Sust. Chem. Proc*. 3 (2015) 3.

[28] J.E. Anthony, *Chem. Rev*. 106 (2006) 5028–5048.

[29] A.R. Murphy, J.M.J. Fréchet, *Chem. Rev*. 107 (2007) 1066–1096.

[30] D. Pérez, E. Guitián, *Chem. Soc. Rev*. 33 (2004) 274–283.

[31] X. Feng, W. Pisula, K. Müllen, *Pure Appl. Chem*. 81 (2009) 2203–2224.

[32] D. Pérez, D. Peña, E. Guitián, *Eur. J. Org. Chem*. (2013) 5981–6013.

[33] T. Truong, M. Mesgar, K.K.A. Le, O. Daugulis, *J. Am. Chem. Soc*. 136 (2014) 8568−8576.

[34] L. Liu, Y. Zhang, B. Xin, *J. Org. Chem*. 71 (2006) 3994–3997.

[35] F. Beaumard, P. Dauban, R. H. Dodd, *Org. Lett*. 11 (2009) 1801–1804.

[36] A.R. Chaudhary, A.V. Bedekar, *Appl. Organometal. Chem*. 26 (2012) 430–437.

[37] S. Reimann, P. Ehlers, M. Sharif, A. Spannenberg, P. Langer, *Tetrahedron* 72 (2016) 1083–1094.

[38] Y.–R. Luo, Handbook of Bond Dissociation Energies in Organic Compounds, CRC Press LLC, Boca Raton, 2003.

Appendix

Tables for atomic coordinates (x 10^4) and equivalent isotropic displacement parameters ($Å^2$ x 10^3). U(eq) is defined as one third of the trace of the orthogonalized U^{ij} tensor.

Table A.1. [Pd(HL^1)Cl] (**1**·Me_2NCHO) **(chapter 2)**

Atom	x	y	z	U(eq)
Pd(1)	411(1)	-960(1)	7775(1)	48(1)
Cl(1)	934(1)	-1903(1)	7803(2)	70(1)
O(1)	1002(2)	-470(2)	6186(4)	60(1)
N(1)	0(2)	-135(2)	7672(5)	41(1)
N(2)	327(2)	287(2)	6770(5)	50(1)
C(1)	-899(3)	-302(3)	9269(6)	46(2)
C(2)	-766(3)	-919(3)	9668(7)	49(2)
C(3)	-1198(3)	-1233(3)	10537(7)	59(2)
C(4)	-1752(3)	-974(4)	10999(7)	66(2)
C(5)	-1873(3)	-361(3)	10582(7)	62(2)
C(6)	-1469(3)	-15(3)	9731(7)	57(2)
C(7)	-165(3)	-1262(3)	9292(7)	69(2)
C(8)	-2209(3)	-1321(3)	11934(7)	97(3)
C(9)	-1634(3)	642(3)	9293(7)	69(2)
C(10)	-497(3)	62(3)	8326(7)	53(2
C(11)	836(3)	82(3)	6054(7)	49(2)
C(12)	1168(3)	532(3)	5091(6)	50(2)
C(13)	1704(3)	315(3)	4401(7)	62(2)
C(14)	2039(3)	700(4)	3481(8)	76(2)
C(15)	1854(3)	1304(4)	3278(7)	74(2)
C(16)	1332(4)	1527(4)	3963(7)	78(2)
C(17)	982(3)	1138(3)	4868(7)	63(2)
O(2)	-261(2)	1456(2)	6889(5)	80(2)
N(3)	-1146(3)	2045(3	6831(6)	62(2)

Table A.1. Continued……

C(18)	-760(4)	1612(3)	6321(7)	62(2)
C(19)	-988(4)	2392(3)	8168(7)	108(3)
C(20)	-1739(3)	2167(4)	6147(8)	110(3)

Table A.2. [Pd(HL^2)Cl] (**2**·Me_2NCHO) **(chapter 2)**

Atom	x	y	z	U(eq)
Pd(1)	3908(1)	1972(1)	2521(1)	38(1)
Cl(1)	3035(2)	3834(1)	2249(1)	63(1)
O(1)	5579(3)	2688(3)	4123(2)	46(1)
O(2)	10325(4)	2435(3)	8433(3)	59(1)
N(1)	4773(4)	417(3)	2737(3)	37(1)
N(2)	5684(4)	554(3)	3787(3)	41(1)
C(1)	3728(5)	-965(4)	941(3)	41(1)
C(2)	2748(4)	-181(4)	536(3)	41(1)
C(3)	2012(5)	-497(4)	-575(3)	48(1)
C(4)	2158(5)	-1594(5)	-1282(3)	50(1)
C(5)	3127(5)	-2346(5)	-870(4)	52(1)
C(6)	3936(5)	-2058(4)	228(4)	46(1)
C(7)	2314(5)	894(4)	1255(4)	51(1)
C(8)	1260(5)	-1940(5)	-2449(3)	63(1)
C(9)	4992(7)	-2922(5)	593(4)	64(1)
C(10)	4595(5)	-674(4)	2072(3)	41(1)
C(11)	6104(4)	1764(4)	4415(3)	39(1)
C(12)	7212(4)	1923(4)	5474(3)	39(1)
C(13)	7259(5)	2949(4)	6323(3)	42(1)
C(14)	8277(5)	3157(4)	7322(3)	46(1)
C(15)	9272(5)	2335(4)	7490(3)	45(1)
C(16)	9262(5)	1316(4)	6637(4)	50(1)
C(17)	8234(5)	1115(4)	5650(4)	48(1)

Table A.2. Continued……

C(18)	10411(7)	3481(6)	9337(4)	69(1)
O(3)	6715(5)	-1709(3)	3914(3)	72(1)
N(3)	7549(4)	-3527(4)	4189(3)	51(1)
C(19)	7314(6)	-2358(5)	4517(5)	63(1)
C(20)	7105(8)	-4175(6)	3063(5)	87(2)
C(21)	8375(10)	-4174(7)	4974(6)	107(2)

Table A.3.[Pd(L^1)(PPh_3)] (3) (chapter 2)

Atom	x	y	z	U(eq)
Pd(1)	6518(1)	4606(1)	7636(1)	38(1)
P(1)	5847(1)	2882(1)	8671(1)	37(1)
O(1)	4575(2)	5653(2)	7323(2)	48(1)
N(1)	7105(3)	6074(2)	6621(2)	36(1)
N(2)	6000(3)	7036(2)	6338(2)	41(1)
C(1)	9677(3)	5375(3)	6331(2)	38(1)
C(2)	9721(3)	4261(3)	7041(2)	40(1)
C(3)	11039(4)	3371(3)	7020(3)	49(1)
C(4)	12282(4)	3566(4)	6357(3)	54(1)
C(5)	12206(4)	4690(4)	5694(3)	54(1)
C(6)	10944(4)	5602(3)	5662(3)	44(1)
C(7)	8477(3)	4031(3)	7844(3)	49(1)
C(8)	13688(4)	2593(4)	6355(3)	78(1)
C(9)	10969(4)	6782(4)	4910(3)	61(1)
C(10)	8353(3)	6268(3)	6211(2)	41(1)
C(11)	4772(3)	6703(3)	6748(3)	42(1)
C(12)	3498(3)	7702(3)	6531(3)	45(1)
C(13)	2181(4)	7408(4)	6868(3)	54(1)
C(14)	980(4)	8378(4)	6733(3)	67(1)
C(15)	1112(5)	9609(4)	6265(3)	74(1)

Table A.3. Continued……

C(16)	2412(4)	9894(4)	5914(3)	74(1)
C(17)	3595(4)	8944(4)	6053(3)	60(1)
C(18)	6765(3)	2187(3)	9581(2)	37(1)
C(19)	7459(3)	877(3)	9727(3)	46(1)
C(20)	8132(4)	412(4)	10447(3)	59(1)
C(21)	8122(4)	1254(4)	11007(3)	62(1)
C(22)	7440(4)	2567(4)	10865(3)	57(1)
C(23)	6787(3)	3038(3)	10147(3)	48(1)
C(24)	6094(3)	1529(3)	8049(2)	36(1)
C(25)	5277(3)	604(3)	8379(3)	49(1)
C(26)	5451(4)	-349(3)	7838(3)	56(1)
C(27)	6416(4)	-387(3)	6979(3)	55(1)
C(28)	7239(4)	507(4)	6653(3)	61(1)
C(29)	7077(3)	1458(3)	7187(3)	49(1)
C(30)	3970(3)	3138(3)	9331(3)	43(1)
C(31)	2968(4)	3634(3)	8811(3)	59(1)
C(32)	1541(4)	3718(4)	9272(4)	73(1)
C(33)	1118(4)	3340(4)	10221(4)	81(2)
C(34)	2093(4)	2903(4)	10733(3)	82(1)
C(35)	3515(4)	2794(4)	10276(3)	64(1)

Table A.4. [Pd(L^2)(PPh_3)] (4) (chapter 2)

Atom	x	y	z	U(eq)
Pd(1)	848(1)	2301(1)	2385(1)	34(1)
P(1)	1639(1))	2188(1)	3957(1)	32(1)
O(1)	2216(2)	1223(2)	1449(2)	45(1)
O(2)	4096(3)	-2733(3)	-1577(3)	66(1)
N(1)	257(3)	2412(2)	906(2)	37(1)
N(2)	841(3)	1593(3)	227(2)	41(1)
C(1)	-1291(3)	4043(3)	1073(3)	38(1)

Table A.4. Continued……

C(2)	-1326(3)	4112(3)	2231(3)	38(1)
C(3)	-2002(3)	5071(3)	2662(3)	44(1)
C(4)	-2627(3)	5952(3)	1995(4)	46(1)
C(5)	-2565(3)	5865(3)	860(3)	48(1)
C(6)	-1923(3)	4930(3)	391(3)	43(1)
C(7)	-771(3)	3165(3)	3046(3)	42(1)
C(8)	-3359(4)	6975(4)	2474(4)	63(1)
C(9)	-1900(4)	4886(4)	-850(3)	56(1)
C(10)	-596(3)	3098(3)	533(3)	41(1)
C(11)	1815(3)	1053(3)	588(3)	38(1)
C(12)	2490(3)	114(3)	-38(3)	38(1)
C(13)	3508(3)	-526(3)	301(3)	48(1)
C(14)	4078(4)	-1473(4)	-199(4)	53(1)
C(15)	3624(4)	-1801(3)	-1045(3)	48(1)
C(16)	2627(4)	-1149(3)	-1414(3)	49(1)
C(17)	2051(4)	-203(3)	-919(3)	45(1)
C(18)	4936(6)	-3552(4)	-1069(5)	80(2)
C(19)	623(3)	2058(3)	5368(3)	35(1)
C(20)	896(4)	2524(3)	6237(3)	46(1)
C(21)	204(4)	2305(4)	7344(3)	55(1)
C(22)	-772(4)	1633(4)	7580(3)	58(1)
C(23)	-1072(4)	1192(3)	6715(4)	53(1)
C(24)	-371(3)	1409(3)	5613(3)	42(1)
C(25)	2447(3)	3473(3)	3895(3)	39(1)
C(26)	1768(4)	4564(3)	3820(4)	54(1)
C(27)	2301(6)	5556(4)	3828(4)	71(1)
C(28)	3509(6)	5494(4)	3875(5)	77(2)
C(29)	4197(5)	4430(5)	3911(5)	77(2)
C(30)	3653(4)	3415(4)	3938(4)	56(1)
C(31)	2773(3)	921(3)	4143(3)	36(1)

Table A.4. Continued……

C(32)	2691(3)	103(3)	5157(3)	45(1)
C(33)	3520(4)	-892(4)	5223(4)	56(1)
C(34)	4429(4)	-1059(4)	4285(4)	57(1)
C(35)	4522(4)	-244(4)	3279(4)	51(1)
C(36)	3692(3)	738(3)	3200(3)	41(1)

Table A.5. [Pd_2(μ-dppb)(L^1)$_2$] (5) (chapter 2)

Atom	x	y	z	U(eq)
Pd(1)	8266(1)	1944(1)	9538(1)	42(1)
P(1)	8478(1)	3565(1)	8485(1)	39(1)
O(1)	8636(2)	2430(1)	10976(1)	52(1)
N(1)	7976(2)	549(2)	10564(2)	45(1)
N(2)	8283(3)	584(2)	11565(2)	54(1)
C(1)	7121(3)	-558(2)	9466(2)	52(1)
C(2)	7313(3)	156(2)	8502(2)	53(1)
C(3)	6731(3)	-52(3)	7674(2)	64(1)
C(4)	6029(3)	-970(3)	7738(3)	72(1)
C(5)	5898(3)	-1675(3)	8683(3)	72(1)
C(6)	6399(3)	-1503(2)	9544(3)	61(1)
C(7)	8203(4)	1084(2)	8269(2)	60(1)
C(8)	5476(5)	-1167(4)	6789(3)	104(1)
C(9)	6136(4)	-2286(2)	10556(3)	76(1)
C(10)	7581(3)	-367(2)	10400(2)	56(1)
C(11)	8585(3)	1577(2)	11682(2)	49(1)
C(12)	8931(3)	1709(2)	12729(2)	55(1)
C(13)	9838(4)	2452(2)	12757(3)	73(1)
C(14)	10254(5)	2533(3)	13700(3)	87(1)
C(15)	9753(5)	1911(4)	14622(3)	92(1)
C(16)	8836(5)	1162(5)	14606(3)	114(2)

Table A.5. Continued……

C(17)	8447(4)	1053(4)	13667(3)	91(1)
C(18)	10155(3)	3427(2)	7304(2)	44(1)
C(19)	10348(3)	4330(2)	6540(2)	62(1)
C(20)	11652(4)	4249(3)	5684(2)	76(1)
C(21)	12769(4)	3264(3)	5574(3)	76(1)
C(22)	12601(3)	2358(3)	6319(3)	77(1)
C(23)	11289(3)	2434(2)	7180(2)	58(1)
C(24)	6920(3)	4207(2)	7886(2)	44(1)
C(25)	6874(3)	3790(2)	6916(2)	58(1)
C(26)	5652(4)	4226(3)	6490(3)	74(1)
C(27)	4480(4)	5083(3)	7022(3)	78(1)
C(28)	4516(3)	5513(3)	7975(3)	69(1)
C(29)	5727(3)	5074(2)	8403(2)	56(1)
C(30)	8594(3	4759(2)	9246(2)	44(1)
C(31)	10043(3)	4540(2)	9604(2)	46(1)

Table A.6. $[Pd_2(\mu\text{-dppb})(L^2)_2]$ (6) (chapter 2)

Atom	x	y	z	U(eq)
Pd(1)	7971(1)	2087(1)	486(1)	62(1)
P(1)	7393(1)	3651(1)	1418(1)	61(1)
O(1)	9246(3)	2538(2)	-949(2)	78(1)
O(2)	14164(6)	1875(4)	-5152(3)	143(2)
N(1)	8401(3)	719(3)	-417(2)	62(1)
N(2)	9383(4)	736(3)	-1375(2)	68(1)
C(1)	6813(4)	-316(3)	720(3)	67(1)
C(2)	6392(4)	389(3)	1595(3)	67(1)
C(3)	5184(5)	260(4)	2373(4)	76(1)
C(4)	4412(5)	-557(4)	2316(4)	83(1)
C(5)	4908(6)	-1279(4)	1481(4)	83(1)
C(6)	6089(5)	-1195(3)	686(4)	76(1)

Table A.6. Continued……

C(7)	7271(5)	1202(3)	1770(3)	68(1)
C(8)	3079(7)	-658(6)	3158(5)	118(2)
C(9)	6531(7)	-2005(4)	-203(4)	99(1)
C(10)	7929(4)	-168(3)	-186(3)	71(1)
C(11)	9722(4)	1696(3)	-1555(3)	67(1)
C(12)	10800(5)	1798(3)	-2547(3)	71(1)
C(13)	11519(6)	2652(4)	-2683(3)	86(1)
C(14)	12633(6)	2703(5)	-3542(4)	98(2)
C(15)	13042(6)	1911(5)	-4294(4)	98(2)
C(16)	12309(7)	1067(5)	-4197(4)	105(2)
C(17)	11201(6)	1003(4)	-3336(3)	87(1)
C(18)	15041(11)	2664(8)	-5228(6)	174(2)
C(19)	5387(4)	4272(3)	1825(3)	67(1)
C(20)	4760(7)	5389(5)	1886(6)	123(2)
C(21)	3232(7)	5778(6)	2229(7)	137(3)
C(22)	2313(6)	5130(6)	2506(6)	111(2)
C(23)	2861(7)	4066(6)	2434(7)	130(2)
C(24)	4401(6)	3622(4)	2083(5)	105(2)
C(25)	8134(4)	3509(3)	2660(3)	65(1)
C(26)	9311(5)	2648(4)	2800(4)	89(1)
C(27)	9894(6)	2535(6)	3731(5)	113(2)
C(28)	9316(8)	3263(7)	4521(5)	120(2)
C(29)	7538(7)	4231(5)	3480(4)	103(2)
C(30)	8147(9)	4095(6)	4421(5)	132(2)
C(31)	8090(5)	4779(4)	691(3)	77(1)
C(32)	9764(5)	4521(4)	349(4)	79(1)

Table A.7. [Pd_2(μ-dppf)(L^2)$_2$] (7) (chapter 2)

Atom	x	y	z	U(eq)
Pd(1)	2990(1)	2335(1)	2446(1)	40(1)
Fe(1)	5000	5000	5000	43(1)
P(1)	4530(1)	4337(1)	2671(1)	39(1)
O(1)	1641(2)	2541(2)	3456(1)	53(1)
O(2)	-2754(3)	1482(2)	6280(2)	75(1)
N(1)	1444(2)	600(2)	2206(1)	41(1)
N(2)	543(2)	382(2)	2875(1)	47(1)
C(1)	1890(3)	-213(2)	718(2)	44(1)
C(2)	3175(3)	782(2)	687(2)	45(1)
C(3)	3609(3)	951(3)	-139(2)	52(1)
C(4)	2841(3)	169(3)	-938(2)	54(1)
C(5)	1649(3)	-848(3)	-888(2)	55(1)
C(6)	1151(3)	-1061(3)	-85(2)	50(1)
C(7)	4110(3)	1619(3)	1510(2)	48(1)
C(8)	3265(4)	441(4)	-1829(2)	75(1)
C(9)	-195(3)	-2171(3)	-94(2)	63(1)
C(10)	1203(3)	-316(2)	1524(2)	47(1)
C(11)	718(3)	1448(2)	3457(2)	45(1)
C(12)	-238(3)	1399(3)	4183(2)	46(1)
C(13)	-29(3)	2482(3)	4840(2)	58(1)
C(14)	-875(4)	2475(3)	5532(2)	65(1)
C(15)	-1961(3)	1381(3)	5572(2)	57(1)
C(16)	-2181(3)	298(3)	4936(2)	56(1)
C(17)	-1316(3)	298(3)	4242(2)	52(1)
C(18)	-3895(4)	422(4)	6344(2)	76(1)
C(19)	6475(3)	4541(3)	2543(2)	47(1)
C(20)	7304(3)	5613(3)	2257(2)	66(1)
C(21)	8791(4)	5743(4)	2188(2)	88(1)
C(22)	9438(4)	4835(5)	2408(2)	88(1)

Table A.7. Continued……

C(23)	8642(4)	3793(4)	2705(2)	74(1)
C(24)	7146(3)	3633(3)	2764(2)	55(1)
C(25)	3884(3)	5208(2)	1858(2)	44(1)
C(26)	3518(3)	6335(3)	2107(2)	61(1)
C(27)	2993(4)	6935(4)	1464(3)	77(1)
C(28)	2846(4)	6418(4)	575(2)	76(1)
C(29)	3190(4)	5297(4)	323(2)	79(1)
C(30)	3691(4)	4678(3)	962(2)	65(1)
C(31)	4607(3)	5352(2)	3734(2)	42(1)
C(32)	3361(3)	5364(3)	4199(2)	49(1)
C(33)	3835(4)	6333(3)	4972(2)	59(1)
C(34)	5349(4)	6917(3)	5004(2)	62(1)
C(35)	5844(3)	6327(2)	4242(2)	52(1)

Table A.8. $[Pd_4(L)_4]$ ($1\cdot CHCl_3$) (chapter 4)

Atom	x	y	z	U(eq)
Pd(1)	3977(1)	1422(1)	607(1)	41(1)
Pd(2)	3337(1)	1786(1)	1105(1)	43(1)
Pd(3)	3278(1)	1039(1)	-420(1)	40(1)
Pd(4)	3468(1)	1641(1)	-1495(1)	44(1)
S(1)	3943(1)	1590(1)	-829(1)	42(1)
S(2)	3110(1)	1330(1)	757(1)	44(1)
S(3)	3740(1)	977(1)	251(1)	41(1)
S(4)	3311(1)	1943(1)	-344(1)	46(1)
N(1)	4145(1)	1830(1)	834(4)	42(2)
N(2)	4182(2)	2033(2)	154(4)	57(2)
N(3)	3337(1)	1613(1)	2306(4)	44(2)
N(4)	3271(2)	1310(2)	2436(4)	48(2)
N(5)	3468(1)	807(1)	-1381(4)	41(2)

Table A.8. Continued……

N(6)	3776(1)	737(2)	-1345(4)	47(2)
N(7)	3053(2)	1713(2)	-1920(4)	49(2)
N(8)	2846(2)	1864(2)	-1398(5)	59(2)
C(1)	4033(2)	1301(2)	1867(5)	48(2)
C(2)	4004(2)	1009(2)	2110(6)	69(3)
C(3)	4006(3)	908(3)	2973(7)	91(4)
C(4)	4024(2)	1107(3)	3610(6)	73(3)
C(5)	4251(3)	2092(3)	4713(7)	100(4)
C(6)	4347(4)	2376(3)	4601(8)	117(5)
C(7)	4391(3)	2478(3)	3762(8)	113(5)
C(8)	4340(3)	2310(2)	3041(6)	79(3)
C(9)	4178(2)	1814(2)	2422(5)	46(2)
C(10)	4115(2)	1611(3)	4108(6)	75(3)
C(11)	4196(2)	1904(3)	3988(6)	64(3)
C(12)	4243(2)	2016(2)	3123(6)	62(3)
C(13)	4097(2)	1511(2)	2553(5)	46(2)
C(14)	4077(2)	1413(2)	3432(5)	55(2)
C(15)	4207(2)	1949(2)	1572(5)	50(2)
C(16)	4080(2)	1957(2)	-593(5)	45(2)
C(17)	4086(2)	2179(2)	-1301(5)	58(2)
C(18)	4091(3)	2103(2)	-2157(6)	88(4)
C(19)	4088(3)	2321(3)	-2784(6)	117(5)
C(20)	4069(3)	2617(3)	-2566(8)	120(5)
C(21)	4069(3)	2695(3)	-1720(8)	110(4)
C(22)	4079(3)	2475(2)	-1099(6)	80(3)
C(23)	3510(2)	2180(2)	1537(5)	44(2)
C(24)	3614(2)	2393(2)	950(6)	59(2)
C(25)	3712(2)	2676(2)	1198(6)	69(3)
C(26)	3713(2)	2760(2)	2019(6)	71(3)
C(27)	3571(2)	2567(2)	5086(6)	77(3)

Table A.8. Continued……

C(28)	3499(3)	2386(3)	5733(6)	81(3)
C(29)	3407(3)	2097(3)	5574(7)	97(4)
C(30)	3390(3)	1985(2)	4756(6)	78(3)
C(31)	3452(2)	2062(2)	3137(5)	44(2)
C(32)	3633(2)	2646(2)	3534(6)	69(3)
C(33)	3555(2)	2461(2)	4221(6)	58(2)
C(34)	3457(2)	2164(2)	4030(6)	55(2)
C(35)	3518(2)	2264(2)	2440(5)	46(2)
C(36)	3622(2)	2556(2)	2681(6)	61(2)
C(37)	3378(2)	1755(2)	3024(5)	48(2)
C(38)	3180(2)	1162(2)	1766(5)	48(2)
C(39)	3113(2)	838(2)	1905(5)	48(2)
C(40)	2938(2)	674(2)	1336(5)	55(2)
C(41)	2877(2)	375(2)	1481(6)	65(3)
C(42)	2985(2)	235(2)	2179(7)	71(3)
C(43)	3159(2)	391(2)	2771(6)	70(3)
C(44)	3222(2)	687(2)	2634(5)	59(2)
C(45)	2876(2)	1052(2)	-1062(5)	41(2)
C(46)	2643(2)	1203(2)	-710(5)	53(2)
C(47)	2360(2)	1233(2)	-1092(6)	72(3)
C(48)	2310(2)	1103(3)	-1847(7)	79(3)
C(49)	2600(3)	475(3)	-4301(7)	100(4)
C(50)	2798(3)	314(3)	-4735(7)	97(4)
C(51)	3084(3)	270(3)	-4406(6)	85(3)
C(52)	3168(3)	410(2)	-3648(6)	77(3)
C(53)	3043(2)	736(2)	-2365(5)	44(2)
C(54)	2471(2)	787(2)	-3057(6)	74(3)
C(55)	2676(2)	620(2)	-3507(6)	69(3)
C(56)	2968(2)	593(2)	-3160(5)	56(2)
C(57)	2828(2)	902(2)	-1883(5)	46(2)

Table A.8. Continued……

C(58)	2534(2)	933(2)	-2269(6)	60(2)
C(59)	3346(2)	709(2)	-2088(5)	47(2)
C(60)	3915(2)	815(2)	-667(5)	44(2)
C(61)	4240(2)	747(2)	-611(6)	59(2)
C(62)	4370(2)	623(3)	89(7)	109(5)
C(63)	4664(3)	544(4)	105(8)	145(7)
C(64)	4840(2)	595(4)	-586(9)	120(5)
C(65)	4718(3)	719(4)	-1296(10)	143(6)
C(66)	4421(2)	789(3)	-1319(8)	111(5)
C(67)	3575(2)	1410(2)	-2595(5)	47(2)
C(68)	3851(2)	1282(2)	-2682(5)	56(2)
C(69)	3940(2)	1095(2)	-3367(5)	64(3)
C(70)	3750(3)	1041(2)	-4010(6)	77(3)
C(71)	2809(3)	1208(3)	-5540(7)	97(4)
C(72)	2544(3)	1335(3)	-5598(7)	102(5)
C(73)	2424(3)	1502(3)	-4918(7)	105(4)
C(74)	2591(3)	1538(3)	-4181(6)	88(4)
C(75)	3072(2)	1465(2)	-3337(5)	48(2)
C(76)	3266(3)	1126(2)	-4717(6)	78(3)
C(77)	3461(2)	1170(2)	-4013(5)	59(3)
C(78)	3366(2)	1350(2)	-3286(5)	47(2)
C(79)	2877(2)	1422(2)	-4079(5)	66(3)
C(80)	2989(3)	1249(3)	-4779(6)	75(3)
C(81)	2935(2)	1626(2)	-2651(5)	58(2)
C(82)	2933(2)	1965(2)	-662(6)	55(2)
C(83)	2706(2)	2117(2)	-127(5)	65(3)
C(84)	2405(2)	2063(3)	-249(7)	95(4)
C(85)	2190(3)	2209(4)	209(9)	130(5)
C(86)	2276(3)	2424(3)	804(10)	133(6)
C(87)	2568(3)	2479(3)	961(8)	106(4)

Table A.8. Continued……

C(88)	2784(2)	2326(2)	492(6)	80(3)
Cl(1)	2638(1)	1847(1)	2583(3)	165(2)
Cl(2)	2011(1)	1880(1)	2614(4)	186(2)
Cl(3)	2291(1)	1366(1)	1923(3)	174(2)
C(89)	2315(3)	1738(4)	2079(9)	127(5)

Table A.9. [Pd(L)(PPh_3)] (2·CH_3CN) (chapter 4)

Atom	x	y	z	U(eq)
Pd(1)	12052(1)	2487(1)	885(1)	32(1)
S(1)	11971(1)	1214(1)	1627(1)	42(1)
P(1)	13252(1)	1534(1)	496(1)	33(1)
N(1)	11150(3)	3279(2)	1367(1)	34(1)
N(2)	10705(3)	2794(2)	1824(1)	37(1)
C(1)	11827(3)	3623(2)	216(2)	35(1)
C(2)	11894(3)	3431(3)	-396(2)	43(1)
C(3)	11791(4)	4183(3)	-875(2)	54(1)
C(4)	11658(4)	5180(3)	-735(2)	52(1)
C(5)	11287(4)	7874(3)	776(2)	57(1)
C(6)	11225(4)	8171(3)	1356(2)	65(1)
C(7)	11173(4)	7436(3)	1820(2)	62(1)
C(8)	11184(4)	6411(3)	1691(2)	50(1)
C(9)	11338(3)	4983(2)	936(2)	34(1)
C(10)	11404(3)	6478(3)	26(2)	47(1)
C(11)	11313(3)	6805(3)	617(2)	45(1)
C(12)	11263(3)	6049(3)	1085(2)	40(1)
C(13)	11574(3)	4673(2)	357(2)	34(1)
C(14)	11538(3)	5452(3)	-119(2)	40(1)
C(15)	11047(3)	4265(2)	1368(2)	37(1)
C(16)	11047(3)	1856(2)	1956(2)	35(1)

Table A.9. Continued……

C(17)	10578(3)	1288(2)	2425(2)	36(1)
C(18)	11090(4)	402(3)	2723(2)	54(1)
C(19)	10638(5)	-128(3)	3147(2)	70(1)
C(20)	9688(5)	199(4)	3272(2)	66(1)
C(21)	9177(4)	1068(3)	2979(2)	60(1)
C(22)	9619(4)	1619(3)	2560(2)	46(1)
C(23)	14172(3)	783(3)	1138(2)	36(1)
C(24)	15162(4)	1185(3)	1491(2)	52(1)
C(25)	15782(4)	650(4)	2024(2)	71(1)
C(26)	15408(5)	-256(4)	2206(2)	66(1)
C(27)	14427(4)	-660(3)	1861(2)	54(1)
C(28)	13816(4)	-144(3)	1327(2)	45(1)
C(29)	14191(3)	2229(2)	131(2)	34(1)
C(30)	14479(3)	1916(3)	-417(2)	42(1)
C(31)	15216(4)	2481(3)	-649(2)	56(1)
C(32)	15687(4)	3355(3)	-345(2)	51(1)
C(33)	15407(4)	3685(3)	191(2)	59(1)
C(34)	14654(4)	3139(3)	422(2)	49(1)
C(35)	12576(3)	544(2)	-66(2)	36(1)
C(36)	13165(4)	-261(2)	-240(2)	44(1)
C(37)	12622(4)	-1027(3)	-646(2)	52(1)
C(38)	11495(4)	-999(3)	-873(2)	56(1)
C(39)	10892(4)	-214(3)	-704(2)	57(1)
C(40)	11442(3)	562(3)	-297(2)	44(1)
N(1)	7819(5)	-1897(4)	2956(3)	107(2)
C(41)	8007(5)	-1662(4)	2498(4)	86(2)
C(42)	8248(7)	-1346(5)	1907(3)	130(3)

Table A.10. [Pd(HL)Cl] (1·Me_2NCHO) (chapter 5)

Atom	x	y	z	U(eq)
Pd(1)	8206(1)	-1475(1)	-623(1)	40(1)
Cl(1)	9324(1)	-1570(2)	-500(1)	64(1)
O(1)	7780(1)	-2928(3)	-1387(1)	48(1)
N(1)	7242(2)	-1440(4)	-732(1)	36(1)
N(2)	6840(2)	-2223(4)	-1195(1)	42(1)
C(1)	7466(2)	940(5)	493(2)	45(1)
C(2)	7570(2)	83(4)	64(2)	37(1)
C(3)	8224(2)	-120(5)	17(2)	40(1)
C(4)	8743(2)	629(5)	410(2)	45(1)
C(5)	9181(2)	2279(5)	1271(2)	60(1)
C(6)	9072(3)	3121(6)	1707(2)	71(2)
C(7)	8440(3)	3239(6)	1754(2)	65(2)
C(8)	7919(3)	2546(5)	1363(2)	56(1)
C(9)	8000(2)	1675(5)	906(2)	43(1)
C(10)	8647(2)	1539(5)	861(2)	44(1)
C(11)	7038(2)	-669(5)	-376(2)	40(1)
C(12)	7162(2)	-2930(5)	-1522(2)	43(1)
C(13)	6764(2)	-3655(5)	-2051(2)	41(1)
C(14)	6084(2)	-3805(6)	-2217(2)	66(1)
C(15)	5757(3)	-4513(7)	-2724(2)	84(2)
C(16)	6087(3)	-5061(6)	-3066(2)	68(2)
C(17)	6763(3)	-4918(6)	-2898(2)	77(2)
C(18)	7101(3)	-4228(6)	-2397(2)	66(1)
O(2)	5518(2)	-1838(4)	-1326(2)	68(1)
N(3)	4591(2)	-1347(5)	-1090(2)	65(1)
C(19)	5191(3)	-1989(6)	-1013(2)	62(1)
C(20)	4237(3)	-1615(7)	-690(3)	110(2)
C(21)	4252(3)	-390(6)	-1570(2)	88(2)

Table A.11. [Pd(L)(PPh_3)] (2) (chapter 5)

Atom	x	y	z	U(eq)
Pd(1)	11190(1)	8755(1)	8710(1)	39(1)
P(1)	11157(1)	8216(1)	7092(1)	39(1)
O(1)	13164(3)	8762(2)	9718(3)	52(1)
N(1)	11263(4)	9237(2)	10139(4)	44(1)
N(2)	12431(4)	9333(2)	11008(4)	48(1)
C(1)	7903(5)	9533(2)	9024(5)	60(1)
C(2)	9097(5)	9334(2)	9130(4)	46(1)
C(3)	9313(5)	8955(2)	8228(4)	41(1)
C(4)	8297(5)	8822(2)	7274(4)	48(1)
C(5)	5998(6)	8884(3)	6148(6)	72(2)
C(6)	4752(6)	9087(3)	6015(7)	79(2)
C(7)	4558(6)	9436(3)	6906(7)	75(2)
C(8)	5560(6)	9574(3)	7866(8)	76(2)
C(9)	6810(5)	9383(2)	8002(5)	55(1)
C(10)	7023(5)	9023(2)	7130(5)	48(1)
C(11)	10213(5)	9470(2)	10136(5)	51(1)
C(12)	13341(5)	9062(2)	10681(4)	45(1)
C(13)	14686(5)	9134(2)	11498(5)	50(1)
C(14)	14922(6)	9371(3)	12654(5)	64(2)
C(15)	16178(7)	9425(3)	13423(7)	82(2)
C(16)	17194(7)	9251(3)	13016(7)	81(2)
C(17)	16927(6)	9029(3)	11836(8)	81(2)
C(18)	15770(5)	8917(3)	11075(5)	61(2)
C(19)	11226(4)	8575(2)	5693(4)	43(1)
C(20)	10800(5)	9074(2)	5540(5)	56(1)
C(21)	10837(6)	9359(3)	4490(7)	76(2)
C(22)	11299(7)	9145(4)	3603(7)	94(3)
C(23)	11730(6)	8655(4)	3743(5)	81(2)
C(24)	11700(6)	8341(3)	4776(5)	65(2)

Table A.11. Continued……

C(25)	9816(5)	7763(2)	6610(5)	48(1)
C(26)	9218(6)	7643(2)	5366(6)	64(2)
C(27)	8197(7)	7288(3)	5045(7)	82(2)
C(28)	7783(7)	7057(3)	5969(8)	83(2)
C(29)	8378(7)	7167(2)	7196(8)	79(2)
C(30)	9398(6)	7529(2)	7530(6)	59(1)
C(31)	12596(5)	7800(2)	7448(5)	48(1)
C(32)	13783(6)	8036(2)	7666(6)	65(2)
C(33)	14899(6)	7741(3)	7976(8)	86(2)
C(34)	14812(8)	7207(3)	8058(9)	100(3)
C(35)	13613(9)	6970(3)	7895(11)	123(4)
C(36)	12525(7)	7259(3)	7582(9)	90(2)
Pd(1')	11453(1)	6158(1)	10080(1)	41(1)
P(1')	11500(1)	6667(1)	11752(1)	41(1)
O(1')	9459(3)	6129(2)	9124(3)	52(1)
N(1')	11363(4)	5695(2)	8607(4)	47(1)
N(2')	10203(4)	5596(2)	7778(4)	50(1)
C(1')	14779(5)	5465(2)	9616(5)	56(1)
C(2')	13558(5)	5648(2)	9530(5)	51(1)
C(3')	13341(5)	5985(2)	10503(5)	45(1)
C(4')	14370(5)	6099(2)	11467(4)	50(1)
C(5')	16549(7)	6038(2)	12589(5)	68(2)
C(6')	17854(6)	5779(3)	12749(7)	84(2)
C(7')	18080(7)	5449(3)	11828(8)	81(2)
C(8')	17089(6)	5363(3)	10788(7)	69(2)
C(9')	15834(6)	5580(2)	10638(6)	57(1)
C(10')	15647(5)	5897(2)	11620(6)	56(1)
C(11')	12441(6)	5508(2)	8510(5)	53(1)
C(12')	9279(5)	5842(2)	8146(4)	45(1)
C(13')	7928(5)	5777(2)	7346(5)	49(1)

Table A.11. Continued……

(14')	7658(6)	5560(2)	6149(5)	68(2)
C(15')	6407(7)	5520(3)	5433(7)	86(2)
C(16')	5394(7)	5688(3)	5845(7)	88(2)
C(17')	5658(6)	5905(3)	7030(7)	80(2)
C(18')	6912(6)	5944(2)	7771(6)	68(2)
C(19')	11451(4)	6274(2)	13100(4)	48(1)
C(20')	11758(5)	5743(2)	13108(5)	54(1)
C(21')	11674(7)	5420(3)	14085(6)	74(2)
C(22')	11283(6)	5634(4)	15072(5)	82(2)
C(23')	11017(8)	6150(5)	15096(6)	98(2)
C(24')	11059(6)	6476(3)	14099(5)	65(2)
C(25')	10071(5)	7080(2)	11456(5)	52(1)
C(26')	10154(7)	7626(2)	11317(9)	92(2)
C(27')	9017(8)	7923(3)	11001(13)	155(5)
C(28')	7862(8)	7691(3)	10912(12)	131(4)
C(29')	7761(7)	7157(3)	10990(8)	86(2)
C(30')	8901(6)	6850(3)	11244(6)	71(2)
C(31')	12848(5)	7118(2)	12288(5)	48(1)
C(32')	13269(6)	7381(2)	11367(6)	61(1)
C(33')	14288(7)	7733(2)	11707(8)	77(2)
C(34')	14883(7)	7822(3)	12970(9)	87(2)
C(35')	14513(7)	7559(3)	13846(7)	81(2)
C(36')	13480(6)	7204(2)	13541(5)	61(1)